

# **SOME STUDIES IN DILEPTON PRODUCTION IN HADRON - HADRON COLLISION**

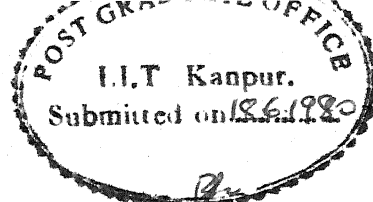
A Thesis Submitted  
in Partial Fulfilment of the Requirements  
for the Degree of  
**DOCTOR OF PHILOSOPHY**

By  
**MOHAMMAD NOMAN**

50205

to the  
**DEPARTMENT OF PHYSICS**  
**INDIAN INSTITUTE OF TECHNOLOGY, KANPUR**

**JUNE 1980**



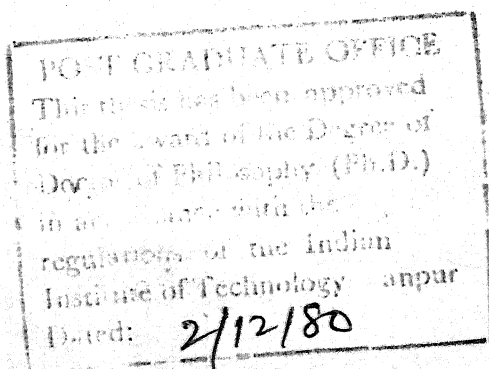
ii

### CERTIFICATE

Certified that the work presented in this thesis entitled 'Some Studies in Dilepton Production in Hadron-Hadron Collision' by Mohammad Noman has been carried out under my supervision and that this has not been submitted elsewhere for a degree.

*H. S. Mani*

H. S. Mani  
Professor  
Physics Department  
Indian Institute of Technology  
Kanpur 208016, India



PHY-1980-D-NOM-SOM

I.I.T. KANPUR  
CENTRAL LIBRARY  
70507  
ALL No A

16 APR 1982

## ACKNOWLEDGEMENTS

I am very much obliged to Professor H. S. Mani for his invaluable guidance throughout this work. I owe him a great deal for his unfailing encouragement and support.

I am grateful to Professors R. Ramachandran, Tulsi Dass, K. Banerjee and Drs. Saurabh D. Rindani and H. S. Sharatchandra from whom I have learnt a lot. To all those who have taught me, both formally and informally, I shall be ever grateful.

I am thankful to Professor K. V. L. Sarma for some clarifications.

To Mr. Razi Nalim, who has helped me in proof-reading and with the graphs, I am grateful.

I gratefully acknowledge the help of many friends and colleagues of whom Messrs. B. P. Singh, C.P.K. Reddy, N. Chandrasekhar, P. K. Srivastava, M. Rafat, J. P. Singh, R. P. Singh, V. K. Srivastava, U. N. L. Mathur, (Miss) V. Chaudhry, M. Saleem, M. Idrees and M. H. Khan deserve special mention.

The indispensable help of my brother, Ataur Rahman, my brother-in-law, Zaheeruddin, and my wife, Nayeema, is also acknowledged.

I also thank Mr. Nihal Ahmad for the speedy and accurate typing and Mr. H. K. Panda for the excellent cyclostyling.

M. Noman



## CONTENTS

	Page
SYNOPSIS	v
Chapter	
1 INTRODUCTION	1
2. DILEPTON PRODUCTION IN HADRONIC COLLISIONS: A REVIEW	8
3 ANGULAR DISTRIBUTION OF DILEPTONS PRODUCED IN HADRONIC COLLISION	23
3.I Introduction	23
3.II Derivation of Angular Distribution	25
3.III Numerical Calculations and Results	35
4 ASYMMETRY PARAMETER AS A FUNCTION OF TRANS- VERSE MOMENTUM IN THE PRODUCTION OF DILEPTON WITH POLARIZED BEAM AND TARGET	54
4.I Introduction	54
4.II Derivation of the QCD Subprocess Cross- section and the Expression for the Asymmetry Parameter	57
4.III Spin Dependence of Parton Distribution Functions	64
4.IV Results and Discussion	71
5 EXTRACTING QUARK AND GLUON DISTRIBUTION IN MESONS FROM DILEPTON DATA	81
5.I Introduction	81
5.II Relation Between Processes $MN \rightarrow \mu^+ \mu^- X$	82
5.III Discussion	89
6 CONCLUSION	93
REFERENCES	96

## SYNOPSIS

Thesis entitled 'Some Studies in Dilepton Production in Hadron-Hadron Collision' by Mohammad Noman in partial fulfilment of the requirements of the Ph.D. degree of the Department of Physics, Indian Institute of Technology, Kanpur.

Quantum chromodynamics (QCD) seems to be a suitable theory for strong interactions. It is a non-abelian gauge theory of interacting coloured quarks and gluons. The quarks come in three colours and the gauge fields called gluons form an octet under SU(3), the underlying symmetry being SU(3) . Colour  
It is the asymptotic freedom that makes QCD interesting and applicable to high energy processes. The effective QCD coupling constant goes to zero logarithmically as the momentum transfer squared  $Q^2$  goes to infinity, i.e. at very high momentum transfer, the theory becomes effectively a free field theory and hence perturbation theory can be applied in such processes. Many calculations have been done involving hadrons in the asymptotic region of QCD and there seems to be fairly good agreement between theoretical perturbative calculations and the experimental data, such as

(i) scaling violation observed in deep inelastic lepton-hadron scattering,

(ii) the ratio  $R = \frac{\sigma(e^+e^- \rightarrow \gamma^* \rightarrow \text{hadron})}{\sigma(e^+e^- \rightarrow \gamma^* \rightarrow \mu^+\mu^-)}$  in the  $e^+e^-$  annihilation,

- (iii) hadron-hadron hard scattering producing particles with large transverse momentum  $q_T$ ,
- (iv) jets of hadrons observed in  $e^+e^-$  annihilation and other hard scattering processes, and
- (v) massive dilepton production in hadronic collisions.

In this thesis we investigate some more aspects of dilepton production in the QCD framework. We study the angular distribution of the dilepton in their rest frame, the  $z$  axis being along the beam direction and  $x$  axis in the plane of the colliding hadron's momenta, i.e. the Gottfried-Jackson frame.. The QCD subprocesses considered are  $q\bar{q} \rightarrow g\gamma^*_{\mu^+\mu^-}$  and  $qg \rightarrow q\gamma^*_{\mu^+\mu^-}$ . The angular distribution is of the form  $1 + A \cos^2 \theta + B \sin^2 \theta \cos \phi + C \sin^2 \theta \cos 2\phi$ .  $A$ ,  $B$  and  $C = \frac{(1-A)}{4}$  are functions of dimuon mass  $m$ ,  $s$  and  $q_T$  (the transverse momentum of the dimuon). We neglect the primordial transverse momentum of the partons, and restrict ourselves to large  $q_T$  in order to avoid mass singularity and infrared divergence.. We compute  $A$  and  $B$  as a function of  $r_T = \frac{q_T}{\sqrt{s}}$  for  $pp$ ,  $p\bar{p}$ ,  $\pi^+p$  and  $\pi^-p$  collisions at  $\sqrt{s} = 27.4$  Gev.  $A$  and  $B$  show striking variations with  $r_T$ . We find that for low values of  $r_T \sim 0.05$ , the angular distribution is of the form  $1 + \cos^2 \theta$  ( $A \cong 1$ ,  $B = C \cong 0$ ) identical to the Drell-Yan prediction. However, for higher values of  $r_T > 0.05$ , there is a strong dependence on both  $\theta$  and  $\phi$ , which shows a striking departure from the Drell-Yan prediction. For example, for  $\tau = m^2/s = 0.1$  and  $r_T = 0.3$ ,  $A = 0.18$  and  $B = 0.12$  for  $pp$

collision. Hence it is the high transverse momentum region where the QCD shows its effects without any ambiguity.

Further we study the asymmetry

$$A_L = \frac{d\sigma(H_1(+)H_2(+)) \rightarrow \mu^+\mu^-X - d\sigma(H_1(+)H_2(-)) \rightarrow \mu^+\mu^-X}{d\sigma(H_1(+)H_2(+)) \rightarrow \mu^+\mu^-X + d\sigma(H_1(+)H_2(-)) \rightarrow \mu^+\mu^-X}$$

associated with dilepton production in longitudinally polarized hadron-hadron collisions  $H_1+H_2 \rightarrow \mu^+\mu^-X$ . We study the variation of  $A_L$  with  $r_T = \frac{q_T}{\sqrt{s}}$  in longitudinally polarized p-p and p- $\bar{p}$  collisions using four different models of spin dependent quark and gluon distribution functions. The basic QCD subprocesses considered are  $q\bar{q} \rightarrow g\gamma^* \rightarrow \mu^+\mu^-$  and  $qg \rightarrow q\gamma^* \rightarrow \mu^+\mu^-$ . For p- $\bar{p}$  collision the asymmetry is quite large (greater than 15%) and shows striking variation with  $r_T$  and is strongly dependent on the model of spin-dependent structure functions. For pp collisions the asymmetry is not large (~5 to 7%) and it is not strongly model dependent because in all the models, we use, the sea and the glue are not strongly polarized. The study of the asymmetry parameter  $A_L$  as a function of  $r_T$  serves two purposes: (i) it distinguishes the QCD subprocesses giving rise to dimuon where  $A_L$  will be non-zero from the quark-meson scattering subprocesses giving rise to dimuon for which  $A_L$  will be zero and (ii) it serves as a good test for the spin dependent quark and gluon distributions in polarized nucleons.

\* Finally we derive relations between dilepton differential cross-sections, based on 1st order QCD subprocesses, in meson-

nucleon collisions:  $\pi^+N$ ,  $k^+N$ ,  $k^0N$ ,  $\bar{k}^0N$ , ( $N = n, p$ ) collisions, assuming the sea to be SU(2) singlet. These relations lead to tests of the parametrizations of (i) nonstrange valence quark distribution in mesons and (ii) gluon distribution in  $\pi$  and  $k$  mesons. The knowledge of the sea quarks either in mesons or nucleons and gluon distribution in nucleons is not required.

## Chapter 1

### INTRODUCTION

Quantum chromodynamics (QCD) seems to be a suitable candidate for strong interactions. It is a nonabelian gauge theory of interacting coloured quarks and gluons. The quarks are supposed to come in three colours and the intermediating gauge fields called gluons form an octet under  $SU(3)$ , the underlying symmetry being  $SU(3)_{\text{Colour}}$ . The QCD Lagrangian<sup>1,2</sup> is

$$\mathcal{L} = -\frac{1}{4} (\partial_\mu A_\nu^a - \partial_\nu A_\mu^a + gf^{abc} A_\mu^b A_\nu^c)^2 + \bar{\psi} [i\gamma^\mu (\partial_\mu - ig \frac{\lambda^a}{2} A_\mu^a)] \psi \quad (1.1)$$

where  $A_\mu^a$  are the 8 gauge fields,  $\psi$  is the quark field,  $g$  is the coupling constant,  $f^{abc}$  are the structure constants of  $SU(3)$  and  $\frac{\lambda^a}{2}$  are the generators of  $SU(3)$  in the triplet representation.

In contrast with quantum electrodynamics, the gauge fields of QCD carry colour and hence interact among themselves. The Feynman rules<sup>1</sup> for QCD are summarized in fig. 1.1. Although there are many hurdles such as the problem of quark and gluon confinement etc. before QCD, yet it becomes useful in calculating processes involving hadrons at very high energies because of 'asymptotic freedom'.<sup>1,2</sup> By 'asymptotic freedom' we mean that the

coupling constant decreases with increasing  $Q^2$ , the momentum transfer squared. This remarkable result of asymptotic freedom arises in the solution of the renormalization group equation for n point Green function of non-abelian gauge theories. One defines a running coupling constant  $\bar{g}(g,t)$  (where  $t = \ln Q^2/Q_0^2$ ) by

$$\frac{\partial \bar{g}(g,t)}{\partial t} = \frac{1}{2} \beta(\bar{g}); \quad \bar{g}(g,0) = g \quad (1.2)$$

$\beta(g)$  is the so-called Callan-Symanzik function. For QCD

$$\beta(g) = \frac{-bg^3}{4\pi}; \quad b = \frac{1}{12\pi} (33 - 2f) \quad (1.3)$$

and fortunately  $\beta(g)$  is negative if the number of quark flavours  $f \leq 16$  and hence  $\bar{g}(g,t) \rightarrow 0$  logarithmically as  $Q^2 \rightarrow \infty$ . Eqs. (1.2) and (1.3) immediately give

$$\bar{g}^2(t) = \frac{\bar{g}^2(0)}{1 + \frac{bt}{4\pi} \bar{g}^2(0)} \quad (1.4)$$

In deep inelastic hadronic processes, it is assumed, because of asymptotic freedom, that the hadron constitutes of almost free quarks and gluons and these quasi free partons interact incoherently with the high  $Q^2$  probe (virtual photon etc.) and hence one needs quark and gluon distribution functions for processes like hadron  $\rightarrow$  parton and quark and gluon fragmentation functions for processes like parton  $\rightarrow$  hadron. In these processes two time scales<sup>3</sup> are involved. One is a

short time scale which is associated with external probe-hadron interaction, and the other is a long time scale associated with the bound state nature of the hadron. In the QCD asymptotic region the short time scale is emphasized. However, till now, there is no prescription as how to incorporate the long time effects in QCD processes.

There is another difficulty of infrared divergence and mass singularity<sup>3</sup> in QCD hard processes involving quarks and gluons. Quarks and gluons are supposed to be massless. Infrared divergence appears because of low energy massless gluons in the final state and the mass singularity appears in the quark propagator. Recently it has been shown<sup>4</sup> that these singularities factor out and hence can be absorbed in the quark and gluon distribution function in hadrons. Many calculations have been done involving hadrons in the asymptotic region of QCD and there seems to be fairly good agreement between theoretical calculations and the experimental data. We mention a few of them.

(i) Deep inelastic lepton-hadron scattering : The main conclusion of deep inelastic lepton-nucleon scattering experiments is that the nucleon structure functions  $F_2$  and  $F_1$  show Bjorken scaling,<sup>5</sup> i.e.  $F_2(x, Q^2) \rightarrow F_2(x)$

$$F_1(x, Q^2) \rightarrow F_1(x)$$

as  $Q^2 \rightarrow \infty$ ,



where  $Q^2 = -q^2 = -$  momentum transfer squared

$$x = \frac{Q^2}{2P \cdot q}, \quad P = 4\text{-momentum of the nucleon target.}$$

But from the asymptotic freedom of QCD one knows that at any finite  $Q^2$ , however large it may be, some interactions among quarks are always present and hence one expects some scaling violation in deep inelastic lepton-nucleon scattering. Using QCD the order of scaling violation<sup>6</sup> has been estimated and it agrees with the experimental data.<sup>7</sup>

(ii)  $e^+e^-$  Annihilation : The ratio  $R = \frac{\sigma(e^+e^- \rightarrow \gamma^* \rightarrow \text{hadrons})}{\sigma(e^+e^- \rightarrow \gamma^* \rightarrow \mu^+\mu^-)}$  has been computed<sup>8</sup> taking leading and next to leading QCD corrections and comes out to be

$$R = 3 \sum_{q=1}^f e_q^2 \left[ 1 + \frac{\alpha_s(Q^2)}{\pi} + (7.35 - 0.442f) \left( \frac{\alpha_s(Q^2)}{\pi} \right)^2 \right] \quad (1.5)$$

$$= 3.84 \text{ for 4 flavours,}$$

which is in good agreement with the experimental value<sup>9</sup> of  $4.17 \pm 0.09$  (stat)  $\pm 0.42$  (syst). The factor 3 on the right hand side of (1.5) is due to the fact that each quark has three colours.

(iii)  $H_1 + H_2 \rightarrow HX$  ; Hadron-hadron hard scattering producing particles with large transverse momentum  $q_T$  : In the framework of QCD these hard scattering phenomena arise due to quark-quark, quark-antiquark, quark-gluon, antiquark-gluon and gluon-gluon

hard elastic scatterings, the scattered quarks and gluons fragmenting into hadrons with large  $q_T$ . Gluck-Owen and Reya<sup>10</sup> have calculated the single pion inclusive cross-sections in p-p, p- $\bar{p}$ ,  $\pi^+p$  collisions in QCD hard scattering formulation using scale breaking  $Q^2$ -dependent quark and gluon distribution and fragmentation functions. The theoretical curve of differential cross-section against  $q_T$  fits the observed curve. It is worth noting that the scale breaking effects play a dominant role in these calculations.

(iv) Jets : In any hard scattering process the predominant QCD radiative corrections are those due to collinear gluonstrahlung and paircreation. These give rise to jets of partons. Thus two jets in  $e^+e^- \rightarrow \gamma^* \rightarrow q\bar{q}$ , three jets in  $e^+e^- \rightarrow \gamma^* \rightarrow q\bar{q}g$  and so on are expected. Production of an additional jet costs an extra factor of  $\alpha_s(Q^2)$ ; hence in  $e^+e^-$  annihilation one expects

$$\sigma(2 \text{ jets}) : \sigma(3 \text{ jets}) : \sigma(4 \text{ jets}) = 1 : \alpha_s : \alpha_s^2 .$$

For 3 jets in  $e^+e^-$  annihilation, it is expected that there should be a large  $q_T$  cross-section. Recently evidence for three jets has been found in  $e^+e^-$  annihilation,<sup>11</sup> which gives another credibility to QCD.

(v) Massive dilepton production in hadronic collisions:

$H_1 + H_2 \rightarrow \mu^+\mu^-X$ . This is another process in which the role of QCD can be tested. In the Drell-Yan<sup>12</sup> picture a quark from one hadron annihilates an antiquark from the other

hadron to produce a massive photon which decays into lepton pair  $q\bar{q} \rightarrow \gamma^* \rightarrow \mu^+\mu^-$ . First order QCD effects such as  $q\bar{q} \rightarrow g\gamma_{\mu}^* \mu^+\mu^-$  and  $qg \rightarrow q\gamma_{\mu}^* \mu^+\mu^-$  are found to be of equal importance.<sup>13</sup>

In this thesis we have investigated some other aspects of dilepton production in the QCD framework. In Chapter 2. we give a survey of experimental status of dilepton production and check it against the theoretical Drell-Yan<sup>12</sup> predictions. In Chapter 3 we investigate the angular distribution of the dilepton in their rest-frame and find that it differs significantly from the Drell-Yan prediction of  $1 + \cos^2\theta$  dependence. In Chapter 4 we study the asymmetry associated with dilepton production in longitudinally polarized hadronic collisions (pp and  $p\bar{p}$  collisions). The asymmetry is quite large and varies with  $q_T$ , the transverse momentum of the dilepton, which can be compared with future data and in turn may throw light on the performance of QCD in dilepton production. In Chapter 5 we derive relations based on QCD expressions between dilepton cross-sections in nucleon-meson collisions, which in turn may be used to determine the distribution functions of nonstrange valence quarks and gluons in  $\pi$  and K mesons without requiring the knowledge of sea and gluon distributions in nucleons.

Feynman propagator

$$\begin{array}{c} \text{---} \rightarrow \end{array} = \delta_{ij} \frac{1}{\not{p} - m + i\epsilon}$$

Gluon propagator

$$\begin{array}{c} \text{---} \end{array} = \delta_{ab} \left[ \frac{-1}{k^2 + i\epsilon} \left( (g_{\mu\nu} - \frac{k_\mu k_\nu}{k^2}) + \alpha \frac{k_\mu k_\nu}{k^2} \right) \right]$$

Ghost propagator

$$\text{---} = \delta_{ab} \frac{1}{k^2 + i\epsilon}$$

Feynman vertex

$$\begin{array}{c} \text{---} \end{array} = ig \gamma_\mu \lambda_{ij}^a / 2$$

Triple gluon vertex

$$\begin{array}{c} \text{---} \end{array} = g f_{abc} [g_{\mu\beta}(k-q)_\sigma + g_{\beta\sigma}(q-r)_\mu + g_{\sigma\mu}(r-k)_\beta]$$

Quadruple gluon Vertex

$$\begin{array}{c} \text{---} \end{array} = -ig^2 [f_{abe} f_{cde} (g_{\mu\sigma} g_{\beta\delta} - g_{\mu\delta} g_{\beta\sigma}) + f_{ace} f_{bde} (g_{\mu\beta} g_{\sigma\delta} - g_{\mu\delta} g_{\beta\sigma}) + f_{ade} f_{cbe} (g_{\mu\sigma} g_{\beta\delta} - g_{\mu\beta} g_{\sigma\delta})]$$

Ghost Vertex

$$\begin{array}{c} \text{---} \end{array} = g f_{abc} \gamma_\mu$$

Feynman rules for QCD

FIG. 1.1

## Chapter 2

### DILEPTON PRODUCTION IN HADRONIC COLLISIONS

In this chapter a short review of experimental situation of massive dilepton production in high energy hadronic collisions

$$H_1 + H_2 \rightarrow \mu^+ \mu^- + \text{anything} \quad (2.1)$$

will be given. We will also be comparing the experimental results with the predictions of the Drell-Yan model<sup>1,2</sup> in which an onshell quark from one hadron annihilates with an onshell antiquark from the other hadron to produce a virtual photon which eventually decays into a lepton pair, (Fig. 2.1)

Assuming that the quarks do not have any intrinsic transverse momentum, the Drell-Yan differential cross-section is given by

$$m^2 \frac{d^2\sigma}{dm^2 d\cos\theta} = \frac{1}{3} \cdot \left(\frac{\pi\alpha^2}{2m^2}\right) (1 + \cos^2\theta) \sum_i e_i^2 \int dx_1 \int dx_2 \\ [f_i(x_1) f_{\bar{i}}(x_2) + (i \leftrightarrow \bar{i})] \delta(x_1 x_2 - \frac{m^2}{s}) \quad (2.2)$$

where  $\theta$  is the polar angle of one of the muons measured from the beam direction, in the  $t$  channel dimuon rest-frame,  $f_i(x)$  is the probability of finding the  $i$ th quark inside the hadron with momentum fraction  $x$  and  $e_i$  is the fractional charge,  $m^2$  the invariant mass square of the dimuon and  $\sqrt{s}$  the c.m.

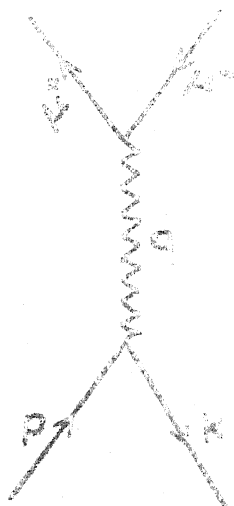


FIG. 2.2

energy of the colliding particles. Some of the predictions of this simple model are:

(i) the differential cross-section is a function of single variable  $\tau = \frac{m^2}{s}$ , i.e. it scales as  $\tau$ .

(ii) the angular distribution of the muon is of the form  $1 + \cos^2\theta$ .

(iii) the dimuon carry no transverse momentum. On introduction of intrinsic transverse momentum  $\sim 600$  MeV, part of which may have its origin in the fermi motion of the quarks inside the hadron, the maximum transverse momentum the dimuon can carry will be of the order 600 MeV in the Drell-Yan picture.

Now one has to check these theoretical Drell-Yan predictions as well as the overall differential cross-section against the experimental data. Data on proton-nucleus collision and pion and nucleus collisions at various energies over a range of dimuon mass are available. We enlist the salient points of the data as follows:

Proton-Nucleus collision : Data<sup>14</sup> on the inclusive production of massive lepton pair in the mass range  $2 \text{ GeV} < m < 15 \text{ GeV}$  by 200, 300, 400, 2000 GeV/c proton on nuclear targets are available at rapidities  $y = 0, 0.23$  to  $0.6$ . The following points emerge out of the data:

(i) Scaling seems to be valid to the 20% level.

(ii) The average transverse momentum  $\langle q_T \rangle$  of the dimuon is independent of mass but rises with beam energy. For 200, 400 and 2000 GeV/c protons  $\langle q_T \rangle$  is respectively 1.01, 1.2 and 1.8 GeV. The data seems to be consistent with the fit

$$\langle q_T \rangle = 0.6 + .022 \sqrt{s}$$

$$\langle q_T^2 \rangle = 0.7 + .0018 s$$

$$E \frac{d^3\sigma}{dq^3} = C [1 + (\frac{q_T}{2.2})^2]^{-6} \quad (2.3)$$

(iii) The angular distribution  $\frac{d\sigma}{d \cos \theta}$  of the muon is being measured in the rest frame of the dimuon, the reference axis for  $\theta$  is either the beam axis (t channel Gottfried-Jackson frame) in which we denote it by  $\theta$ , or the Collins-Soper<sup>15</sup> axis which averages the beam and the reverse target momentum directions, in which we denote it by  $\theta_{c.s.}$ . The Collins-Soper axis is suited for the case when one is incorporating the intrinsic transverse momentum of the partons also. Experimentally the two axes do not differ much. In the t channel frame, where we are ignoring the intrinsic transverse momentum,  $d\sigma/d \cos \theta$  is of the form  $1 + \cos^2 \theta$ , whereas in the Collins-Soper frame  $d\sigma/d \cos \theta_{c.s.}$  is of the form  $1 + \frac{A_0}{2} + (1 - \frac{3}{2} A_0) \cos^2 \theta_{c.s.}$  where  $A_0 = \langle (K_{1T} - K_{2T})^2 \rangle / m^2 \sim 2 \langle K_T^2 \rangle / m^2$ ,  $K_T$  being the intrinsic transverse momentum of the parton. At beam energy 400 GeV/c and  $m \sim 4-10$  GeV  $\langle q_T \rangle \sim 1.2$  GeV,  $k_T$  will be  $\sim 1$  GeV. Hence  $A_0 \sim .1$  to  $.02$  and  $(d\sigma/d \cos \theta_{c.s.}) \sim 1 + \cos^2 \theta_{c.s.}$



According to Antreasyan,<sup>14</sup> the angular distribution fit at  $\sqrt{s} = 62$  Gev is of the form:

$$1 + (1.6 \pm 0.7) \cos^2 \theta_{cs} \quad \text{for } 6 < m < 8 \text{ Gev}$$

$$1 + (0.3 \pm 0.6) \cos^2 \theta_{cs} \quad \text{for } 8 < m < 11 \text{ Gev.}$$

Though the authors claim that above the  $\gamma\gamma$  threshold the angular distribution seems to support the Drell-Yan picture, yet the picture is not very clear because of large uncertainty.

(iv) Shape and normalization of the differential cross-section

$\frac{d\sigma}{dm^2}$  : It all depends on the structure of the sea distribution in nucleons. If one assumes a symmetric sea  $\bar{u}(x) = \bar{d}(x) =$

$s(x) = \bar{s}(x) = c(1-x)^p/x$  where  $p = 7$  or  $9$  and  $c$  is fixed by

the momentum carried by the sea, then the shape of  $\frac{d\sigma}{dm^2}$  agrees

with the experimental curve, over all normalization being

arbitrary. Overall normalization will be all right if the

sea distributions extracted from  $pN \rightarrow \mu^+ \mu^- x$  data and  $\nu N \rightarrow \mu x$

$\bar{\nu} N \rightarrow \mu x$  data are identical at the same values of  $x$  and  $Q^2 (=m^2)$ .

The neutrino data for  $0.05 < x < 0.25$  and  $5 \leq Q^2 \leq 20 \text{ Gev}^2$

overlaps that of the  $pN \rightarrow \mu^+ \mu^- x$  data only for  $x$  near  $0.2$  and

$Q^2 (=m^2) = 20 \text{ Gev}^2$ . E. L. Berger<sup>16</sup> determined the magnitude

of sea from the two data. In the overlap region, the magnitude

of the sea determined from  $\nu N$  data is at most one half of

that determined from the  $pN \rightarrow \mu^+ \mu^- x$  data.

(v) Target dependence: It is assumed that in the asymptotic region partons interact incoherently, hence it is expected that the dimuon cross-section should vary linearly with A, the atomic number of the target. The data<sup>14</sup> indicates that the target dependence changes from  $A^{2/3}$  dependence for  $m \leq 4$  Gev to an A dependence.

Pion-nucleon collisions : Data<sup>14</sup> on the inclusive production of massive dimuons in the mass range  $2 \text{ Gev} < m < 12 \text{ Gev}$  by 150, 175, 200, 225, 280 Gev/c pion beams on nuclear targets are available. The salient features of the data are given below:

(i) With the exception of 225 Gev/c data of Anderson et al<sup>14</sup> scaling is well satisfied within the normalisation error of  $\pm 15\%$ .

(ii) For dimuon mass  $m < 4 \text{ Gev}$ , the average transverse momentum  $\langle q_T \rangle$  seems to rise with m. Above 4 Gev,  $\langle q_T \rangle$  becomes independent of dimuon mass but it increases with increasing beam energy. For instance at 150 Gev/c beam energy it is 1.04 Gev/c whereas for 280 Gev/c it is 1.2 Gev/c. The data seems to give the following fit

$$\langle q_T \rangle = a + b \sqrt{s} \quad a \approx .7 \text{ Gev/c} \\ b = .02$$

$$\frac{1}{q_T} \frac{d\sigma}{dq_T} = D \left[ 1 + \left( \frac{q_T}{E} \right)^2 \right]^F$$

$$D = 0.49 \pm .05 \text{ nb/GeV/c}$$

$$E = 1.7 \pm .05 \text{ Gev/c}$$

$$F = -3.2 \pm 1.3$$

$$\frac{d\sigma}{dX_F} = A [1 - |X_F - B|]^C$$

$$A = .43 \pm .03 \text{ nb}$$

$$B = .14 \pm .02$$

$$C = 2.1 \pm .03 \quad (2.4)$$

(iii) In the pion-nucleus collision, the valence-valence annihilation is the dominant process. Hence in  $\pi^+N \rightarrow \mu^+\mu^-X$   $\bar{d}_\pi(x_1) d_N(x_2)$  annihilation gives the important contribution and in  $\pi^-N \rightarrow \mu^+\mu^-X$  it is the  $\bar{u}_\pi(x_1) u_N(x_2)$  annihilation gives the major contribution, and according to the Drell-Yan formula, it is expected that  $R = \frac{\sigma(\pi^+N \rightarrow \mu^+\mu^-X)}{\sigma(\pi^-N \rightarrow \mu^+\mu^-X)} \xrightarrow{\text{large } x} \frac{e_d^2}{e_u^2} = \frac{1}{4}$ .

. The data of Anderson et al.<sup>14</sup> confirms this tendency: for low dimuon mass  $m$ ,  $R \sim 1$  and near  $m \sim 8$  Gev it is  $\sim .25$ .

(iv) The angular distribution  $\frac{d\sigma}{d \cos\theta}$  in 't channel rest frame' of the dimuon is found to be of the form  $1 + \alpha \cos^2\theta$ . The value of  $\alpha$  as fitted by different groups is not very consistent. According to the fit of Badier et al.<sup>14</sup>,  $\alpha = 0.80 \pm .17$ ; Barate et al.<sup>14</sup> give  $\alpha = 0.52 \pm .46$  but according to Anderson et al.<sup>14</sup>  $\alpha = 1$  at low  $x$  but  $\alpha = -1$  near  $x \sim 1$ . The last quoted result gives a clear evidence that the dimuon production in  $x \sim 1$  region is not predominantly through on-shell quark annihilation.

(v) To check the absolute normalisation one extracts the valence quark (antiquark) distribution in pion from  $\pi N \rightarrow \mu^+\mu^-X$  data using the quark distribution in nucleon determined from

deep inelastic scattering and then checks with the established fact that  $\sim 40\%$  of the pion's momentum is carried by valence quarks. Data of various groups are not consistent. Newmann et al.<sup>17</sup> give the fit  $f_\pi(x) = A(1-x)^p/x$ ,  $p = 1.01 \pm 0.05$ ,  $A = 0.52 \pm .03$  for  $\langle m^2 \rangle \approx 25 \text{ Gev}^2$  and find  $\int x f_\pi(x) dx \approx 0.2$ , showing that 40% of the pion's momentum is carried by valence quarks and anti-quarks which seems to be reasonable. The later data of Barate et al.<sup>14</sup> gives  $\int_0^1 f_\pi(x) dx = 2.8$  which is 2.5 times higher than expected - which shows a clear disagreement with Drell-Yan model. If higher order QCD effects can increase the cross-section by 100% the result can be consistent. Badier et al.<sup>14</sup> also report that the experimental dimuon differential cross-section is almost twice of the Drell-Yan prediction.

(vi) Target dependence: The Chicago-Princeton collaborators<sup>17</sup> find an exponent  $\alpha = 1.12 \pm 0.05$  for  $m > 4 \text{ Gev}$ , whereas recent data of Badier et al.<sup>14</sup> supports the idea of incoherent parton interactions with  $\alpha = 1.03 \pm .03$ .

Thus we get the following important information from the data on  $pN \rightarrow \mu^+ \mu^- x$  and  $\pi N \rightarrow \mu^+ \mu^- x$ :

- (1) that the scaling seems to be valid,
- (2) above  $m = 4 \text{ Gev}$ , the average transverse momentum of the dimuon  $\langle q_T \rangle$  is independent of mass but increases with  $\sqrt{s}$  - a fact unexplainable by simple Drell-Yan model.

(3) the angular distribution  $\frac{d\sigma}{d\cos\theta}$  is of the form  $1 + \alpha\cos^2\theta$  where at low  $x$ ,  $\alpha$  seems to be equal to 1 but in the region  $x \sim 1$ ,  $\alpha = -1$  indicating a clear departure from the simple Drell-Yan model.

(4) The sea distribution extracted from  $pN \rightarrow \mu^+ \mu^- X$  data is twice of that extracted from  $\nu N \rightarrow \mu X$  data,  $\int_0^1 f_\pi(x) dx$  extracted from  $\pi N \rightarrow \mu^+ \mu^- X$  is 2.5 times greater than the expected value of 1.

It is clear that the Drell-Yan model gives only a qualitative but not a quantitative picture of the dilepton production in hadronic collisions. Leaving aside the absolute normalisation, attempts have been made to explain the high transverse momentum of the dilepton by introducing intrinsic transverse momentum for the quarks. Of course the quarks do have a transverse momentum distribution because of fermi motion and quark-gluon interactions inside the hadron. If one assumes a Gaussian type of distribution for quark intrinsic transverse momentum as

$$f(K_T^2) = \frac{1}{2\pi \sigma_0^2} e^{-K_T^2/2\sigma_0^2}$$

$$\sigma_0^2 = \langle K_T^2 \rangle \quad (2.5)$$

then from the Drell-Yan formula, one obtains

$$\frac{d^2\sigma}{dm^2 dq_T^2} = \frac{d\sigma^{DY}}{dm^2} f(q_T^2) \quad (2.6)$$

$$\langle q_T^2 \rangle = \sigma_0^2 = \langle K_T^2 \rangle, \quad \langle q_T \rangle = \frac{\sqrt{\pi}}{2} \sigma_0$$

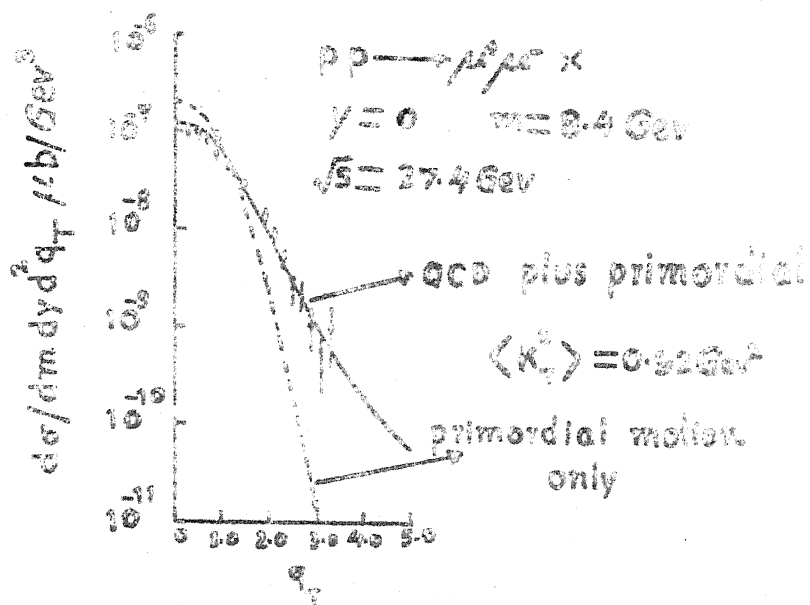


FIG. 2.2

which is decreasing too fast to reproduce the experimental curve (fig. 2.2).<sup>9</sup> Moreover, one requires an unlikely large average intrinsic transverse momentum  $\langle K_T \rangle \sim 1$  GeV/c to explain the observed  $\langle q_T \rangle \sim 1.4$  GeV/c, and this does not explain the increase of  $\langle q_T \rangle$  with incident energy.

Now it is quite natural to look for the higher order QCD effects in the production of massive lepton pair. To the first order of QCD perturbation, either a quark from one hadron can annihilate with an antiquark from the other hadron to produce a gluon and a virtual photon decaying into a lepton pair ( $q\bar{q} \rightarrow q\gamma^*$  fig. 2.3(a)) or a quark (or antiquark) can interact with a gluon from the other hadron to produce a quark (antiquark) and a virtual photon decaying into a lepton pair ( $qg \rightarrow q\gamma^*$  fig. 2.3(b)). For processes where valence-sea contribution is important such as pp collision the second order quark-quark scattering<sup>18</sup> ( $qq \rightarrow qq\gamma^*$ ) producing a virtual photon may be comparable to the first order effect because of the dominance of valence quarks. These QCD processes can give rise to the transverse momentum of the dimuon because the final state recoiling gluon (in the case of  $\bar{q}q$  QCD annihilation) or quark (in the case of  $qg$  compton process) can balance the transverse momentum of the dimuon and thus can explain, after taking the intrinsic transverse momentum of the parton into account, the observed transverse momentum of the dimuon.

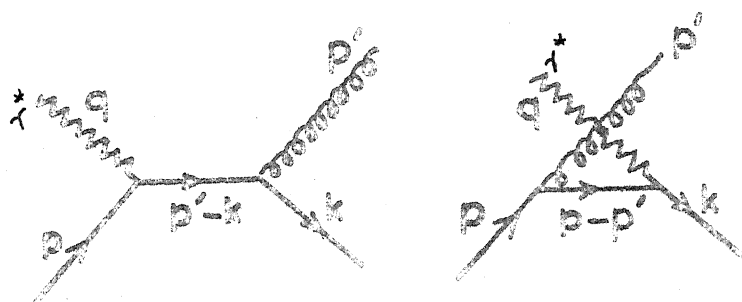


FIG. 2.3 (a)

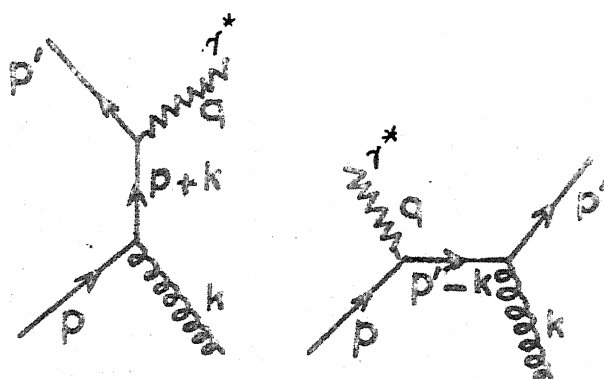


FIG. 2.3 (b)



Explicit calculations on QCD contribution to inclusive dimuon production in hadronic collisions by Fritzsche and Minkowski,<sup>13</sup> Altarelli, Parisi and Petronzio<sup>13</sup> and others<sup>13</sup> show that the quark gluon QCD compton process in pp collision and quark-antiquark QCD annihilation in the  $p\bar{p}$  or  $\pi p$  collision is as important as the Drell-Yan process and the average transverse momentum  $\langle q_T \rangle$  of the dimuon due to these QCD processes increases with  $\sqrt{s}$  at a fixed  $\tau$ . The transverse momentum distribution of dimuon due to first order QCD effect is given by

$$\sigma(s, m^2, q_T^2) = \frac{d^2\sigma}{dm^2 dq_T^2} = \sum_i e_i^2 \iint dx_1 dx_2 \theta((\hat{s} - m^2)^2 - 4\hat{s}q_T^2) \left[ \frac{d^2\hat{\sigma}^{q\bar{q}}}{dm^2 dq_T^2} \{ f_{H_1}^i(x_1) f_{H_2}^{\bar{i}}(x_2) + (i \leftrightarrow \bar{i}) \} + \frac{d^2\hat{\sigma}^{qg}}{dm^2 dq_T^2} \{ (f_{H_1}^i(x_1) + f_{H_1}^{\bar{i}}(x_1)) g_{H_2}(x_2) + g_{H_1}(x_1) (f_{H_2}^i(x_2) + f_{H_2}^{\bar{i}}(x_2)) \} \right] \quad (2.7)$$

where

$$\frac{m^2 d^2\hat{\sigma}^{q\bar{q}}}{dm^2 dq_T^2} = \frac{16\alpha^2\alpha_s}{27 \hat{s} \sqrt{(\hat{s} - m^2)^2 - 4\hat{s}q_T^2}} \left( \frac{\hat{s}^2 + m^4}{\hat{s}^2 q_T^2} - 2 \right)$$

$$m^2 \frac{d^2\hat{\sigma}^{qg}}{dm^2 dq_T^2} = \frac{\alpha^2\alpha_s}{9\hat{s} \sqrt{(\hat{s} - m^2)^2 - 4\hat{s}q_T^2}} \left[ \frac{\hat{s} + 3m^2}{\hat{s}} + \frac{(\hat{s} - m^2)}{q_T^2} \left( 1 - \frac{2m^2(\hat{s} - m^2)}{\hat{s}^2} \right) \right]$$

$$\text{and } \hat{s} = x_1 x_2 s. \quad (2.8)$$

The QCD contribution is not enough to produce the observed  $q_T$  spectrum of the dimuon - the contribution due to the intrinsic transverse momentum of the partons is also needed.<sup>9</sup> The intrinsic contribution is added to  $\sigma(s, m^2, q_T^2)$  after convoluting  $\sigma(s, m^2, q_T^2)$  with the quark premordial motion which is assumed to be  $f(K_T^2) = \frac{1}{2\pi\sigma_0^2} e^{-K_T^2/2\sigma_0^2}$  where  $\sigma_0^2 = \langle K_T^2 \rangle$ .

Thus one obtains

$$\sigma_{\text{total}}(s, m^2, q_T^2) = f(q_T^2) \frac{d\sigma^{\text{DY}}}{dm^2} + \int d^2\vec{K}_T \sigma(s, m^2, (\vec{q}_T - \vec{K}_T)^2) f(K_T^2) \quad (2.9)$$

Taking  $\sigma_0 = .68 \text{ Gev}$   $\langle K_T \rangle = \frac{\sqrt{\pi}}{2} \sigma_0 \approx 600 \text{ Mev}$ , the experimental data<sup>19</sup> on  $pp \rightarrow \mu^+ \mu^- X$  at  $\sqrt{s} = 27.4 \text{ Gev}$  is exactly reproduced.

As the QCD quarkgluon contribution in  $pN$  collisions and QCD quark-antiquark annihilation contribution in  $\pi N$  collisions are of the order of Drell-Yan contribution, the problem of normalization of sea distribution in  $pN \rightarrow \mu^+ \mu^- X$  data and valence quark (antiquark) distribution in pions in  $\pi N \rightarrow \mu^+ \mu^- X$  data may be taken care of.

It looks as if QCD is playing a very important role in the production of dilepton and hence it is desirable to study some other properties of the dimuon production which may reveal something more about the QCD effect in dilepton production. We study the angular distribution of dimuon coming via first order QCD effects. At high transverse momentum the intrinsic momentum

of the partons can be forgotten and hence the angular distribution will be only due to first order QCD processes. Hence it is desirable to study the dimuon angular distribution at large  $q_T$  in order to understand the QCD role in dimuon production. We also study the asymmetry associated in the production of dimuon with polarized beam and target. The asymmetry can arise due to subprocesses involving particles with spin, the nonzero asymmetry will rule out the models of subprocesses involving mesons such as quark-meson scattering etc. Moreover, this study may lead to the knowledge of spin dependent distribution functions of partons inside polarized hadrons.

## Chapter 3

### ANGULAR DISTRIBUTION OF DILEPTONS PRODUCED IN HADRONIC COLLISIONS

#### 3.1 Introduction

The mechanism of Drell and Yan<sup>12</sup> for lepton-pair production in hadronic collisions, involving on-shell quark-antiquark annihilation (Fig. 2.1) into a massive virtual photon, is not adequate to explain all the details of the massive dilepton data, particularly the high transverse momentum of the dilepton pair.

The first order QCD effects<sup>13</sup>, viz., (i)  $q\bar{q} \rightarrow g\gamma^*$  (Fig. 2.3(a)) and (ii)  $qg \rightarrow q\gamma^*$  (Fig. 2.3(b)) in the production of massive dilepton have been investigated by Fritzsche and Minkowski, Petronzio and others,<sup>13</sup> and these first order effects in addition to the contribution of primordial transverse momentum of the partons give the observed transverse momentum of the dilepton and its variation with incident energy i.e.  $\langle q_T \rangle = a + b\sqrt{s}$ . It is natural then to investigate some other aspects of the dilepton production which may give additional information about the mechanism of dilepton production, especially regarding the QCD contribution to the dilepton production. One such aspect would be the study of angular distribution of one of the dileptons in

the dilepton rest frame. In contrast with the simple Drell-Yan angular distribution of the form  $1 + \cos^2 \theta$ , one expects a nontrivial  $\theta, \phi$  dependence in the angular distribution if first order QCD effects  $q\bar{q} \rightarrow g\gamma^*$  and  $qg \rightarrow q\gamma^*$  are taken into account and then consequently one can find out the asymmetry associated with the number of events on two opposite sides of a chosen plane, which can be checked with the experimental data.

In this chapter we study the angular distribution of muons in  $H p \rightarrow \mu^+ \mu^- X$ ,  $H = p, \bar{p}, \pi^+, \pi^-$  by taking into account the first order QCD effects  $q\bar{q} \rightarrow g\gamma^*$  and  $qg \rightarrow q\gamma^*$ . We calculate the coefficients A, B, C occurring in the angular distribution of muons in the  $\mu^+ \mu^-$  centre-of-mass frame, which is given by  $1 + A \cos^2 \theta + B \sin 2\theta \cos \phi + C \sin^2 \theta \cos 2\phi$ , where  $\theta, \phi$  are the polar and azimuthal angles of a muon with respect to some specified axis. A, B, C can be functions of various kinematic variables like  $s, m^2, q_T$ , where  $q_T$  is the invariant generalization of the c.m. transverse momentum, and the prediction of their dependence on the kinematic variables, as well as their actual magnitudes can be tested experimentally.

We obtain the coefficients A, B and C occurring in  $\frac{d^4 \sigma}{dm^2 dq_T^2 d\cos\theta d\phi}$  as functions of  $s, m^2$  and  $q_T^2$ . We restrict ourselves to large  $q_T$  ( $q_T > 1$  Gev) for two reasons. One reason is that we neglect parton transverse momenta  $\sim 0.6$  Gev,

which via the Drell-Yan process would contribute at low  $q_T$ . For large  $q_T$ , where the Drell-Yan process does not contribute significantly, the values of A, B, C become independent of the QCD running coupling constant  $\alpha_s = g_s^2/4\pi$ , and so arbitrariness due to the choice of  $\alpha_s$  is avoided. This is fortunate, since for time like  $q^2$  (which is the present case), the value for  $\alpha_s$  has to be obtained as an extrapolation of the value measured in inelastic scattering for spacelike  $q^2$ . The second reason is that by restricting to large  $q_T$ , our results are independent of mass-singularity regularization procedure,<sup>20</sup> whose effect would be important for low values of  $q_T$ . Our calculations of angular distribution are done in the Gottfried-Jackson frame, i.e., in the  $\mu^+\mu^-$  c.m. frame, we measure the angular distribution with the beam direction as the z axis and with the x axis in the plane of the two hadron momenta.

Kajantie, Lindfors and Raitio<sup>21</sup> have also studied the QCD angular correlations for dimuons with rapidity  $y = 0$ . Our study<sup>22</sup> is for y-integrated distributions. Also, we have calculated the coefficient, we call B. in addition to A which they calculate.

### 3.II Derivation of Angular Distribution

To study the angular distribution of a muon in the process

$$H_1(P_1) + H_2(P_2) \rightarrow \mu^+(K_1) + \bar{\mu}(K_2) + \text{anything} \quad (3.1)$$

(the quantities in the parantheses denote the respective four momenta of the particles), we must obtain the differential cross-section  $d^4\sigma/dm^2 dq_T^2 d\cos\theta d\phi$  for this process,  $\theta, \phi$  being the polar and azimuthal angles of one muon with respect to some specified axes. We shall be working in the  $\mu^+\mu^-$  c.m. frame, and we choose the direction of  $\vec{P}_1$  as the z axis and the direction of  $\vec{P}_1 \times \vec{P}_2$  as the y axis. This is the Gottfried-Jackson or the t-channel helicity frame. Assuming the muonpair to arise from a virtual photon of mass  $m$ , we can conveniently express this differential cross-section in terms of the density matrix elements. For the process  $a + b \rightarrow c + \gamma^*_{\mu^+\mu^-}$ , the matrix element can be expressed as

$$M = A_i^* (a+b \rightarrow c + \gamma^* (\text{helicity}=i)) \cdot \frac{1}{q^2} B^i (\gamma^* (\text{helicity}=i) \rightarrow \mu^+ \mu^-) \quad (3.2)$$

which gives

$$\left[ \sum_{\text{all spins}} |M|^2 \right] = A_i A_j^* \cdot \frac{1}{q^4} B^{*i} B^j = \rho_{ij} \beta^{*ij} \quad (3.3)$$

$i, j = 1, 0, -1.$

The matrix  $\beta$  in the restframe of the virtual photon of 4 momentum  $q$  is given by

$$\beta = e^2 q^2 \begin{pmatrix} 1 + \cos^2\theta & \frac{\sin 2\theta}{\sqrt{2}} e^{i\phi} & \sin^2\theta e^{2i\phi} \\ \frac{\sin 2\theta}{\sqrt{2}} e^{-i\phi} & 2 \sin^2\theta & -\frac{\sin 2\theta}{\sqrt{2}} e^{i\phi} \\ \sin^2\theta e^{-2i\phi} & -\frac{\sin 2\theta}{\sqrt{2}} e^{-i\phi} & 1 + \cos^2\theta \end{pmatrix} \quad (3.4)$$

So the differential cross-section  $(\frac{d^4\sigma}{dm^2 dq_T^2 d\Omega_\mu}) / (\frac{d^2\sigma}{dm^2 dq_T^2})$  can be expressed in terms of the density matrix elements as

$$\begin{aligned} \left( \frac{d^4\sigma}{dm^2 dq_T^2 d\Omega_\mu} \right) / \left( \frac{d^2\sigma}{dm^2 dq_T^2} \right) = \frac{3}{8\pi} [ \rho_{11} (1 + \cos^2\theta) + \rho_{00} \sin^2\theta \\ + \sqrt{2} \operatorname{Re} \rho_{10} \sin 2\theta \cos \phi + \rho_{1,-1} \sin^2\theta \cos 2\phi ] \end{aligned} \quad (3.5)$$

where the density matrix is normalised so that  $2\rho_{11} + \rho_{00} = 1$ . We shall henceforth work with unnormalised  $\rho_{ij}$ , in terms of which, the distribution is

$$I(\theta, \phi) = 1 + A \cos^2\theta + B \sin 2\theta \cos \phi + C \sin^2\theta \cos 2\phi \quad (3.6)$$

with

$$\begin{aligned} A &= \frac{\rho_{11} - \rho_{00}}{\rho_{11} + \rho_{00}} \\ B &= \frac{\sqrt{2} \rho_{10}}{\rho_{11} + \rho_{00}} \\ C &= \frac{\rho_{1,-1}}{\rho_{11} + \rho_{00}} \end{aligned} \quad (3.7)$$

The density matrix elements are sums of contributions from all incoherent processes, and they are integrals over parton distributions of the corresponding density matrix elements (denoted by  $\hat{\rho}_{ij}$ ) for the subprocesses involving partons.

$\hat{\rho}$  for a particular subprocess involving two partons in the initial state can be written as



$$\hat{\rho}_{ij} = \frac{e^2}{q^2 \text{ flux}} \sum A_i A_j^* \quad (3.8)$$

where  $A_i$  is the amplitude for the production of photon of mass  $m$ , helicity  $i$ , and fixed transverse momentum  $q_T$  in the parton c.m. frame; the summation refers to averaging over all initial spins, summation over spins and integration over momenta of all final particles but the photons; and summation over initial and final colours and averaging over initial colour. Thus,

$$\sum \hat{\rho}_{ii} = \frac{3}{16\pi} d^2\sigma/dm^2 dq_T^2 \quad (3.9)$$

We shall be evaluating  $\rho_{ij}$  for the first order QCD subprocesses (i)  $q\bar{q} \rightarrow g\gamma^*$  and (ii)  $qg \rightarrow q\gamma^*$  in addition to the Drell-Yan  $q\bar{q}$  annihilation process ( $q\bar{q} \rightarrow \gamma^*$ ).

The Drell-Yan process : The amplitude for the subprocess

$$q(p) + \bar{q}(k) \rightarrow \gamma^*(q) \quad (3.10)$$

given in fig. 2.1 is

$$A_i^{DY} = e e_q \epsilon_i^{\mu} (q) \bar{v}(k) \gamma_\mu u(p) \quad (3.11)$$

where  $\epsilon_i^{\mu}(q)$  is the photon polarisation vector for helicity  $i$ , and  $e_q$  is the quark charge in the units of the positron charge  $e$ . Taking

$$\begin{aligned} \epsilon_{\pm 1}^{\mu} &= \frac{1}{\sqrt{2}} (0, \mp 1, -i, 0) \\ \epsilon_0^{\mu} &= (0, 0, 0, 1) \end{aligned} \quad (3.12)$$

as the representation for the polarisation vector of a massive photon at rest, we obtain

$$\hat{\rho}_{11}^{DY} = \frac{1}{3} \cdot \frac{e^2 \alpha^2 \hat{s}}{8m^2} \delta(\hat{s}-m^2) \delta(q_T^2) = \hat{\rho}_{-1,-1}^{DY} \quad (3.13)$$

remaining  $\hat{\rho}_{ij}^{DY}$  are zero.

where the factor  $\frac{1}{3}$  comes because summing and averaging over the initial colours of the quark and antiquark i.e.  $\sum_{c=1}^3 1/3 \times 3 = \frac{1}{3}$ ,  $\alpha^2 = \frac{e^2}{4\pi}$ ,  $\sqrt{\hat{s}}/2 =$  parton c.m. energy and  $m^2$  is the invariant mass squared of the photon.

It is clear that for large  $q_T$ , with which we shall be dealing, the contribution of  $\hat{\rho}^{DY}$  will be zero.

### The subprocess $q\bar{q} \rightarrow g\gamma^*$

The amplitude for the subprocess

$$q(p) + \bar{q}(k) \rightarrow g(p') + \gamma^*(q) \quad (3.14)$$

according to the diagram (fig. 2.3a) is given by

$$A_1^{q\bar{q}} = g_s e^2 e_q \varepsilon^{*a\mu}(p') \varepsilon_1^{\nu}(q) \bar{v}(k) \left[ \gamma_\mu \frac{1}{\not{p}-\not{p}'} \gamma_\nu + \gamma_\nu \frac{1}{\not{p}'-\not{k}} \gamma_\mu \right] u(p) \left[ \chi^+ \frac{\lambda^a}{2} \chi \right] \quad (3.15)$$

where  $g_s$  is the strong coupling constant,  $\varepsilon^{a\mu}(p')$  is the polarization vector for the coloured gluon  $a$  ( $a = 1, 2, \dots, 8$ ),  $\lambda^a$  are the usual Gell-Mann matrices for  $SU(3)_{\text{colour}}$  with the normalisation

$$\text{Tr}[\lambda^a \lambda^b] = 2\delta^{ab} \quad (3.16)$$

and  $\chi$  is the SU(3) colour spinor. Using (3.12) for  $\epsilon_i^{\nu}(q)$  and summing over all gluon final states we can express  $\rho_{ij}^{q\bar{q}}$  in terms of the following invariants:

$$\begin{aligned}
 s &= (P_1 + P_2)^2 \approx 2P_1 P_2 \\
 q^2 &= m^2 = \text{invariant mass square of the virtual photon} \\
 \hat{s} &= (p+k)^2 = (x_1 P_1 + x_2 P_2)^2 \approx 2x_1 x_2 s \\
 \hat{t} &= (p-p')^2 \\
 \hat{u} &= (q - p)^2 \\
 \hat{s} + \hat{t} + \hat{u} &= m^2 \\
 q_T &= \sqrt{\frac{\hat{u}\hat{t}}{\hat{s}}} = \text{Transverse mom. of the virtual photon} \\
 \hat{r}_T &= \frac{q_T}{\sqrt{\hat{s}}} \quad r_T = \frac{q_T}{\sqrt{s}} \\
 \tau &= m^2/s \\
 x_1, x_2 &\text{ are the fractions of the hadron momenta} \\
 &\text{carried by the partons.}
 \end{aligned} \tag{3.17}$$

We get the following expressions for  $\rho_{ij}^{q\bar{q}}$ :

$$\hat{\rho}_{00}^{q\bar{q}} = 2 \hat{\rho}_{1-1}^{q\bar{q}} = \frac{e_q^2 \alpha^2 \alpha_s (m^4 + \hat{s}^2 - 2\hat{s} q_T^2)}{18\pi m^2 \hat{s}^2 \sqrt{(\hat{s}-m^2)^2 - 4\hat{s}q_T^2}} \left[ \frac{2m^2}{(m^2 + q_T^2)^2} \right] \tag{3.18}$$

$$\hat{\rho}_{11}^{q\bar{q}} = \hat{\rho}_{-1,-1}^{q\bar{q}} = \frac{e_q^2 \alpha^2 \alpha_s (m^4 + \hat{s}^2 - 2\hat{s} q_T^2)}{18\pi m^2 \hat{s}^2 \sqrt{(\hat{s}-m^2)^2 - 4\hat{s}q_T^2}} \left[ \frac{1}{q_T^2} - \frac{m^2}{(m^2 + q_T^2)^2} \right] \tag{3.19}$$

$$\hat{\rho}_{10}^{q\bar{q}} = -(\hat{\rho}_{10}^{q\bar{q}})^* = \frac{e_q^2 \alpha^2 \alpha_s (m^4 + \hat{s}^2 - 2\hat{s} q_T^2)}{18\pi m^2 \hat{s}^2 \sqrt{(\hat{s}-m^2)^2 - 4\hat{s}q_T^2}} \left[ \frac{m(q_T^2 - m^2)}{\sqrt{2} q_T (m^2 + q_T^2)^2} \right] \tag{3.20}$$

The above expressions have been obtained on the assumption that the quark momentum  $\vec{p}$  is along the z axis, that is, the quark comes from the hadron whose beam direction is along the z axis. However, it turns out that the contribution  $\rho^{q\bar{q}}$  when the quark comes from the other hadron and the antiquark  $\bar{q}$  is along the z direction, is the same as  $\rho^{q\bar{q}}$ , i.e.,

$$\rho_{ij}^{q\bar{q}} = \rho_{ij}^{\bar{q}q} \quad (3.21)$$

Here  $\alpha_s = g_s^2/4\pi$ ,  $q_T^2 \leq (\hat{s}-m^2)/2\hat{s}$ .

All the expressions for  $\rho^{q\bar{q}}$  include the colour factor

$$\frac{1}{3 \times 3} \sum_{a,b} \text{Tr} \left[ \frac{\lambda^a}{2} \frac{\lambda^b}{2} \right] = \frac{2 \sum \delta^{ab}}{36} = \frac{2 \times 8}{36} = \frac{4}{9}.$$

The subprocess  $qg \rightarrow q\gamma^*$

The amplitude  $A_i^{qg}$ , for the subprocess

$$q(p) + g(k) \rightarrow q(p') + \gamma^*(q), \quad (3.22)$$

obtained from the diagrams in Fig. 2.3(b),

$$A_i^{qg} = e e_q g_s \varepsilon_i^{*\mu}(q) \varepsilon^{a\nu}(k) \bar{u}(p') \left[ \gamma_\mu \frac{1}{\not{p} + \not{k}} \gamma_\nu + \gamma_\nu \frac{1}{\not{p}' - \not{k}} \gamma_\mu \right] u(p) \left[ x^+ \frac{\lambda^a}{2} x \right] \quad (3.23)$$

Notations are the same as defined in the previous section.

Using (3.12) for  $\varepsilon_i^\mu(q)$  and integrating over the quark final states in (3.8), we get for  $\hat{\rho}_{ij}^{qg}$  the following expressions:

$$\hat{\rho}_{00}^{qg} = 2\hat{\rho}_{1,-1}^{qg} = \frac{e_q^2 \alpha^2 \alpha_s}{96\pi \hat{s}^2 m^2 \sqrt{(\hat{s}-m^2)^2 - 4\hat{s}q_T^2}} \left[ \frac{4m^2(\hat{s}+m^2)^2}{(m^2+q_T^2)^2} - \frac{4m^2(3\hat{s}+m^2)}{m^2+q_T^2} \right] \quad (3.24)$$

$$\begin{aligned} \hat{\rho}_{11}^{qg} = \hat{\rho}_{-1,-1}^{qg} &= \frac{e_q^2 \alpha^2 \alpha_s}{96\pi \hat{s}^2 m^2 \sqrt{(\hat{s}-m^2)^2 - 4\hat{s}q_T^2}} \left[ \frac{\hat{s}-m^2}{\hat{s} q_T^2} \{ (\hat{s}-m^2)^2 + m^4 \} \right. \\ &\quad \left. + (3m^2+\hat{s}) \right] - \frac{1}{2} \hat{\rho}_{00}^{qg} \end{aligned} \quad (3.25)$$

$$\begin{aligned} \hat{\rho}_{10}^{qg} = -(\hat{\rho}_{-1,0}^{qg})^* &= \frac{e_q^2 \alpha^2 \alpha_s}{96\pi \hat{s}^2 m^2 \sqrt{(\hat{s}-m^2)^2 - 4\hat{s} q_T^2}} \left( \frac{m^2}{2q_T^2} \right)^{\frac{1}{2}} \left[ -2(\hat{s}+m^2) \right. \\ &\quad \left. - 2 \frac{m^2(\hat{s}+m^2)^2}{(m^2+q_T^2)^2} + \frac{(\hat{s}^2 + 8\hat{s}m^2 + 3m^4)}{(m^2+q_T^2)} \right] \end{aligned} \quad (3.26)$$

The above expressions have been obtained on the assumption that the quark momentum  $\vec{p}$  is along the z direction, that is, the quark comes from the hadron whose direction is defined as the z axis. However, we have also to consider the contribution when the quark comes from the other hadron i.e. the gluon momentum  $\vec{k}$  is along the z axis. We obtain the following expressions for the corresponding density matrix  $\hat{\rho}^{gq}$ .

$$\hat{\rho}_{00}^{gq} = 2\hat{\rho}_{1,-1}^{gq} = \frac{e_q^2 \alpha^2 \alpha_s}{96\pi \hat{s}^2 m^2 \sqrt{(\hat{s}-m^2)^2 - 4\hat{s} q_T^2}} \left[ \frac{8m^2(\hat{s}+3m^2)}{m^2+q_T^2} - \frac{8m^4(\hat{s}+m^2)^2}{\hat{s}(m^2+q_T^2)^2} \right] \quad (3.27)$$

$$\hat{\rho}_{11}^{gq} = \hat{\rho}_{-1,-1}^{gq} = \frac{e_q^2 \alpha^2 \alpha_s}{96\pi \hat{s}^2 m^2 \sqrt{(\hat{s}-m^2)^2 - 4\hat{s} q_T^2}} \left[ \frac{\hat{s}-m^2}{\hat{s} q_T^2} \{ (\hat{s}-m^2)^2 + m^4 \} \right. \\ \left. + (3m^2 + \hat{s}) \right] - \frac{1}{2} \hat{\rho}_{00}^{gq} \quad (3.28)$$

$$\hat{\rho}_{10}^{gq} = -(\hat{\rho}_{-1,0}^{gq})^* = \frac{e_q^2 \alpha^2 \alpha_s}{96\pi \hat{s}^2 m^2 \sqrt{(\hat{s}-m^2)^2 - 4\hat{s} q_T^2}} \left( \frac{m^2}{2q_T^2} \right)^{\frac{1}{2}} \left[ \frac{8m^4 (\hat{s}+m^2)^2}{\hat{s} (m^2+q_T^2)^2} \right. \\ \left. - \frac{4m^2 (3\hat{s}^2 + 8\hat{s}m^2 + m^4)}{\hat{s} (m^2+q_T^2)} + 2(3\hat{s} + 5m^2) \right] \quad (3.29)$$

All expressions for  $\hat{\rho}^{qg}$  and  $\hat{\rho}^{gq}$  include the colour factor  $\frac{1}{3 \times 8} \sum_{a,b} \text{Tr}(\lambda^a/2 \lambda^b/2) = \frac{1}{6}$  which arises because we sum over the colours of initial and final quarks and gluons and average over the initial colours.

To obtain the complete density matrix elements  $\rho_{ij}$  for the process  $H_1 H_2 \rightarrow \gamma^* X$ , the  $\hat{\rho}_{ij}$  have to be convoluted with the appropriate structure functions and then added together. If we denote by  $f_H^q(x)$  and  $f_H^{\bar{q}}(x)$ ,  $g_H(x)$  the structure functions of a quark  $q$ , an antiquark  $\bar{q}$  and a gluon respectively inside the hadron  $H$ , then the convoluted density matrix elements are given by:

$$\rho_{ij}^{q\bar{q}} = \int_0^1 dx_1 \int_0^1 dx_2 \theta((\hat{s}-m^2)^2 - 4\hat{s} q_T^2) \hat{\rho}_{ij}^{q\bar{q}} f_{H_1}^q(x_1) f_{H_2}^{\bar{q}}(x_2) \quad (3.30)$$

$$\rho_{ij}^{\bar{q}q} = \int_0^1 dx_1 \int_0^1 dx_2 \theta((\hat{s}-m^2)^2 - 4\hat{s} q_T^2) \hat{\rho}_{ij}^{\bar{q}q} f_{H_1}^{\bar{q}}(x_1) f_{H_2}^q(x_2) \quad (3.31)$$

$$\rho_{ij}^{qg} = \int_0^1 dx_1 \int_0^1 dx_2 \theta((\hat{s}-m^2)^2 - 4\hat{s} q_T^2) \hat{\rho}_{ij}^{qg} f_{H_1}^q(x_1) g_{H_2}(x_2) \quad (3.32)$$

$$\rho_{ij}^{gq} = \int_0^1 dx_1 \int_0^1 dx_2 \theta((\hat{s}-m^2)^2 - 4\hat{s} q_T^2) \hat{\rho}_{ij}^{gq} g_{H_1}(x_1) f_{H_2}^q(x_2) \quad (3.33)$$

$$\rho_{ij}^{\bar{q}g} = \int_0^1 dx_1 \int_0^1 dx_2 \theta((\hat{s}-m^2)^2 - 4\hat{s} q_T^2) \hat{\rho}_{ij}^{\bar{q}g} f_{H_1}^{\bar{q}}(x_1) g_{H_2}(x_2) \quad (3.34)$$

$$\rho_{ij}^{g\bar{q}} = \int_0^1 dx_1 \int_0^1 dx_2 \theta((\hat{s}-m^2)^2 - 4\hat{s} q_T^2) \hat{\rho}_{ij}^{g\bar{q}} g_{H_1}(x_1) f_{H_2}^{\bar{q}}(x_2) \quad (3.35)$$

The last two expressions (3.34) and (3.35) are the contributions of antiquark-gluon scattering. The Drell-Yan contribution is zero because  $q_T^2 > 0$ . Hence the density matrix elements  $\rho_{ij}$  for the process  $H_1 + H_2 \rightarrow \gamma^* X$  at  $q_T > 0$  is

$$\rho_{ij} = \sum_{\text{all flavours}} (\rho_{ij}^{q\bar{q}} + \rho_{ij}^{\bar{q}q} + \rho_{ij}^{qg} + \rho_{ij}^{gq} + \rho_{ij}^{\bar{q}g} + \rho_{ij}^{g\bar{q}}) \quad (3.36)$$

$\rho_{ij}$  are functions of  $s$ ,  $m^2$  and  $q_T$  which may be expressed in terms of  $s$ ,  $\tau = \frac{m^2}{s}$  and  $r_T = \frac{q_T}{\sqrt{s}}$ . Once this is done the  $s$  dependence is factored out and is the same for all  $\rho_{ij}$ . Knowing  $\rho_{ij}$ , A, B, C can be computed using equation (3.7).

A, B and C are functions of the scaled variables  $\tau = m^2/s$  and  $r_T = q_T/\sqrt{s}$ , because the  $s$  dependence and  $\alpha_s(m^2)$  cancel out in the numerator and denominator of eq. (3.7). Of course, we are treating the structure functions to be  $q^2$ -independent.

### 3.III Numerical Calculations and Results

We have evaluated A, B and C from  $p_{ij}$  given by equation (3.36) using (3.7) for various values of  $\tau$  and  $r_T$  for the processes  $pH \rightarrow \mu^+ \mu^- X$ ,  $H = p, \bar{p}, \pi^+, \pi^-$ . In our calculations, we have used the expression

$$\alpha_s(m^2) = \alpha_s(m_0^2) \left[ 1 + \frac{25}{12\pi} \alpha_s(m_0^2) \ln \frac{m^2}{m_0^2} \right]^{-1} \quad (3.37)$$

given by QCD and the renormalization group equation for three colours and four flavours. We take  $\alpha_s(m_0^2)=0.25$  for  $m_0=2$  GeV. As we restrict ourselves to nonzero transverse momentum of the dimuon, the Drell-Yan process does not contribute to  $p_{ij}$  and consequently in the calculation of A, B, C,  $\alpha_s(m^2)$  cancels out and our results become independent of the choice of  $\alpha_s(m^2)$ . We have neglected the  $m^2(=q^2)$  dependence of the structure functions.

The process  $pp \rightarrow \mu^+ \mu^- X$ : For evaluating  $p_{ij}$  for this process we need the quark and gluon distributions in protons. For the quark distributions, we use the parametrization of Peierls, Trueman and Wang<sup>23</sup>:



$$f_p^u(x) = u_p(x) = 1.79 (1-x)^3(1+2.3x)/\sqrt{x} + s(x)$$

$$f_p^d(x) = d_p(x) = 1.07 (1-x)^{3.1}/\sqrt{x} + s(x)$$

$$f_p^{\bar{u}}(x) = f_p^{\bar{d}}(x) = f_p^{\bar{s}}(x) = s_p(x) = 0.15 (1-x)^7/x \quad (3.38)$$

For the gluon distribution, we use

$$g_p(x) = \frac{(m+1)}{2} (1-x)^m/x \quad (3.39)$$

with  $m = 5$  and  $8$ . The factor  $\frac{m+1}{2}$  takes care of the fact that gluons carry 50% of the proton momentum.

The values of  $A$  and  $B$  as functions of  $r_T$  are presented for various values of  $\tau$  in Figs. 3.1(a), 3.2(a) for  $g_p(x) = 3(1-x)^5/x$  and in Figs. 3.1(b) and 3.2(b) for  $g_p(x) = 4.5(1-x)^8/x$ . ( $C$  is given by  $C = \frac{1}{4}(1-A)$ .)  $A$ ,  $B$  do not separately depend on  $s$ ,  $m^2$  and  $q_T$  but on scaled variables  $\tau$  and  $r_T$ . For evaluating  $\rho_{ij}$ , we have used  $\sqrt{s} = 27.4$  Gev. The shape and size of  $A$  and  $B$  do not change much for the two different gluon distribution  $3(1-x)^5/x$  and  $4.5(1-x)^8/x$ , although  $\rho_{ij}$  change appreciably.  $A$  and  $B$  show interesting variations with  $r_T$ . For low values of  $r_T < 0.05$ ,  $A$  is almost 1 and then decreases with  $r_T$  to a minimum of about 0.1 and then increases.  $B$  starts with a value near zero for  $r_T \approx 0$ , decreases with increasing  $r_T$  to a minimum of about -0.12 and then increases to a value of about +0.2, after which, the curve flattens, and  $B$  decreases slowly.

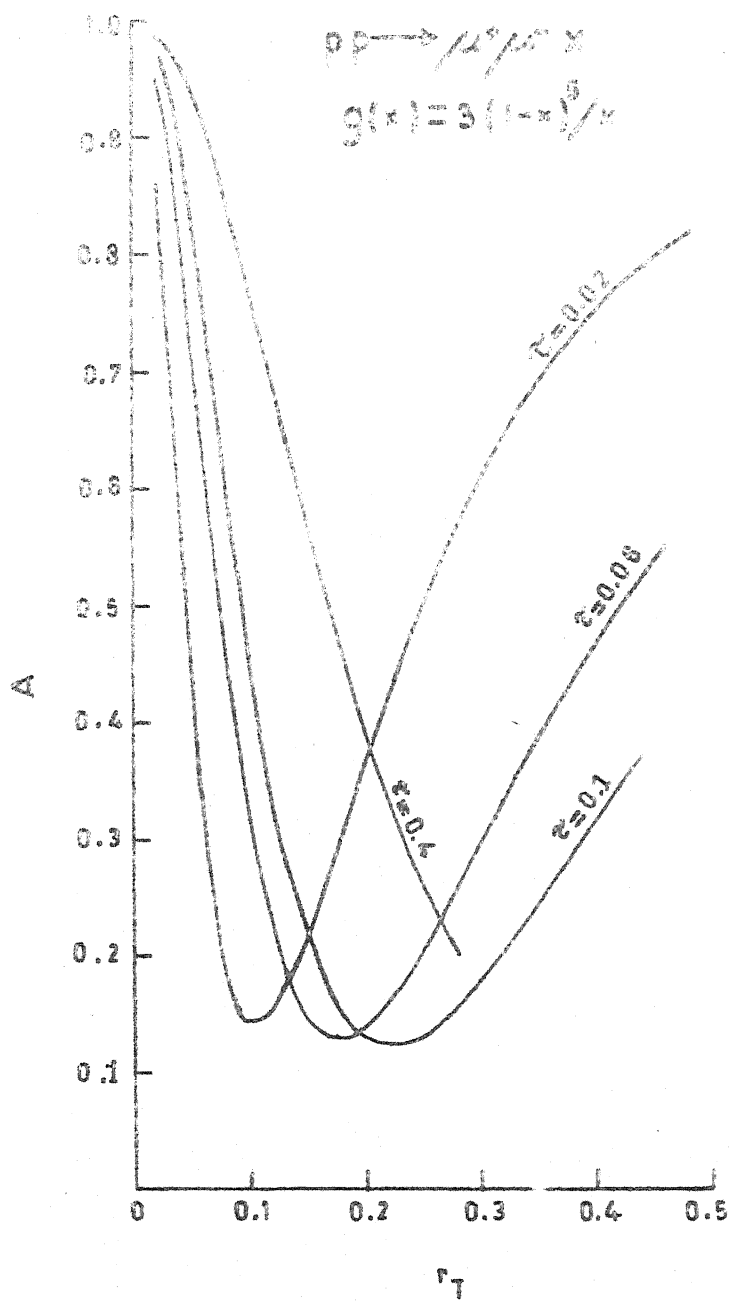


FIG. 3.1(d)

$$pp \rightarrow \mu^+ \mu^- X$$

$$g(x) = 3(1-x)^5/x$$

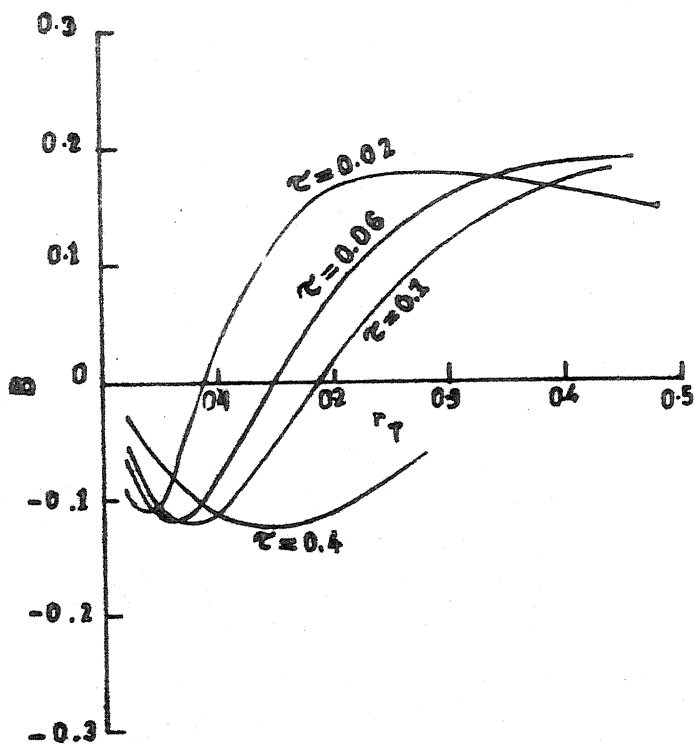


FIG. 3.2 (a)

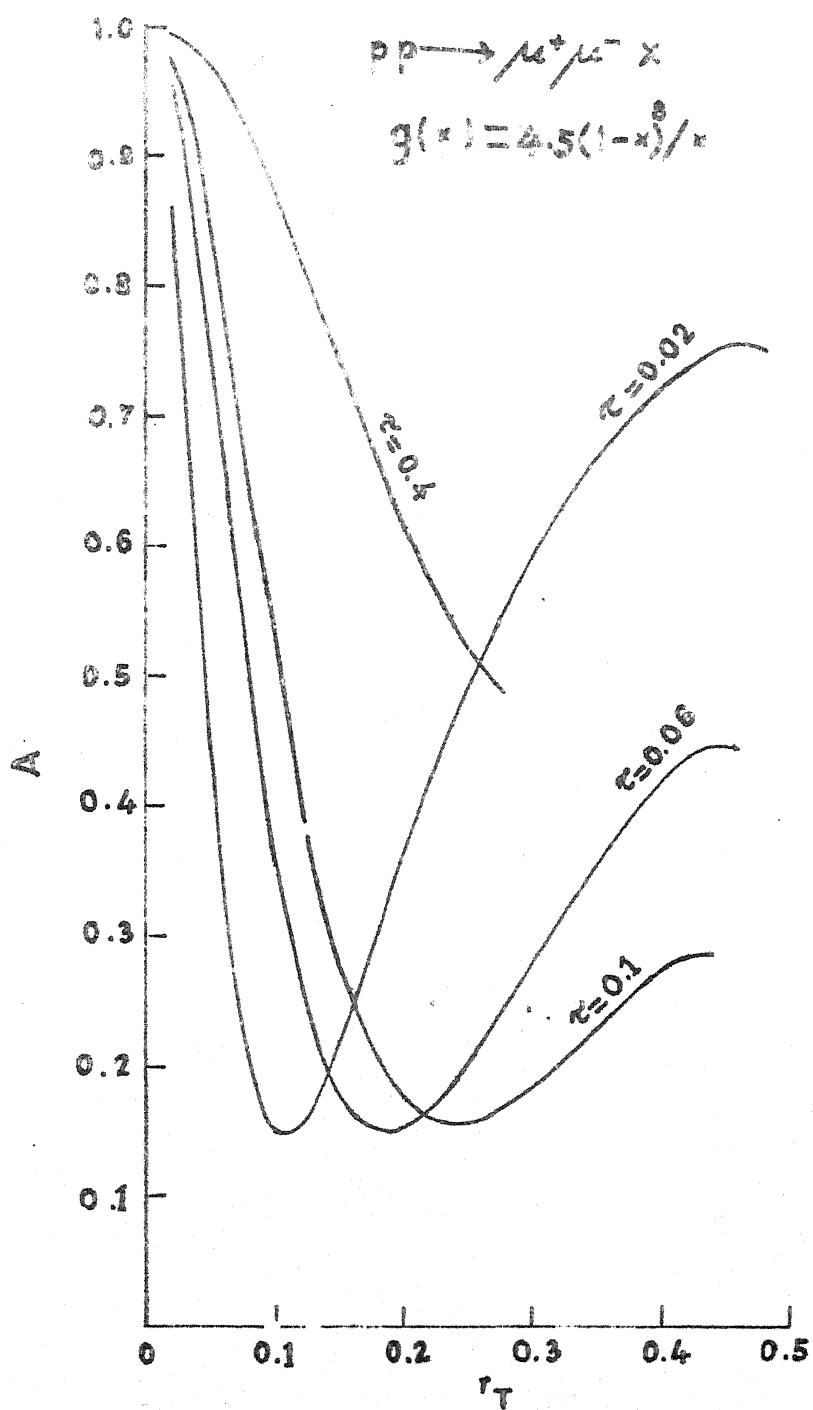


FIG. 3.1 (b)

$$pp \rightarrow \mu^+ \mu^- \gamma$$

$$g(x) = 4.5(1-x)^3/x$$

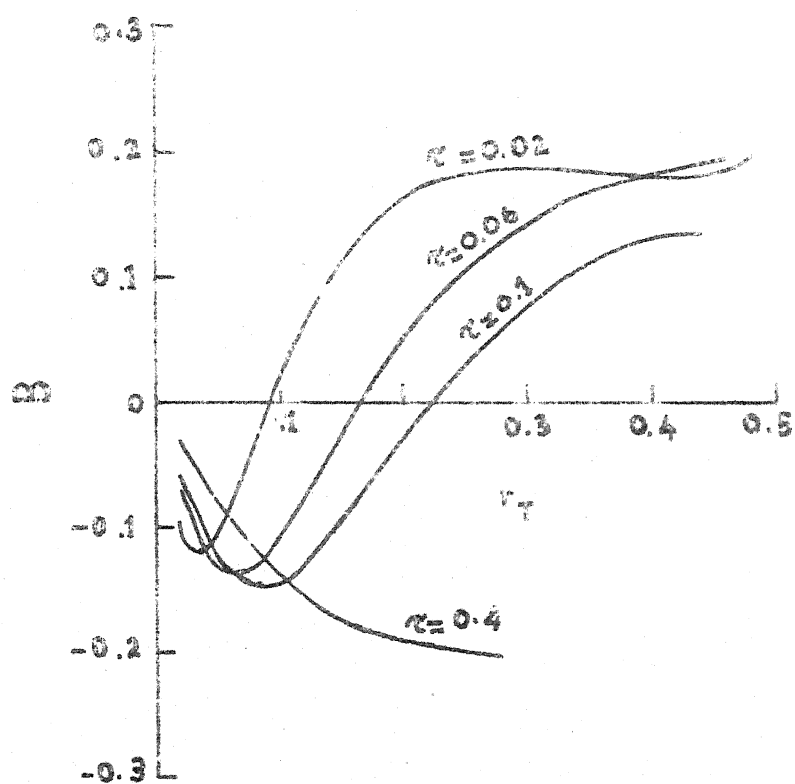


FIG. 3.2 (b)

These variations of A and B with  $r_T$  clearly indicate that  
 (i) at low  $r_T < .05$ , the angular distribution is almost of the form  $1 + \cos^2\theta$  and hence low transverse momentum data on dimuon production is not fit for the investigation of the QCD effects.

(ii) for  $r_T > .05$ , there is quite strong dependence on both  $\theta$  and  $\phi$ . This region is suitable for the investigation of the QCD role in the dimuon production.

A is measured in the  $\phi$ -integrated distribution, which is of the form  $1 + A \cos^2\theta$ . An interesting way of observing nonzero B is to consider the difference in the fractional number of events occurring in the two sides of the yz plane, with  $\theta$  restricted to values  $0 \leq \theta_0 \leq \theta \leq \theta_1 \leq \pi/2$ .

For  $\theta_0 = 0$ , the corresponding asymmetry is

$$\begin{aligned} \delta(\theta_1) &= \frac{\int_0^{\theta_1} \sin\theta \, d\theta \left\{ \int_{\pi/2}^{3\pi/2} I(\theta, \phi) d\phi - \int_{-\pi/2}^{\pi/2} I(\theta, \phi) d\phi \right\}}{\int_0^{\theta_1} \sin\theta \, d\theta \left\{ \int_{\pi/2}^{3\pi/2} I(\theta, \phi) d\phi + \int_{-\pi/2}^{\pi/2} I(\theta, \phi) d\phi \right\}} \\ &= -\frac{4B}{\pi} \cot \frac{\theta_1}{2} \frac{\sin^2 \theta_1}{3 + A(1 + \cos \theta_1 + \cos^2 \theta_1)} \end{aligned} \quad (3.40)$$

$\delta$  is, thus, proportional to B. For  $\theta_1 = \pi/2$

$$\delta(\pi/2) = -\frac{4B}{\pi(A+3)} \quad (3.41)$$

For  $\theta_1 = \pi/3$

$$\delta(\pi/3) = - \frac{12\sqrt{3} B}{\pi(12+7A)} \quad (3.42)$$

At  $\tau = 0.1$  and  $r_T = 0.3$ , for example,  $A = 0.18$  and  $B = 0.12$ ,  $\delta(\pi/2) \approx -.06$ ,  $\delta(\pi/3) \approx -.07$ . Thus the asymmetry can be quite large.

As pointed by Georgi<sup>18</sup> it is a bit dangerous to ignore the higher order QCD subprocess  $qq \rightarrow qq\gamma^* \rightarrow \mu^+\mu^-$  in  $pp \rightarrow \mu^+\mu^-X$ , but fortunately an explicit calculation by Kripfganz and Contogouris<sup>24</sup> shows that the contribution due to this subprocess is negligible over most of the kinematic region.

The process  $p\bar{p} \rightarrow \mu^+\mu^-X$ : To evaluate  $\rho_{ij}$  for this process, we need the parton distributions in antiprotons in addition to the parton distributions in protons given by (3.38) and (3.39). The parton distributions in antiprotons are related to the parton distributions in protons by charge conjugation.

$$\begin{aligned} f_{\bar{p}}^{\bar{u}}(x) &= f_p^u(x) = u_p(x) \\ f_{\bar{p}}^{\bar{d}}(x) &= f_p^d(x) = d_p(x) \\ f_p^u(x) &= f_{\bar{p}}^{\bar{u}}(x) = f_p^{\bar{d}}(x) = f_{\bar{p}}^d(x) = f_p^s(x) = f_{\bar{p}}^{\bar{s}}(x) = \\ f_p^s(x) &= f_{\bar{p}}^{\bar{s}}(x) = s_p(x) \end{aligned} \quad (3.43)$$

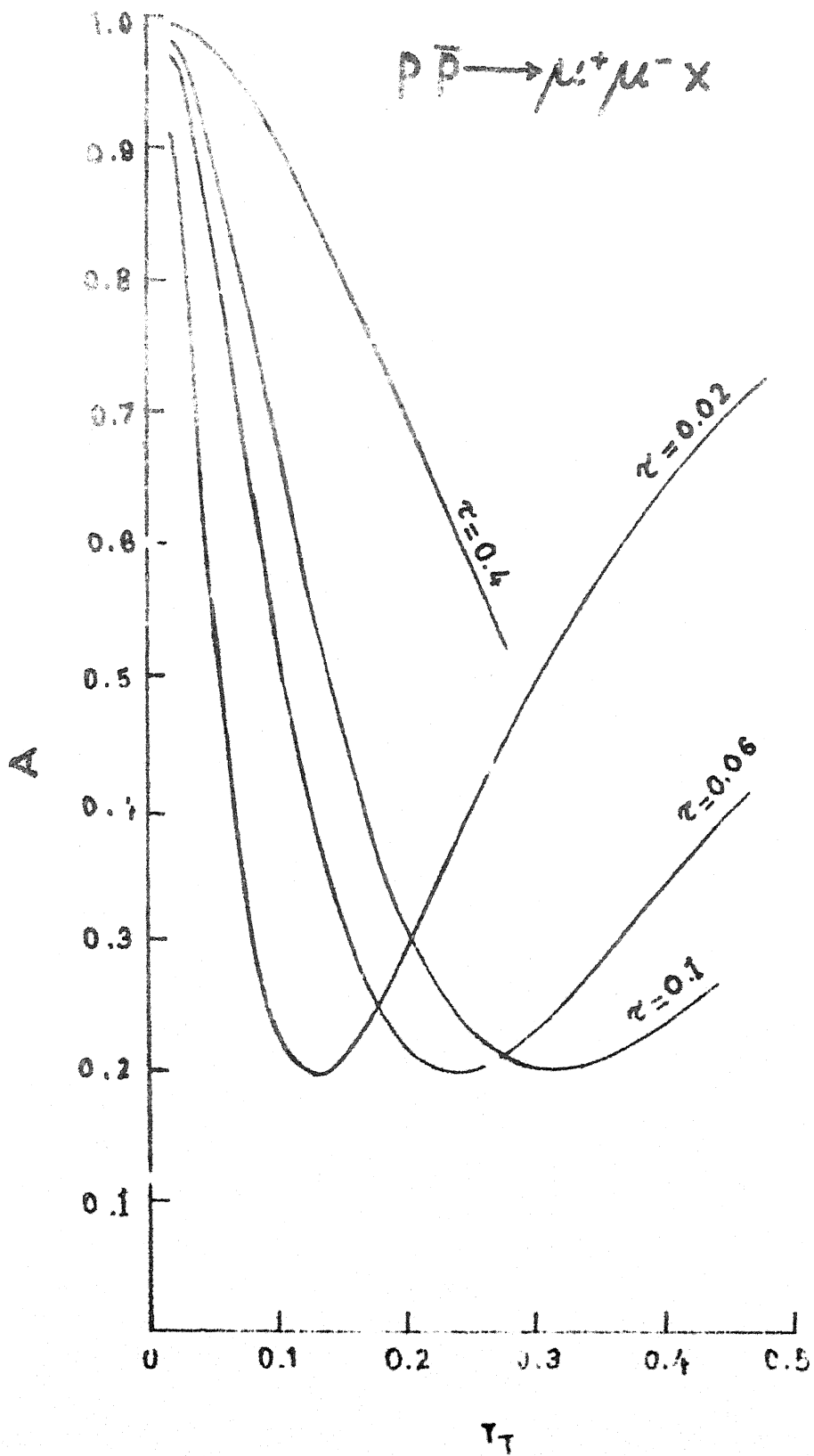


FIG. 3.3 (a)



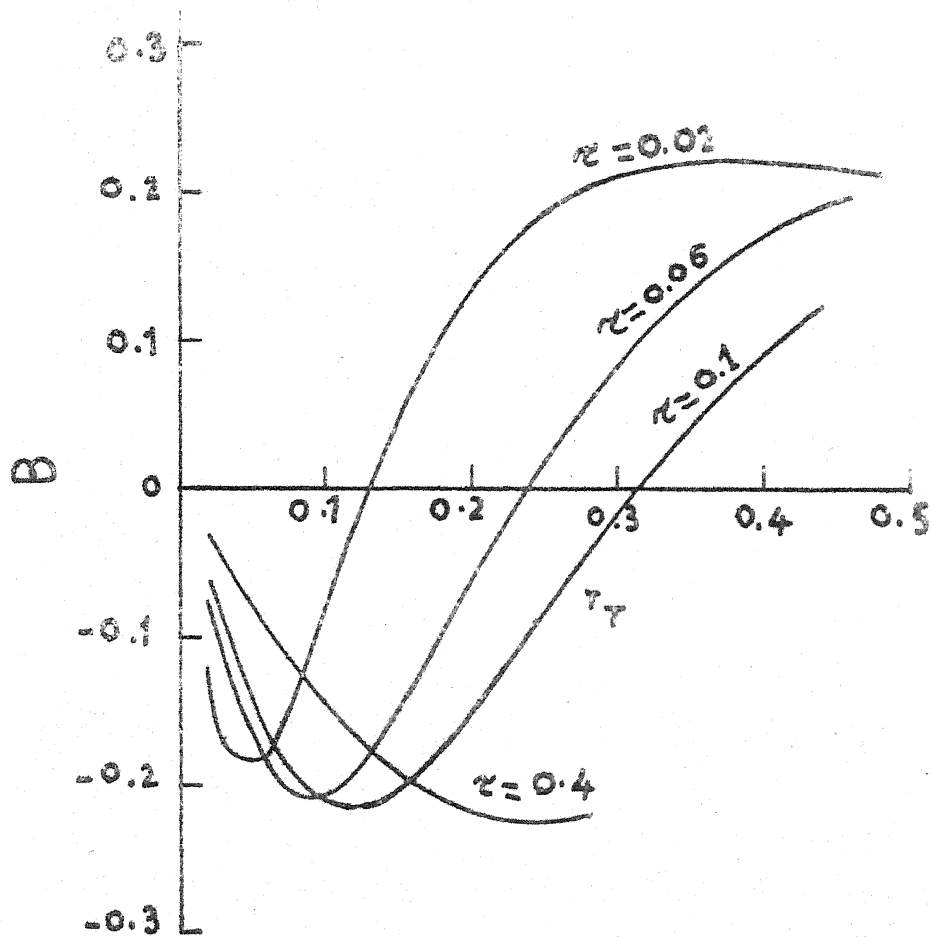


FIG. 3.4 (d)

The gluon distribution in  $\bar{p}$  is assumed to be the same as that in  $p$ .

$$g_{\bar{p}}(x) = g_p(x) = \frac{m+1}{2}(1-x)^m/x \quad (3.44)$$

We compute  $\rho_{ij}$  using the functions  $u_p(x)$ ,  $d_p(x)$ ,  $s_p(x)$  given by equation (3.38) and then calculate A, B and C for various values of  $\tau$  and  $r_T$ . The plot of A and B against  $r_T$  is shown in figs. 3.3(a) and fig. 3.4(a) for  $g_p(x) = 3.0 (1-x)^5/x$ . The shape and size of A and B do not change if we change the gluon distribution to  $g_p(x) = 4.5 (1-x)^8/x$ . This is understandable because for  $p\bar{p} \rightarrow \mu^+\mu^-X$ , the quark-gluon compton subprocess is negligible in comparison with the quark-antiquark QCD-annihilation subprocess. Following comments are in order.

(i) The shape of A, B versus  $r_T$  curves for  $p\bar{p} \rightarrow \mu^+\mu^-X$  are similar to those in  $pp \rightarrow \mu^+\mu^-X$  process.

(ii) A starts at  $\sim 1$  for  $r_{T\sim} 0.02$  and goes to a minimum of 0.2 and then rises with  $r_T$ .

(iii)  $B \approx 0$  for  $r_T \approx 0$  and then decreases to a minimum of  $\sim -0.2$  and then increases with  $r_T$  and goes up to .22.

(iv) The angular distribution for  $r_T < .02$  is of the form  $1 + \cos^2\theta$ , same as the Drell-Yan prediction. Hence this region is not suitable for the study of QCD effects in dimuon production.

(v) For  $r_T > 0.05$ , both  $\theta$  and  $\phi$  dependences are appreciable and quite different from  $1 + \cos^2\theta$  behaviour and thus large  $r_T$  region is suitable for the study of the role of QCD processes playing in the dimuon production. The asymmetry  $\delta(\theta_1)$  defined in (3.40) is appreciable for this process too. For instance at  $\tau = .1$  and  $r_T = 0.2$ ,  $A = .22$  and  $B = -.15$  and hence  $\delta(\pi/2) = .06$  and  $\delta(\pi/3) \approx .08$ . It is to be noted that the asymmetry  $\delta(\theta_1)$  can change sign if  $r_T$  is changed because  $B$  varies from -ve to +ve value as  $r_T$  increases.

The process  $\pi^+ p \rightarrow \mu^+ \mu^- X$ : Here, in addition to the parton distribution in proton, the knowledge of parton distributions in pions is also required. No parametrization based on deep inelastic scattering on pions, due to the lack of data, is available. We use the following parametrization due to Farrar<sup>25</sup>, derived on the basis of SU(2) symmetry, charge conjugation symmetry, quark counting rule and the fact that 40% of pions momentum is carried by valence quark and the rest by the gluon (50%) and the sea

$$\begin{aligned}
 f_{\pi^+}^{uv}(x) &= f_{\pi^-}^{dv}(X) = f_{\pi^-}^{\bar{u}v}(X) = f_{\pi^+}^{\bar{d}v}(X) = u_{\pi}^v(X) \\
 &= 0.4 (1-x)/x \quad \text{for } x \geq 0.5 \\
 &= (0.1 + 0.72\sqrt{x})/x
 \end{aligned}$$

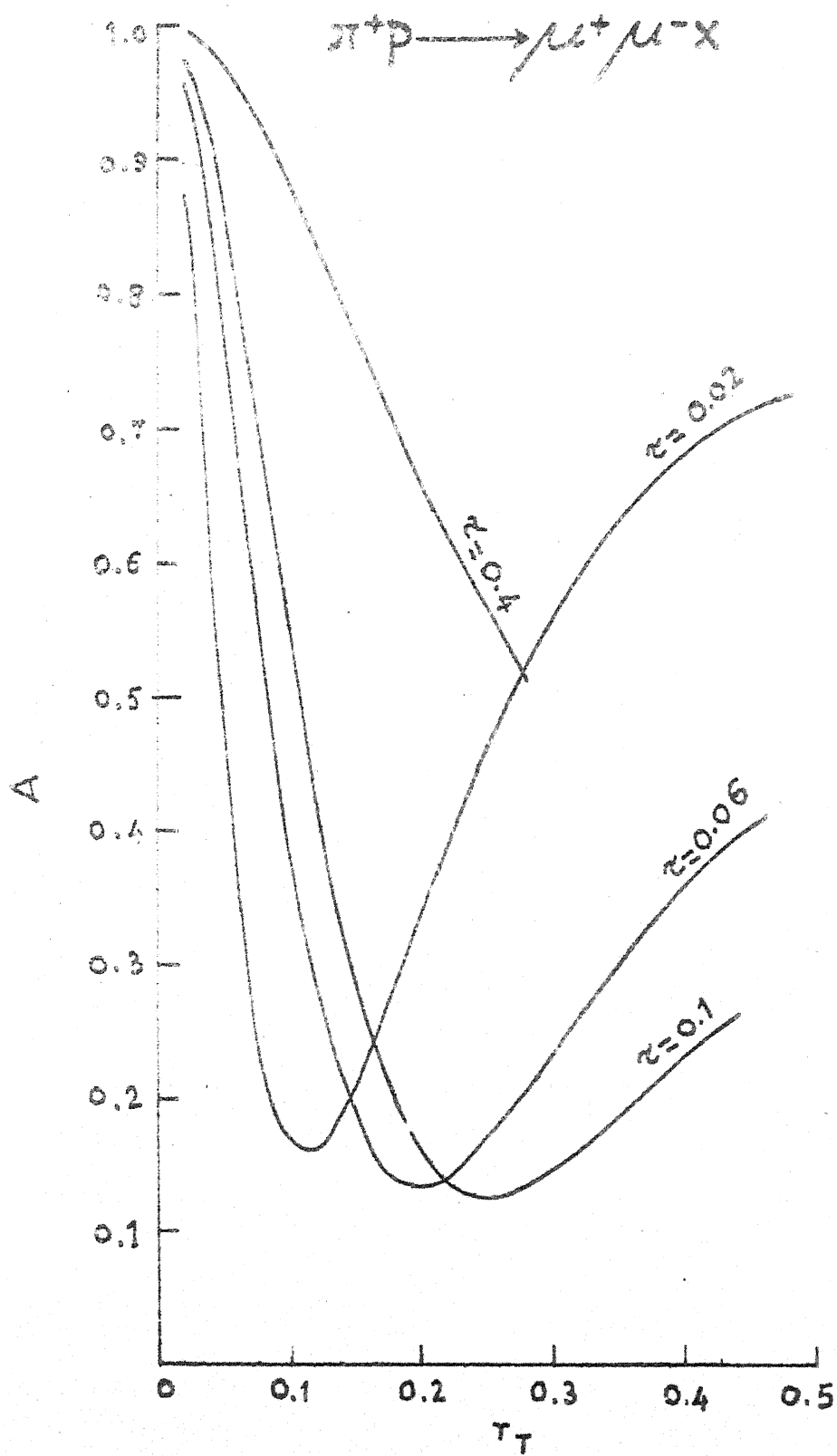


FIG. 3.5 (a)

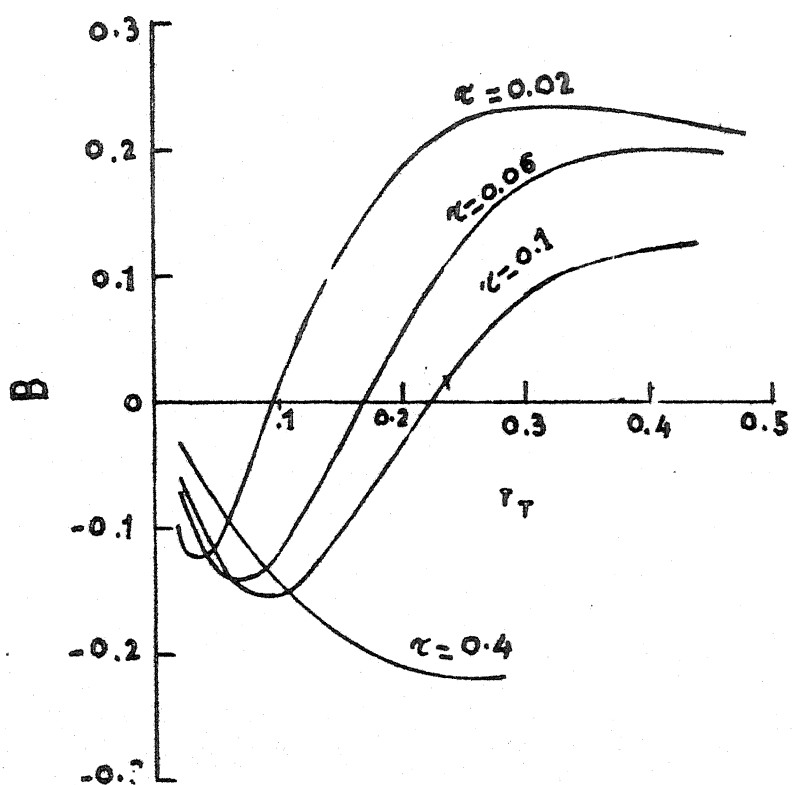
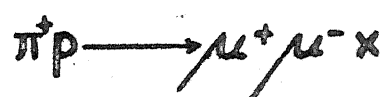


FIG. 3.6 (d)

$$\begin{aligned}
S_{\pi}(x) &= f_{\pi+}^{us}(x) = f_{\pi+}^{ds}(x) = f_{\pi-}^{us}(x) = f_{\pi-}^{ds}(x) = f_{\pi+}^{ss}(x) \\
&= f_{\pi-}^{ss}(x) = 0.1 (1-x)^5/x \\
g_{\pi+}(x) &= g_{\pi-}(x) = 2(1-x)^3/x \\
u_{\pi}(x) &= u_{\pi}^v(x) + s_{\pi}(x) \tag{3.45}
\end{aligned}$$

The superscripts v and s refer to valence and sea quarks.

Using the parton distributions in pion given by (3.45) and in proton given by (3.38), we calculate A, B for  $\pi^+p \rightarrow \mu^+\mu^-X$  for various values of  $\tau$  and  $r_T$ . For various values of  $\tau$ , A and B are plotted against  $r_T$ . Figs. 3.5(a), 3.6(a) show A and B against  $r_T$  for  $g_p(x) = 3.0 (1-x)^5/x$  respectively.

No appreciable change is noticed in going from  $g_p = 3.0 (1-x)^5/x$  to  $g_p(x) = 4.5 (1-x)^8/x$ . Following points are worth mentioning regarding the variations of A and B with  $r_T$ .

- (i) The shapes of the curves are similar to the curves for  $pp \rightarrow \mu^+\mu^-X$ .
- (ii) Starting from  $\sim 1$  at  $r_T \sim 0.05$ , A decreases to a minimum of  $\sim 0.15$  and then increases again with  $r_T$ .
- (iii) B is almost zero for  $r_T < .02$  and then decreases with  $r_T$  to a minimum of  $\sim -0.15$  and increases and flattens beyond  $r_T \geq .3$ .

- (iv) The angular distribution for low  $r_T$  ( $< 0.02$ ) is of the form  $1 + \cos^2\theta$ , same as the Drell-Yan process.
- (v) Beyond  $r_T = 0.1$ , effects of QCD show up in the dimuon angular distribution, the angular distribution being quite different from  $1 + \cos^2\theta$  behaviour. The asymmetry  $\delta(\theta_1)$  for  $\tau = .1$  and  $r_T = .3$  is  $\delta(\pi/2) \approx -.03$ . The asymmetry will be large for low value of  $\tau$ .

The process  $\pi^- p \rightarrow \mu^+ \mu^- X$  : We calculate A, B and C for this process for various values of  $\tau$  and  $r_T$  using the parton distributions given by (3.38) and (3.45). In Figs. 3.7(a), 3.8(a) for  $g_p(x) = 3(1-x)^5/x$ , we show the variation of A and B with  $r_T$  keeping  $\tau$  fixed. There is no significant change if we take  $g_p(x) = 4.5(1-x)^8/x$ .

It is found that

- (i) the shape of the curves are similar to those in  $p\bar{p} \rightarrow \mu^+ \mu^- X$ .
- (ii) A starts near 1 for  $r_T \sim .05$  and goes to a minimum of 0.2 and then increases with  $r_T$ .
- (iii) B is  $\sim 0$  near  $r_T \sim .02$  and takes a minimum value of  $\sim -0.2$  and then increases with  $r_T$  and goes up to  $+0.22$ .
- (iv) The angular distribution for low  $r_T$  ( $< 0.02$ ) is of the form  $1 + \cos^2\theta$ .
- (v) For large values of  $r_T$  ( $> .05$ ), the angular distribution is different from the Drell-Yan prediction  $1 + \cos^2\theta$ , showing a significant role being played by QCD effects in dimuon production.

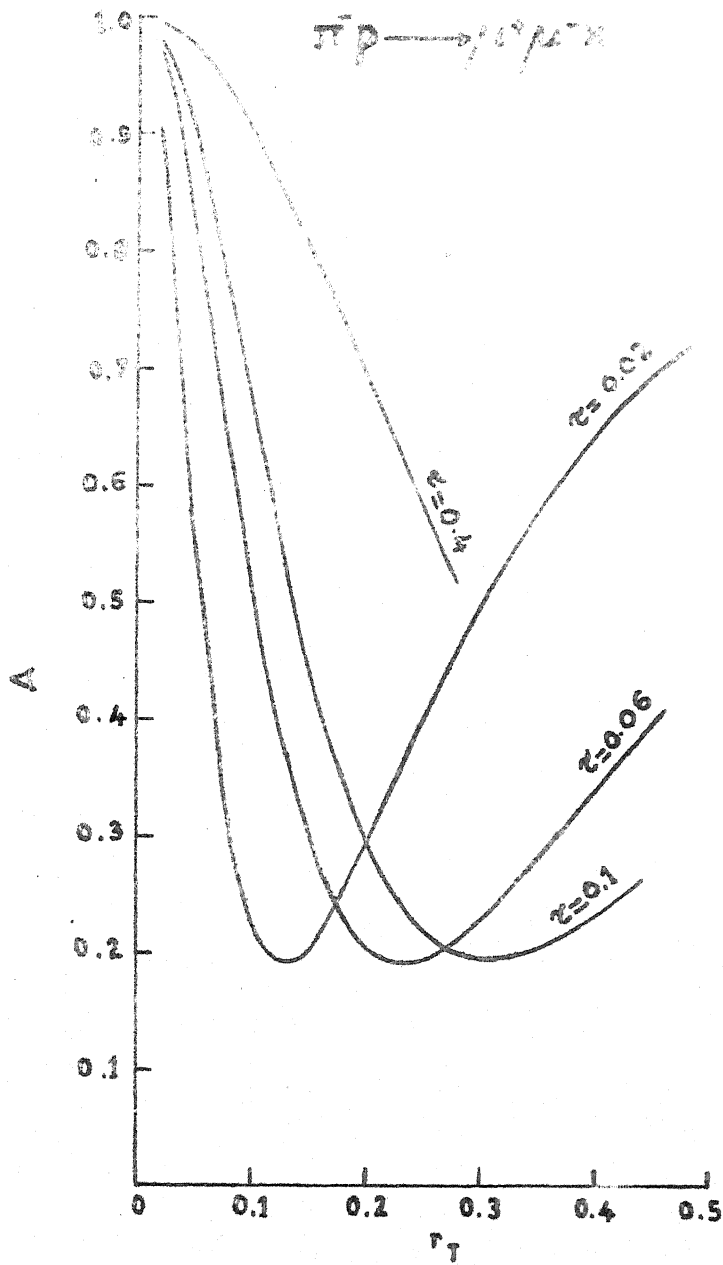


FIG. 3.7 (a)



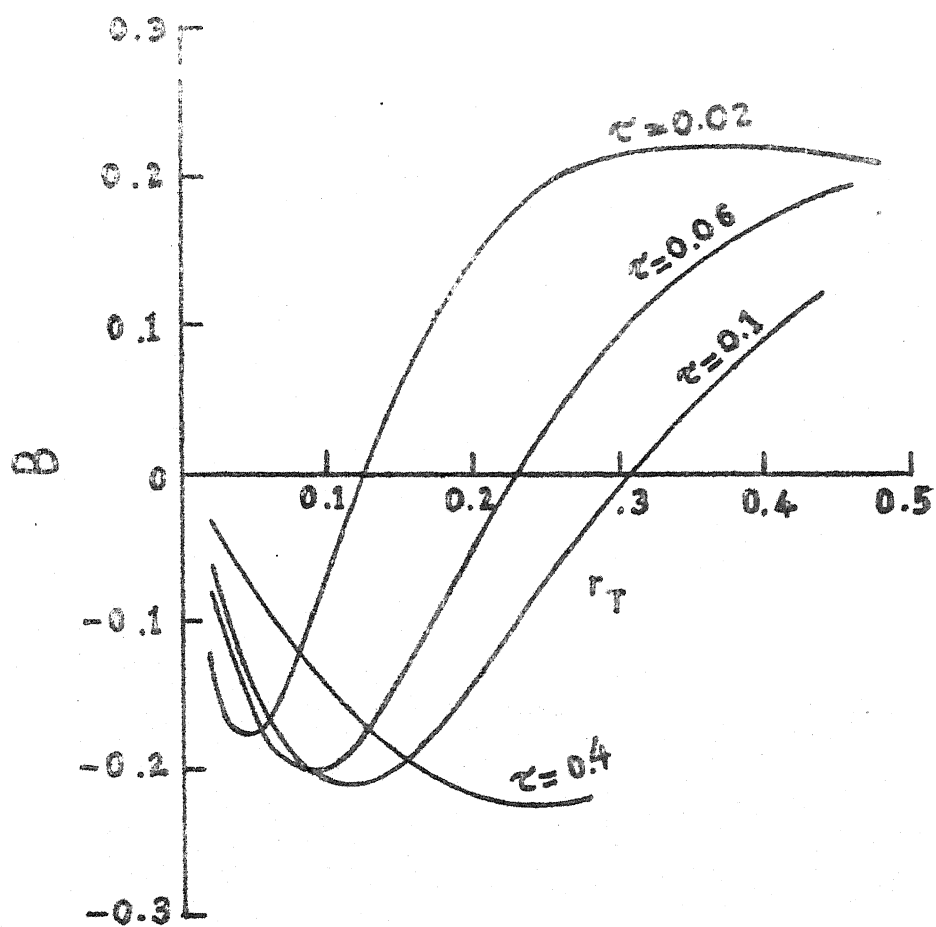
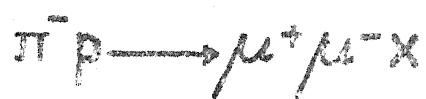


FIG. 3.8 (a)

(vi) The asymmetry  $\delta(\pi/2)$  at  $r_T = .2$  and  $\tau = .1$  is  $\sim .05$ . It will be a bit larger for lower values of  $\tau$ .

A part of this work<sup>22</sup> was done in collaboration with Dr. Saurabh D. Rindani.

## Chapter 4

### ASYMMETRY PARAMETER AS A FUNCTION OF TRANSVERSE MOMENTUM IN THE PRODUCTION OF DILEPTON WITH POLARIZED BEAM AND TARGET

#### 4.1 Introduction

In the previous chapter we investigated the angular distribution of one of the dimuon in dimuon restframe in order to study the role of first order QCD effects<sup>13</sup> in the dilepton production. This was necessitated because of the fact that the simple Drell-Yan<sup>12</sup> model does not explain all the details of dilepton data. In this chapter we study the production of massive lepton pair produced in longitudinally polarized hadronic collisions. We calculate the asymmetry parameter

$$A_L = \frac{m^2 \frac{d^2\sigma}{dm^2 dq_T^2} (H_1(+)H_2(+) \rightarrow \mu^+\mu^-X) - m^2 \frac{d^2\sigma}{dm^2 dq_T^2} (H_1(+)H_2(-) \rightarrow \mu^+\mu^-X)}{m^2 \frac{d^2\sigma}{dm^2 dq_T^2} (H_1(+)H_2(+) \rightarrow \mu^+\mu^-X) + m^2 \frac{d^2\sigma}{dm^2 dq_T^2} (H_1(+)H_2(-) \rightarrow \mu^+\mu^-X)} \times 100 \quad (4.1)$$

as a function of  $r_T = \frac{q_T}{\sqrt{s}}$ . The study of  $A_L$  as a function of  $r_T$  will help us in two ways. At high values of  $q_T$  (greater than the average intrinsic transverse momentum of partons  $\langle K_T \rangle \approx 0.6$  GeV), the asymmetry  $A_L$  is solely due to QCD processes because at high values of  $q_T$  the Drell-Yan contribution to the dilepton production

is almost zero. Consequently the variation of  $A_L$  with  $q_T$  computed via first order QCD processes can be compared with experimental data without any ambiguity and it can provide a good check on the performance of the QCD effects in dilepton production. Secondly, the variation of  $A_L$  with  $r_T$  being dependent on the model chosen for the distribution of polarized partons inside polarized hadrons, will serve as a check on the different models proposed for spin-dependent parton distribution functions inside polarized hadrons.

The first order QCD subprocesses giving rise to non-zero dilepton transverse momentum are: (i)  $q\bar{q}$  annihilation giving rise to a gluon and a virtual photon eventually decaying into lepton pair, fig. 4.1(a), and (ii)  $qg$  Compton type interaction giving rise to a virtual photon which decays into a lepton pair, fig. 4.1(b). We calculate the asymmetry parameter  $A_L$  for four different models of spin dependent parton distribution function in polarized nucleon for  $p-\bar{p}$  collision and  $pp$  collision. The Drell-Yan subprocess does not contribute because we restrict ourselves to high transverse momentum of dilepton.

A similar calculation for polarized  $pp$  collision has been done by Keisho Hideka.<sup>26</sup>

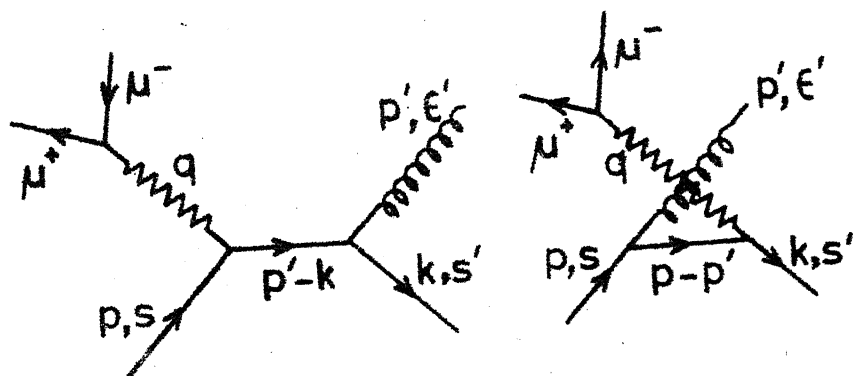


FIG. 4.1(a)

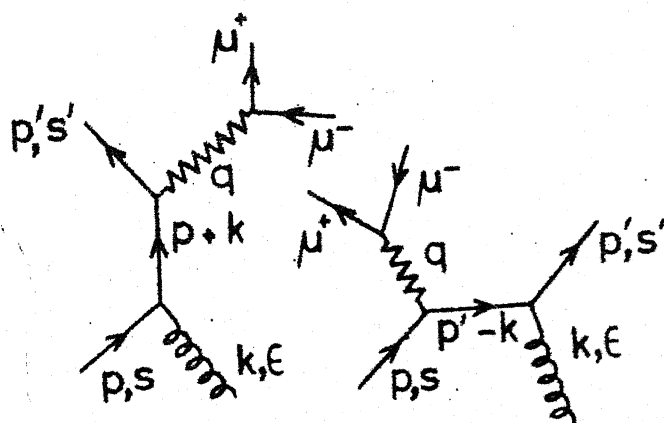


FIG. 4.1(b)

#### 4.II Derivation of the QCD subprocess Cross-section and the Expression for the Asymmetry Parameter $A_L$

We consider the following process:

$$H_1(P_1) + H_2(P_2) \rightarrow \mu^+(k_1) \mu^-(k_2) + \text{anything} \quad (4.2)$$

$H_1$  and  $H_2$  denote colliding hadrons with momenta  $P_1$  and  $P_2$  respectively and  $k_1, k_2$  are the momenta of the muon pair. We will work in the hadron centre of mass frame. The QCD subprocesses producing lepton pair are:

$$(i) \quad q(p,s) + \bar{q}(k,s') \rightarrow g(p',\epsilon') + \mu^+(k_1) + \mu^-(k_2) \quad (4.3)$$

where  $q, \bar{q}$  are the annihilating quark and antiquark with momenta,  $p, k$  and spin  $s, s'$  respectively and  $g$  is the gluon produced with momentum  $p'$  and polarization  $\epsilon'$ . This process is depicted in fig. 4.1(a).

$$(ii) \quad \begin{aligned} q(p,s) + g(k,\epsilon) &\rightarrow q(p',s') + \mu^+(k_1) + \mu^-(k_2) \\ \bar{q}(p,s) + g(k,\epsilon) &\rightarrow \bar{q}(p',s') + \mu^+(k_1) + \mu^-(k_2) \end{aligned} \quad (4.4)$$

Fig. 4.1(b) depicts this process in which a quark or an antiquark of momentum  $p$  and spin  $s$  interact with a gluon of momentum  $k$  and polarization  $\epsilon$  giving rise to a quark or antiquark of momentum  $p'$  and spin  $s'$  and a pair of leptons.

We define

$$q = k_1 + k_2 \quad (4.5)$$

and  $s, m^2, \tau, \hat{s}, \hat{t}, \hat{u}, q_T$  and  $r_T$  are defined in (3.17).

$f_{H(+)}^q(x, \pm), f_{H(-)}^q(x, \pm)$  denote the probabilities of finding

a quark  $q$  of helicity  $\pm$  with fraction  $x$  of the parent hadron's momentum inside a hadron  $H$  of helicity  $+$  and  $-$  respectively and  $g_{H(+)}(x, \pm)$ ,  $g_{H(-)}(x, \pm)$  are the respective probabilities for gluons.

$$\begin{aligned}
 \Delta f_{H(\pm)}^q(x) &= f_{H(\pm)}^q(x, +) - f_{H(\pm)}^q(x, -) \\
 \Delta g_{H(\pm)}(x) &= g_{H(\pm)}(x, +) - g_{H(\pm)}(x, -) \\
 f_H^q(x) &= f_{H(+)}^q(x, +) + f_{H(+)}^q(x, -) = f_{H(-)}^q(x, +) + f_{H(-)}^q(x, -) \\
 g_H(x) &= g_{H(+)}(x, +) + g_{H(+)}(x, -) = g_{H(-)}(x, +) + g_{H(-)}(x, -)
 \end{aligned}
 \tag{4.6}$$

Parity invariance demands that

$$\begin{aligned}
 f_{H(+)}^q(x, +) &= f_{H(-)}^q(x, -) & f_{H(+)}^q(x, -) &= f_{H(-)}^q(x, +) \\
 g_{H(+)}(x, +) &= g_{H(-)}(x, -) & g_{H(+)}(x, -) &= g_{H(-)}(x, +)
 \end{aligned}$$

and thus

$$\begin{aligned}
 \Delta f_{H(+)}^q(x) &= -\Delta f_{H(-)}^q(x) = \Delta f_H^q(x) \\
 \Delta g_{H(+)}(x) &= -\Delta g_{H(-)}(x) = \Delta g_H(x)
 \end{aligned}
 \tag{4.7}$$

The process  $q(p, s) + \bar{q}(k, s') \rightarrow g(p', \epsilon') + \mu^+(k_1) + \mu^-(k_2)$

The amplitude for this process according to the diagram 4.1(a) is

$$M = g e^2 e_q [\bar{v}(k, s') [\gamma^\mu \frac{1}{\not{p}-\not{k}}, \gamma^\nu + \gamma^\nu \frac{1}{\not{p}'-\not{k}} \gamma^\mu] u(p, s)]$$

$$\epsilon_\mu^{*a}(p') [x + \frac{\lambda^a}{2} x] \frac{1}{q^2} [\bar{u}(k_1) \gamma_\nu v(k_2)] \quad (4.8)$$

After mod squaring  $M$  and then introducing the spin projection operators  $\frac{1 + \gamma_5 \not{s}}{2}$ ,  $\frac{1 + \gamma_5 \not{s}'}{2}$  for the initial spins, we sum over all spins, polarization and colours and average over the initial colours and get

$$|M|^2 = \left(\frac{4}{9}\right) (-g^2 e^2 e_q^2 / q^4) H^{\mu\nu} L_{\mu\nu} \quad (4.9)$$

where

$$L_{\mu\nu} = 4(k_{1\mu} k_{2\nu} + k_{1\nu} k_{2\mu} - k_1 \cdot k_2 g_{\mu\nu}) \quad (4.10)$$

$$H^{\mu\nu} = \text{Tr} [(\not{k} - m_q)(\gamma^\mu \frac{\not{p}-\not{p}'}{2p \cdot p'}, \gamma^\sigma + \gamma^\sigma \frac{\not{p}'-\not{k}}{2p' \cdot k} \gamma^\mu) (\frac{1+\gamma_5 \not{s}}{2})(\not{p}+m_q) \cdot$$

$$(\gamma_\sigma \frac{\not{p}-\not{p}'}{2p \cdot p'} \gamma^\nu + \gamma^\nu \frac{\not{p}'-\not{k}}{2p' \cdot k} \gamma_\sigma) (\frac{1+\gamma_5 \not{s}'}{2})] \quad (4.11)$$

By straightforward calculation we arrive at the differential cross-section

$$m^2 \frac{d^2 \hat{\sigma}}{dm^2 d\hat{t}} (q(\eta_1) \bar{q}(\eta_2) \rightarrow \mu^+ \mu^- X) = \frac{4}{9} (1 - \eta_1 \eta_2) \left( \frac{2\alpha^2 \alpha_s e_q^2}{3} \right) \frac{1}{\hat{s}^2} \left( \frac{\hat{s}^2 + m^4}{\hat{t}\hat{u}} - 2 \right) \quad (4.12)$$

$\eta_1$  and  $\eta_2$  are the helicities of the quark and the antiquark respectively, other symbols have already been defined in

Chapter 3. Using the identity  $q_T^2 = \hat{u} \hat{t} / \hat{s}$ , we deduce

$$m^2 \frac{d^2 \hat{\sigma}}{dm^2 dq_T^2} (q(\eta_1) \bar{q}(\eta_2) \rightarrow \mu^+ \mu^- X) = \left( \frac{16}{27} \right) \frac{(1 - \eta_1 \eta_2) \alpha^2 \alpha_s e_q^2}{\hat{s} \sqrt{(\hat{s} - m^2)^2 - 4 \hat{s} q_T^2}}$$

$$\left( \frac{\hat{s}^2 + m^4}{\hat{t}\hat{u}} - 2 \right) \quad (4.13)$$



It is to be observed that the quark and the antiquark of the same helicity decouple. [The helicities are defined in reference to the momentum directions of the individual particles.]

The process  $q(p,s) + g(k,\epsilon) \rightarrow q(p',s') + \mu^+(k_1) + \mu^-(k_2)$

The amplitude for this process depicted in fig. 4.1(b) is

$$M = g^2 e^2 e_q [\bar{u}(p',s') [\gamma^\mu \frac{1}{\not{p} + \not{k}} \gamma^\nu + \gamma^\nu \frac{1}{\not{p}' - \not{k}} \gamma^\mu] u(p,s)] \epsilon_\nu^a(k) \cdot [x + \frac{\lambda^a}{2} x] \cdot \frac{1}{2} [\bar{u}(k_1) \gamma_\mu v(k_2)] \quad (4.14)$$

We mod square M and introduce the spin projection operator  $\frac{1 + \gamma_5 \not{s}}{2}$  for initial quark spin and then sum over initial and final spins and colours and average over the initial colours. We get

$$|M|^2 = \left(\frac{1}{6}\right) \left(\frac{g^2 e^4 e_q^2}{q^4}\right) H'^{\mu\nu} L_{\mu\nu} \quad (4.15)$$

where  $L_{\mu\nu}$  is the same as given by (4.10) and

$$H'^{\mu\nu} = \epsilon_\rho^*(k) \epsilon_\sigma(k) \text{Tr} [(\not{p}' + m_q)(\gamma^\mu \frac{\not{p} + \not{k}}{2p \cdot k} \gamma^\rho - \gamma^\rho \frac{\not{p}' - \not{k}}{2p' \cdot k} \gamma^\mu) \left(\frac{1 + \gamma_5 \not{s}}{2}\right) (\not{p} + m_q)(\gamma^\sigma \frac{\not{p} + \not{k}}{2p \cdot k} \gamma^\nu - \gamma^\nu \frac{\not{p}' - \not{k}}{2p' \cdot k} \gamma^\sigma)] \quad (4.16)$$

A straightforward calculation gives

$$m^2 \frac{d^2 \hat{\sigma}}{dm^2 d\hat{u}} (q(\eta)g(\Lambda) \rightarrow \mu^+ \mu^- X) = \frac{\alpha^2 \alpha_s e_q^2}{9 \hat{s}^2} \left[ - \frac{(\hat{u}^2 + \hat{s}^2 + 2m^2 \hat{t})}{\hat{s} \hat{u}} \right. \\ \left. + \eta \Lambda \left\{ \frac{\hat{u} - 2m^2}{\hat{s}} - \frac{\hat{s} - 2m^2}{\hat{u}} \right\} \right] \quad (4.17)$$

where  $\eta$  and  $\Lambda$  are the helicities of the quark and gluon respectively.

Using the identity  $q_T^2 = \hat{u} \hat{t} / \hat{s}$  we get

$$m^2 \frac{d^2 \hat{\sigma}}{dm^2 dq_T^2} (q(\eta)g(\Lambda) \rightarrow \mu^+ \mu^- X) = \frac{\alpha^2 \alpha_s e_q^2}{9 \hat{s} \sqrt{(\hat{s} - m^2)^2 - 4 \hat{s} q_T^2}} \\ \left[ \frac{\hat{s} + 3m^2}{\hat{s}} + \frac{(\hat{s} - m^2)}{q_T^2} \left\{ 1 - \frac{2m^2(\hat{s} - m^2)}{\hat{s}^2} \right\} + \eta \Lambda \left\{ - \frac{(\hat{s} + 3m^2)}{\hat{s}} + \right. \right. \\ \left. \left. \frac{(\hat{s} - m^2)}{q_T^2} (1 - 2m^2/\hat{s}) \right\} \right] \quad (4.18)$$

### Expression for the asymmetry parameter $A_L$

To write an expression for the asymmetry parameter  $A_L$ , we need the convoluted cross-section  $m^2 \frac{d^2 \sigma_{\text{Annih}}}{dm^2 dq_T^2} (H_1(h_1) H_2(h_2) \rightarrow \mu^+ \mu^- X)$  due to quark-antiquark annihilation subprocess (fig. 4.1(a)) and  $m^2 \frac{d^2 \sigma_{\text{Comp.}}}{dm^2 dq_T^2} (H_1(h_1) H_2(h_2) \rightarrow \mu^+ \mu^- X)$  due to quark-gluon compton process (fig. 4.1(b)). Using equations (4.13) and (4.18) we get the following expressions for these cross-sections.

$$m^2 \frac{d^2 \sigma_{\text{Annih}}}{dm^2 dq_T^2} (H_1(h_1) H_2(h_2) \rightarrow \mu^+ \mu^- X) = \frac{16\alpha^2 \alpha_s}{27} \int_0^1 dx_1 \int_0^1 dx_2$$

$$\theta\{(\hat{s}-m^2)^2 - 4\hat{s}q_T^2\} \sum_{q=u,d,s} \sum_{\eta_1, \eta_2 = \pm} [m^2 \frac{d^2 \hat{\sigma}}{dm^2 dq_T^2} (q(\eta_1) \bar{q}(\eta_2) \rightarrow \mu^+ \mu^- X)]$$

$$[f_{H_1}^q(h_1)(x_1, \eta_1) \cdot f_{H_2}^{\bar{q}}(h_2)(x_2, \eta_2) + f_{H_2}^q(h_2)(x_2, \eta_1)$$

$$f_{H_1}^{\bar{q}}(h_1)(x_1, \eta_2)] \quad (4.19)$$

$$m^2 \frac{d^2 \sigma_{\text{Comp.}}}{dm^2 dq_T^2} (H_1(h_1) H_2(h_2) \rightarrow \mu^+ \mu^- X) = \frac{\alpha^2 \alpha_s}{9} \int_0^1 dx_1 \int_0^1 dx_2$$

$$\theta\{(\hat{s}-m^2)^2 - 4\hat{s}q_T^2\} \sum_{q=u,d,s} \sum_{\eta, \Lambda = \pm} [m^2 \frac{d^2 \hat{\sigma}}{dm^2 dq_T^2} (q(\eta) g(\Lambda) \rightarrow \mu^+ \mu^- X)]$$

$$[ \{ f_{H_1}^q(h_1)(x_1, \eta) + f_{H_1}^{\bar{q}}(h_1)(x_1, \eta) \} g_{H_2}(h_2)(x_2, \Lambda) + \{ f_{H_2}^{\bar{q}}(h_2)(x_2, \eta)$$

$$+ f_{H_2}^q(h_2)(x_2, \eta) \} g_{H_1}(h_1)(x_1, \Lambda) ] \quad (4.20)$$

where  $h_1$  and  $h_2$  are the helicities of the hadrons  $H_1$  and  $H_2$  respectively.

Using equation (4.19), (4.20), (4.6) and (4.7) we arrive at the following expression for the asymmetry parameter  $A_L$ .

$$A_L = \left[ \frac{D_{\text{Annih}}}{\sigma_{\text{Annih}} + \sigma_{\text{Comp}}} + \frac{D_{\text{Comp}}}{\sigma_{\text{Annih}} + \sigma_{\text{Comp}}} \right] \times 100 \quad (4.21)$$

$$\begin{aligned}
D^{\text{Annih}} &= m^2 \frac{d^2 \sigma^{\text{Annih}}}{dm^2 dq_T^2} (H_1(+)H_2(+) \rightarrow \mu^+ \mu^- X) - m^2 \frac{d^2 \sigma^{\text{Annih}}}{dm^2 dq_T^2} \\
&\quad (H_1(+)H_2(-) \rightarrow \mu^+ \mu^- X) = \int_0^1 dx_1 \int_0^1 dx_2 \theta \{(\hat{s}-m^2)^2 - 4\hat{s}q_T^2\} \\
&\quad \{ m^2 \frac{d^2 \hat{\sigma}}{dm^2 dq_T^2} (q(+) \bar{q}(+) \rightarrow \mu^+ \mu^- X) - m^2 \frac{d^2 \hat{\sigma}}{dm^2 dq_T^2} \\
&\quad (q(+) \bar{q}(-) \rightarrow \mu^+ \mu^- X) \} \left[ \sum_{q=u,d,s} e_q^2 \{ \Delta f_{H_1}^q(+)(x_1) \Delta f_{H_2}^{\bar{q}}(+) + \right. \\
&\quad \left. (q \leftrightarrow \bar{q}) \} \right] \quad (4.22)
\end{aligned}$$

$$\begin{aligned}
D^{\text{Comp}} &= m^2 \frac{d^2 \sigma^{\text{Comp}}}{dm^2 dq_T^2} (H_1(+)H_2(+) \rightarrow \mu^+ \mu^- X) - m^2 \frac{d^2 \sigma^{\text{Comp}}}{dm^2 dq_T^2} \\
&\quad (H_1(+)H_2(-) \rightarrow \mu^+ \mu^- X) = \int_0^1 dx_1 \int_0^1 dx_2 \theta \{(\hat{s}-m^2)^2 - 4\hat{s}q_T^2\} \\
&\quad \{ m^2 \frac{d^2 \hat{\sigma}}{dm^2 dq_T^2} (q(+)g(+) \rightarrow \mu^+ \mu^- X) - m^2 \frac{d^2 \hat{\sigma}}{dm^2 dq_T^2} \\
&\quad (q(+)g(-) \rightarrow \mu^+ \mu^- X) \} \left[ \sum_{q=u,d,s} e_q^2 \left[ \Delta g_{H_1}(+)(x_1) \{ \Delta f_{H_2}^q(+)(x_2) \right. \right. \\
&\quad \left. \left. + \Delta f_{H_2}^{\bar{q}}(x_2) \} + \{ \overset{x_1 \leftrightarrow x_2}{H_1 \leftrightarrow H_2} \} \right] \right] \quad (4.23)
\end{aligned}$$

$$\begin{aligned}
\sigma^{\text{Annih}} &= m^2 \frac{d^2 \sigma^{\text{Annih}}}{dm^2 dq_T^2} (H_1(+)H_2(+) \rightarrow \mu^+ \mu^- X) + m^2 \frac{d^2 \sigma^{\text{Annih}}}{dm^2 dq_T^2} \\
&\quad (H_1(+)H_2(-) \rightarrow \mu^+ \mu^- X) = \int_0^1 dx_1 \int_0^1 dx_2 \theta \{(\hat{s}-m^2)^2 - 4\hat{s}q_T^2\} \\
&\quad \{ m^2 \frac{d^2 \hat{\sigma}}{dm^2 dq_T^2} (q(+) \bar{q}(+) \rightarrow \mu^+ \mu^- X) + m^2 \frac{d^2 \hat{\sigma}}{dm^2 dq_T^2} \\
&\quad (q(+) \bar{q}(-) \rightarrow \mu^+ \mu^- X) \} \left[ \sum_{q=u,d,s} e_q^2 \{ f_{H_1}^q(x_1) f_{H_2}^{\bar{q}}(x_2) + (q \leftrightarrow \bar{q}) \} \right] \quad (4.24)
\end{aligned}$$

$$\begin{aligned}
\sigma^{\text{Comp}} &= m^2 \frac{d^2 \sigma^{\text{Comp}}}{dm^2 dq_T^2} (H_1(+)H_2(+) \rightarrow \mu^+ \mu^- X) + m^2 \frac{d^2 \sigma^{\text{Comp}}}{dm^2 dq_T^2} \\
&\quad (H_1(+)H_2(-) \rightarrow \mu^+ \mu^- X) = \int_0^1 dx_1 \int_0^1 dx_2 \theta\{(\hat{s}-m^2)^2 - 4\hat{s}q_T^2\} \\
&\quad \{m^2 \frac{d^2 \hat{\sigma}}{dm^2 dq_T^2} (q(+)g(+) \rightarrow \mu^+ \mu^- X) + m^2 \frac{d^2 \sigma}{dm^2 dq_T^2} (q(+)g(-) \rightarrow \\
&\quad \mu^+ \mu^- X)\} \left[ \sum_{q=u,d,s} e_q^2 [g_{H_1}(x_1) \{f_{H_2}^q(x_2) + f_{H_2}^{\bar{q}}(x_2)\} \right. \\
&\quad \left. + \{ \overset{x_1 \leftrightarrow x_2}{H_1 \leftrightarrow H_2} \} \right] \quad (4.25)
\end{aligned}$$

#### 4.III Spin Dependence of Parton Distribution Functions

We take the following four different models for the spin dependent parton distribution functions in longitudinally polarized nucleons.

A. We assume the sea and the gluon to be unpolarized and take the spin dependence of quark distribution  $f(x, \pm)$  based on a nonrelativistic SU(6) wavefunction of the nucleon:

$$\begin{aligned}
f_{p(+)}^u(x, +) &= \frac{5}{6} f_p^{uv}(x) + \frac{1}{2} f_p^{us}(x) = f_{p(+)}^{\bar{u}}(x, +) \\
f_{p(+)}^u(x, -) &= \frac{1}{6} f_p^{uv}(x) + \frac{1}{2} f_p^{us}(x) = f_{p(+)}^{\bar{u}}(x, -) \\
f_{p(+)}^d(x, +) &= \frac{1}{3} f_p^{dv}(x) + \frac{1}{2} f_p^{ds}(x) = f_{p(+)}^{\bar{d}}(x, +) \\
f_{p(+)}^d(x, -) &= \frac{2}{3} f_p^{dv}(x) + \frac{1}{2} f_p^{ds}(x) = f_{p(+)}^{\bar{d}}(x, -) \quad (4.26)
\end{aligned}$$

where the second superscripts v and s denote valence and sea contributions respectively. Then

$$\begin{aligned}
 \Delta f_p^u(x) &= \Delta f_{\bar{p}}^{\bar{u}}(x) = \frac{2}{3} f_p^{uv}(x) \\
 \Delta f_p^d(x) &= \Delta f_{\bar{p}}^{\bar{d}}(x) = -\frac{1}{3} f_p^{dv}(x) \\
 \Delta f_p^{\bar{u}}(x) &= \Delta f_p^{\bar{d}}(x) = \Delta f_{\bar{p}}^u(x) = \Delta f_{\bar{p}}^d(x) = \Delta f^s(x) = \Delta f^{\bar{s}}(x) = 0 \\
 \Delta g_p(x) &= \Delta g_{\bar{p}}(x) = 0.
 \end{aligned} \tag{4.27}$$

We call it SU(6) model.

B. Sehgal's model : In this model we use the Sehgal's parametrization for  $\Delta f_p^u(x)$  and  $\Delta f_p^d(x)$ . Since for a nucleon

$$\langle J_z \rangle = \langle S_z \rangle_{\text{quarks}} + \langle S_z \rangle_{\text{gluon}} + \langle L_z \rangle \tag{4.28}$$

We take  $\langle L_z \rangle = 0$ .

$$\begin{aligned}
 \langle S_z \rangle_{\text{quark}} &= \frac{1}{2} \int dx [\Delta f^u(x) + \Delta f^{\bar{u}}(x) + \Delta f^{\bar{d}}(x) + \Delta f^d(x) + \Delta f^s(x) \\
 &\quad + \Delta f^{\bar{s}}(x)]
 \end{aligned} \tag{4.29}$$

$$\left( \frac{G_A}{G_V} \right)_{n \rightarrow p} = \int dx [\Delta f^u(x) + \Delta f^{\bar{u}}(x) - \Delta f^d(x) - \Delta f^{\bar{d}}(x)] \tag{4.30}$$

$$\left( \frac{G_A}{G_V} \right)_{\Xi^- \rightarrow \Xi^0} = \int dx [\Delta f^d(x) + \Delta f^{\bar{d}}(x) - \Delta f^s(x) - \Delta f^{\bar{s}}(x)] \tag{4.31}$$

Thus

$$\langle S_z \rangle_{\text{quark}} = \frac{1}{2} \left[ \left( \frac{G_A}{G_V} \right) n \rightarrow p + 2 \left( \frac{G_A}{G_V} \right) \Xi^- \rightarrow \Xi^0 \right] + \frac{3}{2} \int dx [\Delta f^S(x) + \Delta f^{\bar{S}}(x)] \quad (4.32)$$

Neglecting the strange quark contribution, one gets

$$\langle S_z \rangle_{\text{quark}} = \frac{1}{2} (3F - D) \quad (4.33)$$

where

$$\left( \frac{G_A}{G_V} \right) n \rightarrow p = F + D$$

$$\left( \frac{G_A}{G_V} \right) \Xi^- \rightarrow \Xi^0 = F - D$$

Using the experimental values of  $D+F = 1.25 \pm 0.01$  and

$F/D = 0.5 \pm 0.03$ , one gets  $\langle S_z \rangle_{\text{quark}} = 0.3 \pm 0.03$ .

Hence

$$\langle S_z \rangle_{\text{gluon}} = 0.2 \pm 0.05 \quad (4.34)$$

Assuming the sea to be unpolarized, we get

$$0.3 = \langle S_z \rangle_{\text{quark}} = \frac{1}{2} \int_0^1 dx [\Delta f^u(x) + \Delta f^d(x)] \quad (4.35)$$

The Bjorken sum rule is

$$1.23 = \int_0^1 dx [\Delta f^u(x) - \Delta f^d(x)] \quad (4.36)$$

Assuming  $\Delta f^u(x)$  and  $\Delta f^d(x)$  to be proportional to  $f^{uv}(x)$  and  $f^{dv}(x)$  respectively, the equations (4.35) and (4.36) give

$$\Delta f^u(x) = 0.456 f^{uv}(x)$$

$$\Delta f^d(x) = -0.315 f^{dv}(x) \quad (4.37)$$

We parametrize the spin dependent gluon distribution as

$$\Delta g(x) = \beta x g(x)$$

Such that (4.34) is satisfied.

$$0.2 = \langle S_z \rangle_{\text{gluon}} = \int_0^1 x \beta g(x) dx = \frac{\beta(m+1)}{2} \int_0^1 (1-x)^m dx = \beta/2$$

and hence  $\beta = 0.4$  and we get

$$\Delta g(x) = 0.4x g(x)$$

$$g(x) = \left(\frac{m+1}{2}\right)(1-x)^m/x \quad (4.38)$$

We call this Sehgal's model.

C. Carlitz and Kaur's model : In this model, valence quarks interact with the sea and hence their spins are diluted. Let  $\sin^2 \theta$  be the probability that a valence quark's spin changes in interaction with the sea. Suppose  $H(x)$  be the probability of spin flip interaction between the valence and sea and  $N(x)$  be the density of the sea relative to the valence. Suppose the number of particles having spin  $s$  before interaction be 1, then the number of particles having the same spin will be  $1 + \frac{1}{2} N(x) H(x)$  and the number of particles having the opposite spin will be  $\frac{1}{2} N(x) H(x)$  and hence



$$\sin^2 \theta = \frac{\frac{1}{2} N(x) H(x)}{N(x) H(x) + 1} \quad (4.39)$$

Carlitz and Kaur<sup>28</sup> assuming the sea to be unpolarized, deduce the expression

$$H(x) N(x) = H_0 (1-x)^2 x^{-\frac{1}{2}} \quad (4.40)$$

The value  $H_0 = 0.052$  is set by the Bjorken sum rule, Eq. (4.36). A measure of the spin dilution induced by these interactions is given by

$$\cos 2\theta = [H(x) N(x) + 1]^{-1} = [1 + H_0 (1-x)^2 x^{-\frac{1}{2}}]^{-1} \quad (4.41)$$

The spin dependent structure functions are simply given as the product of a function describing the asymmetries of valence-quark spins as given by broken SU(6) model of Close<sup>29</sup> in the absence of the interaction, with the spin dilution factor  $\cos 2\theta$ . The structure functions for scattering off longitudinally polarized nucleons thus have the form

$$\begin{aligned} 2g_1^p(x) &= \cos 2\theta \left[ \frac{4}{9} f_p^u(x) - \frac{3}{9} f_p^d(x) \right] \\ 2g_1^n(x) &= \cos 2\theta \left[ \frac{1}{9} f_p^u(x) - \frac{2}{9} f_p^d(x) \right] \end{aligned} \quad (4.42)$$

Since

$$\begin{aligned} 2g_1^p(x) &= \frac{4}{9} \Delta f_p^u(x) + \frac{1}{9} \Delta f_p^d(x) \\ 2g_1^n(x) &= \frac{4}{9} \Delta f_p^d(x) + \frac{1}{9} \Delta f_p^u(x) \end{aligned} \quad (4.43)$$

Eqs. (4.42) and (4.43) give

$$\begin{aligned}\Delta f_p^u(x) &= \cos 2\theta \left[ f_p^{uv}(x) - \frac{2}{3} f_p^{dv}(x) \right] \\ \Delta f_p^d(x) &= \cos 2\theta \left[ -\frac{1}{3} f_p^{dv}(x) \right]\end{aligned}\quad (4.44)$$

The  $\langle J_z \rangle$  sum rule that the spin carried by the nucleon is  $\frac{1}{2}$  indicates that 11.6% of proton helicity is due to gluons. We parametrize the spin dependence of gluon distribution as before, i.e.

$$\Delta g(x) = cx \, g(x) = c \left( \frac{m+1}{2} \right) (1-x)^m \quad (4.45)$$

and fix  $c$  such that 11.6% of the proton's helicity is carried by gluons. We get

$$\Delta g(x) = 0.058 (m+1)(1-x)^m \quad (4.46)$$

D. Siver's model : This is a model of spin dependent distribution functions in nucleons given by Babcock, Monsey and Sivers.<sup>30</sup> In this model they assume the sea to be polarized and parametrize the sea distribution, based on perturbation theory diagram in QCD and the generation of the sea,<sup>31</sup> as

$$\begin{aligned}f_{p(+)}^{sea}(x,+) &= c f_p^{sea}(x) [2 + (1-x)^2] \\ f_{p(+)}^{sea}(x,-) &= c f_p^{sea}(x) [1 + 2(1-x)^2]\end{aligned}\quad (4.47)$$

where  $c$  is to be fixed by the amount of momentum carried by the sea. Then

$$\Delta f_p^{\text{sea}}(x) = c f_p^S(x) x(2-x) \quad (4.48)$$

They parametrize the gluon distribution, on similar consideration, as

$$\begin{aligned} g_p(+)(x, +) &= k g(x) [2 + (1-x)^2] \\ g_p(+)(x, -) &= k g(x) [1 + 2(1-x)^2] \end{aligned} \quad (4.49)$$

Hence

$$\Delta g(x) = k g(x) x(2-x) \quad (4.50)$$

where  $k$  is to be fixed by the fact that 50% of the nucleon's momentum is carried by the gluon. For  $g(x)$  of the form

$(1-x)^m/x$ ,  $k$  comes to be

$$\begin{aligned} k &= \frac{(m+1)(m+3)}{12(m+2)} \\ g(x) &= (1-x)^m/x \end{aligned} \quad (4.51)$$

$\Delta f_p^{\text{uv}}(x)$  and  $\Delta f_p^{\text{dv}}(x)$  are fixed by Bjorken sum rule (4.36) and the  $\langle J_z \rangle$  sum rule (4.28). If one assumes the spin averaged parton distribution as given in equation (3.38), we get

$$\begin{aligned} \Delta f_p^S(x) &= \Delta f_p^{\bar{d}}(x) = \Delta f_p^{\bar{u}}(x) = 0.028(1-x)^7(2-x) \\ \Delta f_p^{\text{uv}}(x) &= 0.456 f_p^{\text{uv}}(x) \\ \Delta f_p^{\text{dv}}(x) &= -0.315 f_p^{\text{dv}}(x) \end{aligned} \quad (4.52)$$

#### 4.IV Results and Discussion

We compute the asymmetry parameter  $A_L$  as a function of scaled transverse momentum  $r_T = q_T/\sqrt{s}$  for the longitudinally polarized proton-antiproton collision and proton-proton collision for the various models of spin dependent parton distribution functions given in section 4.III for  $\sqrt{s} = 27.4$  Gev. For the spin averaged parton distribution we take the ones of Peierles, Trueman and Wang<sup>23</sup> given in equation (3.38) and the spin averaged gluon distribution is taken of the form  $k(1-x)^m/x$  where  $k$  is to be fixed by the fact that 50% of nucleon's momentum is carried by the gluons. We do our calculations for  $m = 5$  and 8.

For  $p-\bar{p}$  collision, the gluon contribution is understandably very much less than the valence quark-antiquark contribution. We make the following remarks regarding  $p-\bar{p}$  collision.

- (i) For all spin dependent parton distributions  $A_L$  is negative for all values of  $r_T$ .
- (ii) For the distribution obtained from SU(6),  $|A_L|$  increases as  $r_T$  increases, the value of  $A_L$  ranging between -30% to -44%. The variation of  $A_L$  with  $r_T$  for this model is shown in fig. 4.2(a) and 4.2(b), the gluon distributions  $g(x)$  being  $3.0 (1-x)^5/x$  and  $4.5(1-x)^8/x$  respectively. The Drell-Yan model (with  $r_T = 0$ )<sup>32</sup> also gives -44% when SU(6) is used. This limit can be understood simply because the  $u$  quarks dominate  $A_L$  and  $\Delta f^u(x) = \frac{2}{3} f^{uv}(x)$ . Thus

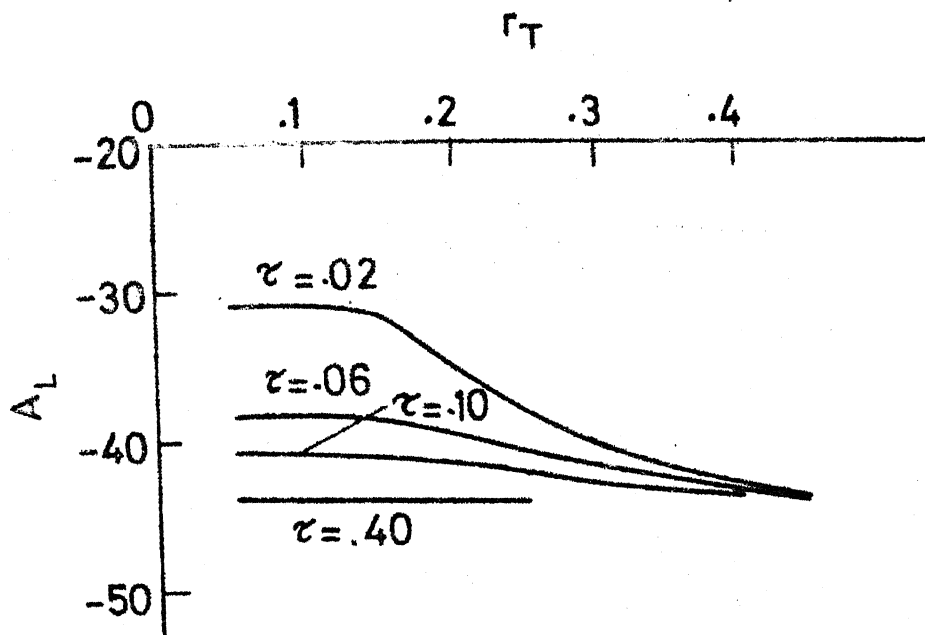


FIG. 4.2(a)

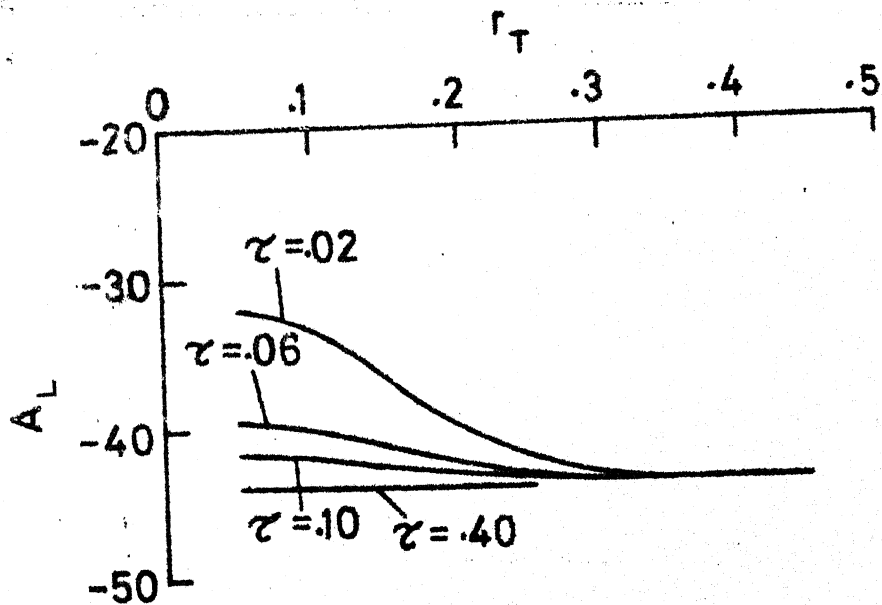


FIG. 4.2(b)

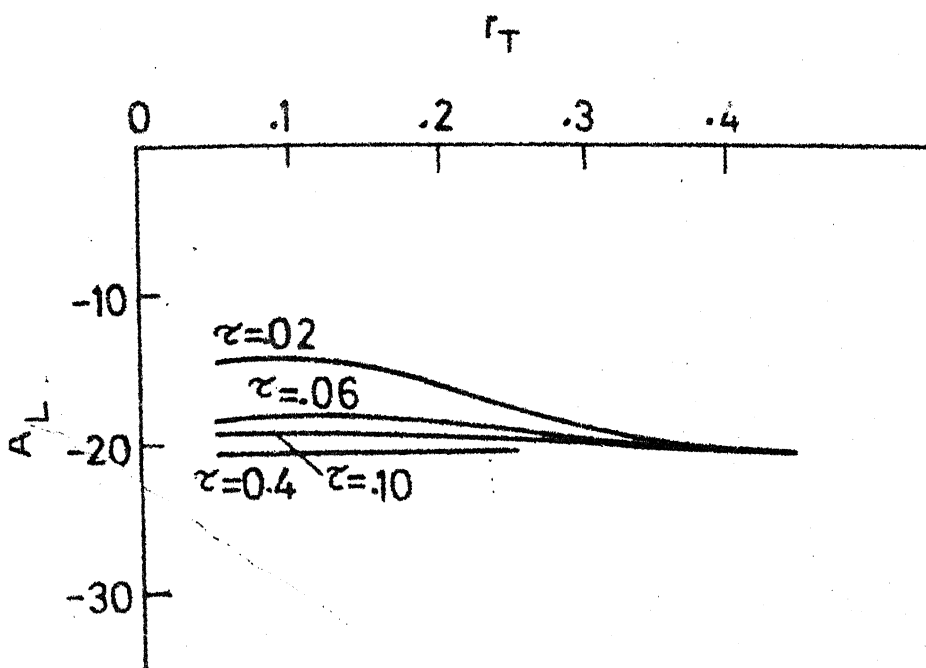


FIG. 4.3(a)

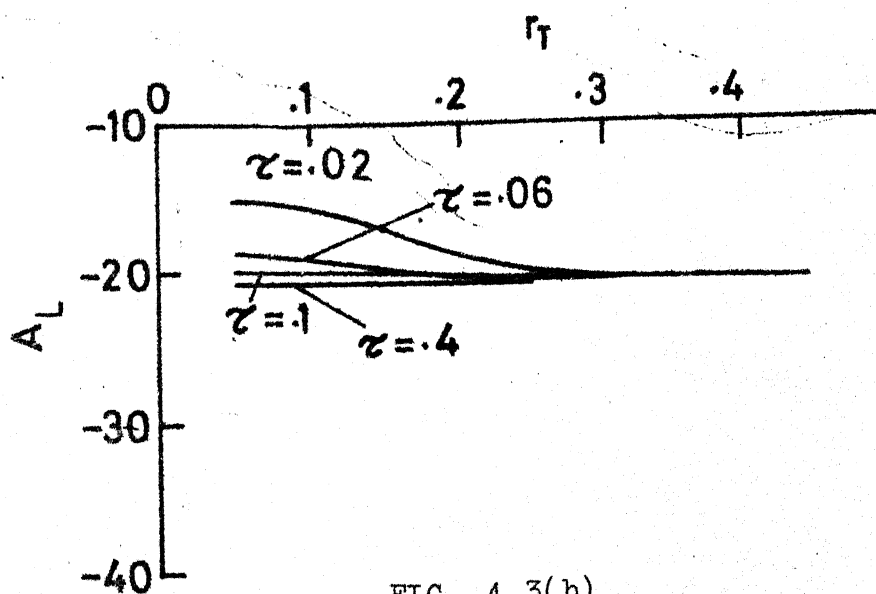


FIG. 4.3(b)

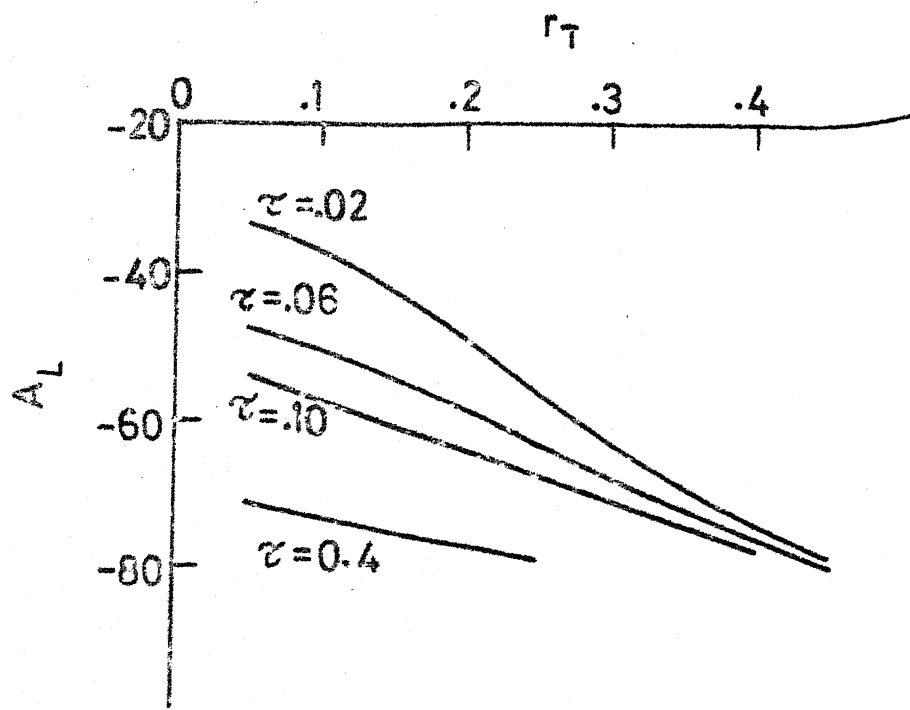


FIG. 4.4(a)

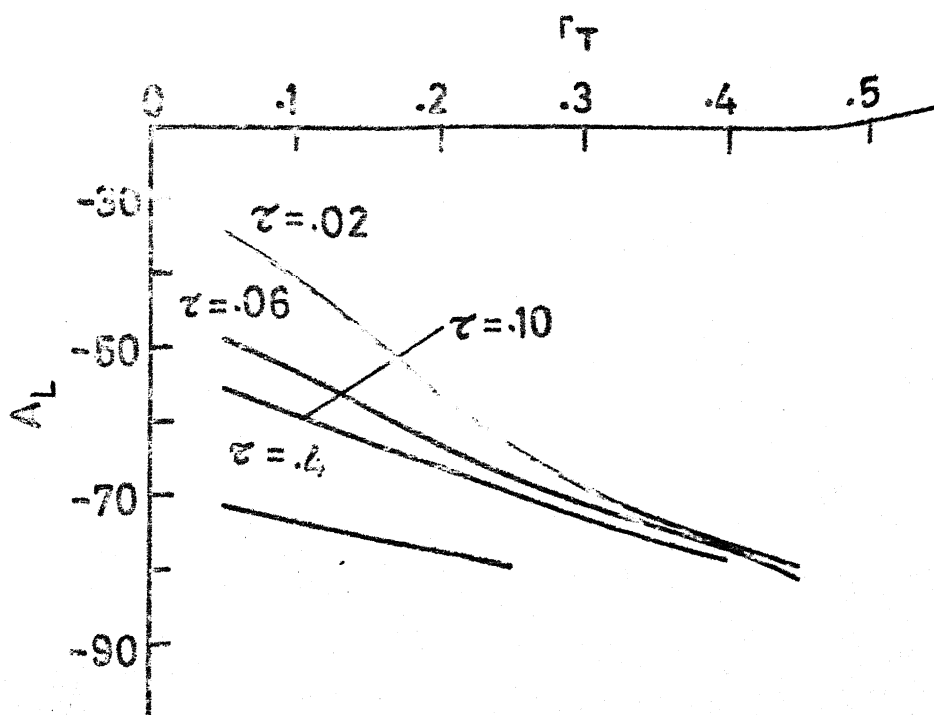


FIG. 4.4(b)

$$A_L \approx \frac{\frac{4}{9} \cdot \frac{2}{3} f_p^{uv}(x) \cdot \frac{2}{3} f_{\bar{p}}^{\bar{u}\bar{v}}(x)}{\frac{4}{9} f_p^{uv}(x) f_{\bar{p}}^{\bar{u}\bar{v}}(x)} = \frac{4}{9} .$$

- (iii) For Sehgal's model the parameter  $A_L$  is more or less similar to SU(6) model but the values are less. The results are shown in figs. 4.3(a) and 4.3(b).  $A_L$  varies from -12% to -20% as  $r_T$  goes from .05 to .45.
- (iv) The Carlitz and Kaur model has a much larger value of  $\Delta f^u(x)$  for large  $x$ . This leads to a much larger asymmetry for large  $x$  as shown in figs. 4.4(a) and 4.4(b). Even though the model is not very reliable in this limit, it will be of interest to test where the asymmetry is as large as 80% for  $r_T = 0.45$ . This would clearly distinguish it from the other models.  $A_L$  varies from -30% to -80% as  $r_T$  goes from .05 to .45.
- (v) Silver's distribution, when the sea is also polarized, does not lead to any significant difference from the Sehgal's distribution. This is understandable because the contribution due to the sea is insignificant.

We now turn to the p-p case where the quark-gluon contribution is dominant over the quark-antiquark contribution. This happens because antiquark distribution in a proton is suppressed. We give the following comments.

- (i) For SU(6)  $A_L$  is zero because neither the antiquarks nor the gluons are assumed to be polarized.



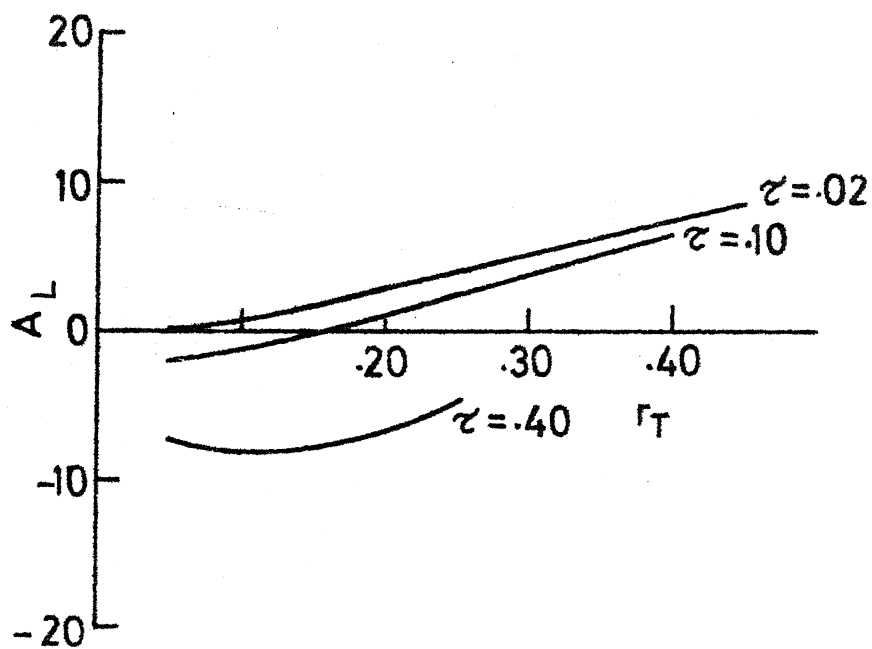
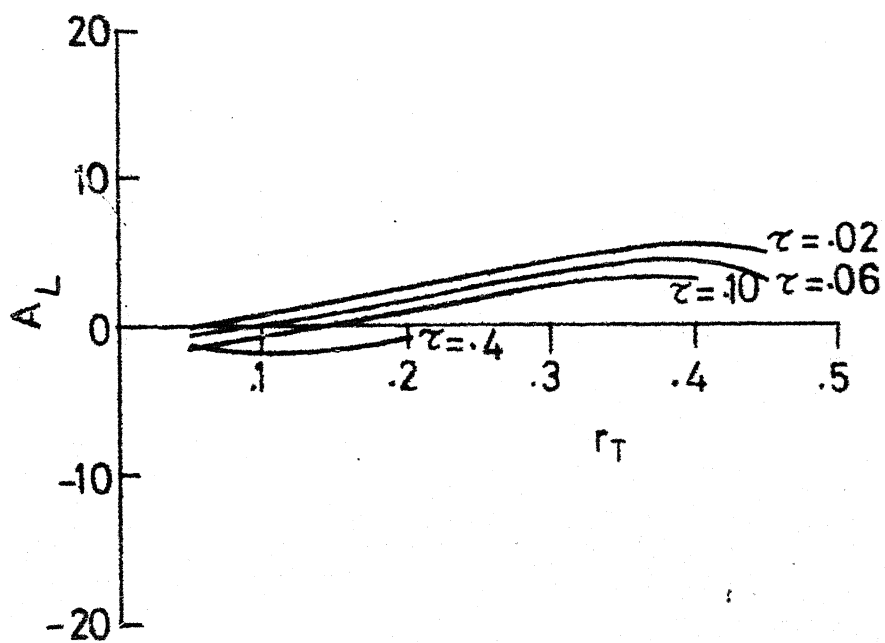


FIG. 4.5(a)



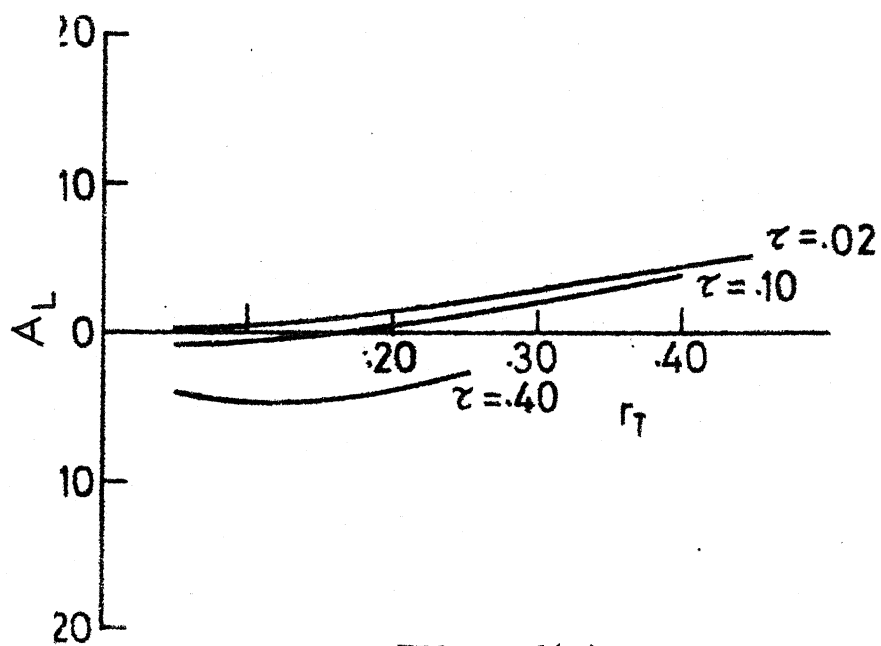


FIG. 4.6(a)

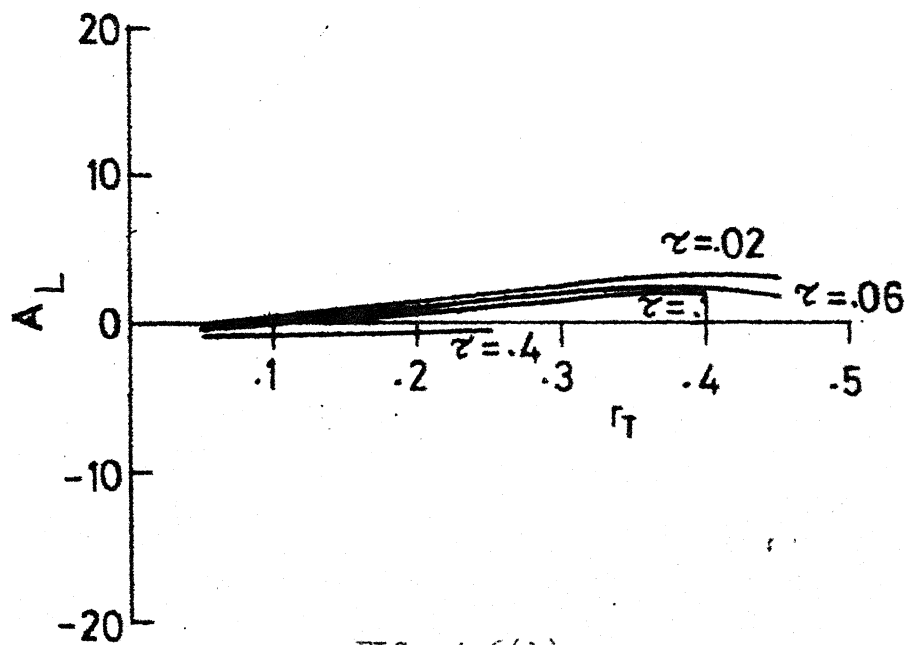


FIG. 4.6(b)

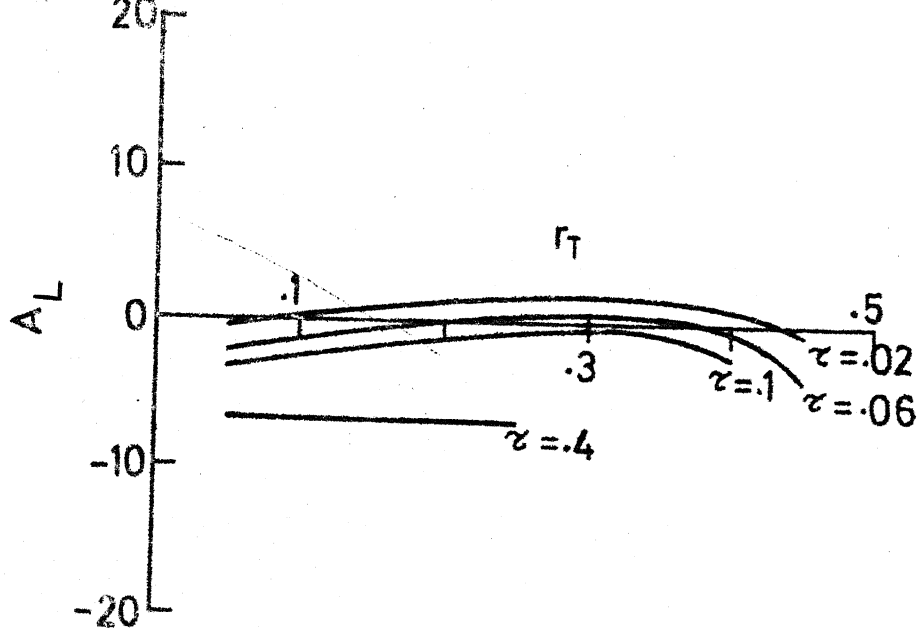


FIG. 4.7(b)

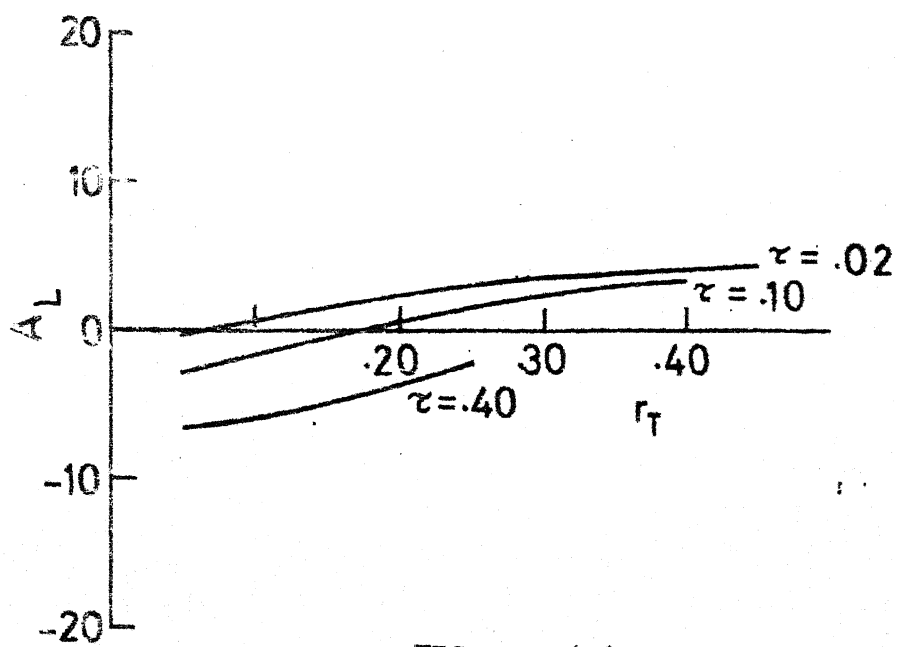


FIG. 4.7(a)

(ii) For Sehgal's distribution the asymmetry  $A_L$  is shown in fig. 4.5(a) for  $g(x) = 3(1-x)^5/x$  and in fig. 4.5(b) for  $g(x) = 4.5(1-x)^8/x$ . This comes entirely from quark-gluon scattering, as the antiquarks are assumed to be unpolarized. The asymmetry has a strong dependence on the gluon distribution. For  $g(x) = 3(1-x)^5/x$ ,  $A_L$  varies from -5% to +10% and for  $g(x) = 4.5(1-x)^8/x$ ,  $A_L$  varies from  $\sim 0$  to +5%. The same remark holds for the Carlitz-Kaur distribution. The variation of  $A_L$  with  $r_T$  for Carlitz-Kaur distribution are shown in fig. 4.6(a) for  $g(x) = 3(1-x)^5/x$  and in fig. 4.6(b) for  $g(x) = 4.5(1-x)^8/x$ .

(iii) The antiquarks are polarized in the Siver's model and hence both quark-antiquark and the quark-gluon processes contribute to the asymmetry. For  $g(x) = 3(1-x)^5/x$ ,  $A_L$  as a function of  $r_T$  is shown in fig. 4.7(a) and it is in the range of 1% to -8%; for  $g(x) = 4.5(1-x)^8/x$  the variation of  $A_L$  with  $r_T$  is shown in fig. 4.7(b) where  $A_L$  is in the range of -5% to 5%.

We have calculated the asymmetry parameter  $A_L$  in the scaling limit. However, we have also repeated our calculations by treating the parton functions as a function of  $q^2 (=m^2)$  and find no appreciable change in  $A_L$ . We use the Gluck-Reya<sup>33</sup> distributions for the  $q^2$  dependence which is

$$f_p^{uv}(x, q^2) = f_p^{uv}(x, q_0^2) \left[ \frac{\ln(q^2/3 \times 10^{-6})}{\ln(q_0^2/3 \times 10^{-6})} \right]^{0.951-x \ln(q^2/0.012)}$$

$$f_p^{dv}(x, q^2) = f_p^{dv}(x, q_0^2) \left[ \frac{\ln(q^2/7 \times 10^{-7})}{\ln(q_0^2/7 \times 10^{-7})} \right]^{0.791-x \ln(q^2/0.0015)}$$

$$f_p^s(x, q^2) = f_p^s(x, q_0^2) \left[ \frac{\ln(q^2/1 \times 10^{-3})}{\ln(q_0^2/1 \times 10^{-3})} \right]^{0.67-x \ln(q^2/0.583)}$$

$$g(x, q^2) = g(x, q_0^2) \left[ \frac{\ln(q^2/4 \times 10^{-5})}{\ln(q_0^2/4 \times 10^{-5})} \right]^{0.288-x \ln(q^2/0.031)}$$

$$\text{with } q_0^2 = 3 \text{ GeV}^2 \quad (4.53)$$

We conclude by observing that the striking variation of  $A_L$  with  $r_T$  is a typical QCD phenomenon and hence is worth measurement in order to study the role of QCD in dilepton production. It also serves as a good test for the correct spin dependent distribution functions of quarks and gluons in polarized nucleons.

This work has been submitted to Phys. Rev. D for publication.

## Chapter 5

### EXTRACTING THE QUARK AND GLUON DISTRIBUTION IN MESONS FROM DILEPTON DATA

#### 5.I Introduction

The parton model idea and the underlying QCD theory seems to work well in the asymptotic region of hadronic collisions. For explicit calculations one needs the quark and gluon distribution functions inside hadrons. The quark distribution in nucleons are usually extracted from deep inelastic  $eN \rightarrow eX$  and  $\nu N \rightarrow \mu X$  data. The gluon distribution is parametrized in the light of some theoretical guidance such as quark counting rules,<sup>25</sup> but there is no direct experimental check on the gluon parametrization. The data on inclusive production of massive dilepton in hadronic collisions can also be used to extract the quark and gluon distribution. The usual extraction<sup>17</sup> based on simple Drell-Yan model where gluons do not play any role cannot be very reliable. Considering the dilepton production in  $MN \rightarrow \mu^+ \mu^- X$ , where  $M$  is  $\pi^\pm$ ,  $K^\pm$ ,  $K^0$ ,  $\bar{K}^0$  meson and  $N$  is proton or neutron, and using first order QCD perturbative effects at high transverse momentum of the dilepton we deduce in section 5.II certain relations which can be used

as a direct check on the quark and gluon distribution in meson, which requires only the valence quark distribution in nucleon (i.e. the knowledge of sea quarks either in mesons or nucleons and gluon distribution in nucleons is not at all required). The basic assumption made is that the sea is an SU(2) singlet.

### 5.II Relations Between Processes $MN \rightarrow \mu^+ \mu^- X$

We will be restricting ourselves to high value of dilepton transverse momentum and consequently the simple Drell-Yan contribution from fig. 2.1 drops out. The non-zero contribution comes from diagrams 4.1(a) and 4.1(b) and the differential cross-section is given by

$$m^2 \frac{d^2\sigma}{dm^2 dq_T^2} = \int_0^1 dx_1 \int_0^1 dx_2 \theta\{(\hat{s}-m^2) - 4\hat{s}q_T^2\} \\ \sum_{q=u,d,s} e_q^2 [B \{f_M^q(x_1) f_N^{\bar{q}}(x_2) + (q \leftrightarrow \bar{q})\} \\ + C \{g_M(x_1)[f_N^q(x_2) + f_N^{\bar{q}}(x_2)] + [\overset{x_1}{\underset{M}{\leftrightarrow}} \overset{x_2}{\underset{N}{\leftrightarrow}}]\}] \quad (5.1)$$

where B and C are the differential cross-sections for the subprocess  $q\bar{q} \rightarrow \gamma^* \rightarrow \mu^+ \mu^-$  and  $qg \rightarrow q\gamma^* \rightarrow \mu^+ \mu^-$  respectively and are given below

$$B = \frac{16\alpha^2\alpha_s}{27\hat{s}\sqrt{(\hat{s}-m^2)^2-4\hat{s}q_T^2}} \left[ \frac{\hat{s}^2 + m^4}{\hat{s} q_T^2} - 2 \right] \quad (5.2)$$

$$C = \frac{\alpha^2\alpha_s}{9\hat{s}\sqrt{(\hat{s}-m^2)^2-4\hat{s}q_T^2}} \left[ \frac{\hat{s} + 3m^2}{\hat{s}} + \frac{(\hat{s}-m^2)}{q_T^2} \left\{ 1 - \frac{2m^2(\hat{s}-m^2)}{\hat{s}^2} \right\} \right] \quad (5.3)$$

All other symbols have the same meanings as defined in earlier chapters.

We will use equation (5.1) and the internal symmetries to derive a hierarchy of sum rules. The most reliable one will be the one based on SU(2). We assume that the valence quark distribution  $f_{p,n}^{qv}(x)$  of nucleons (p,n) and the  $f_{\pi}^{qv}(x)$ ,  $f_K^{qv}(x)$  of the meson doublets ( $\pi^+, \pi^-$ ), ( $K^+, K^0$ ), ( $K^-, \bar{K}^0$ ) are related through isospin rotation and charge conjugation.

$$f_p^{uv}(x) = f_n^{dv}(x) = u_p^v(x) \quad f_p^{dv}(x) = f_n^{uv}(x) = d_p^v(x) \quad (5.4)$$

$$f_{\pi^+}^{uv}(x) = f_{\pi^-}^{dv}(x) = f_{\pi^+}^{\bar{d}v}(x) = f_{\pi^-}^{\bar{u}v}(x) = u_{\pi}^v(x)$$

$$f_{K^+}^{uv}(x) = f_{K^0}^{dv}(x) = f_{K^0}^{\bar{d}v}(x) = f_{\bar{K}}^{\bar{u}v}(x) = u_K^v(x) \quad (5.5)$$

$$f_{K^+}^{\bar{s}v}(x) = f_{K^0}^{\bar{s}v}(x) = f_{K^0}^{sv}(x) = f_{\bar{K}}^{sv}(x) = s_K^v(x)$$

We assume the sea quark distribution  $f^{qs}(x)$  and the gluon distribution  $g(x)$  in mesons to be an SU(2) singlet, i.e.



$$g_{\pi^+}(x) = g_{\pi^-}(x) = g_{\pi}(x) \quad g_{K^+}(x) = g_{K^0}(x) = g_{\overline{K^0}}(x) = g_{K^-}(x) \\ = g_K(x)$$

$$f_{\pi^+}^{us}(x) = f_{\pi^+}^{ds}(x) = f_{\pi^-}^{us}(x) = f_{\pi^-}^{ds}(x) = u_{\pi}^s(x),$$

$$f_{\pi^+}^{ss}(x) = f_{\pi^-}^{ss}(x) = s_{\pi}^s(x)$$

$$f_{K^+}^{us}(x) = f_{K^+}^{ds}(x) = f_{K^0}^{us}(x) = f_{K^0}^{ds}(x) = f_{\overline{K^0}}^{us}(x) = f_{\overline{K^0}}^{ds}(x) =$$

$$f_{K^-}^{us}(x) = f_{K^-}^{ds}(x) = u_K^s(x)$$

$$f_{K^+}^{ss}(x) = f_{K^-}^{ss}(x) = f_{K^0}^{ss}(x) = f_{\overline{K^0}}^{ss}(x) = s_K^s(x) \quad (5.6)$$

Further the gluon distribution  $g(x)$  in nucleons is assumed to be SU(2) singlet and the up, down and strange quark sea are separately the same in proton and neutron

$$g_p(x) = g_n(x)$$

$$u_p^s(x) = u_n^s(x) \quad d_p^s(x) = d_n^s(x) \quad s_p^s(x) = s_n^s(x) \quad (5.7)$$

The superscripts v and s refer to valence and sea quarks respectively.

Now consider the following six sets of reactions:

$$1. \quad \pi^+ p \rightarrow \mu^+ \mu^- X_1$$

$$\pi^- p \rightarrow \mu^+ \mu^- X_2$$

$$2. \quad K^+p \rightarrow \mu^+\mu^-X_3$$

$$K^-p \rightarrow \mu^+\mu^-X_4$$

$$3. \quad \pi^+n \rightarrow \mu^+\mu^-Y_1$$

$$\pi^-n \rightarrow \mu^+\mu^-Y_2$$

$$4. \quad K^+n \rightarrow \mu^+\mu^-Y_3$$

$$K^-n \rightarrow \mu^+\mu^-Y_4$$

$$5. \quad K^0p \rightarrow \mu^+\mu^-Z_1$$

$$\overline{K^0}p \rightarrow \mu^+\mu^-Z_2$$

$$6. \quad K^0n \rightarrow \mu^+\mu^-Z_3$$

$$\overline{K^0}n \rightarrow \mu^+\mu^-Z_4$$

Using equation (5.1) we can write the following two expressions.

$$m^2 \frac{d^2\sigma(MN)}{dm^2 dq_T^2} - m^2 \frac{d^2\sigma(\overline{MN})}{dm^2 dq_T^2} = \int_0^1 dx_1 \int_0^1 dx_2 \theta[(\hat{s}-m^2)^2 - 4\hat{s}q_T^2]$$

$$\sum_{q=u,d,s} e_q^2 [B[\{f_N^{qv}(x_2) + f_N^{qs}(x_2)\} \{f_M^{\bar{q}v}(x_1) + f_M^{\bar{q}s}(x_1)$$

$$- f_{\overline{M}}^{\bar{q}v}(x_1) - f_{\overline{M}}^{\bar{q}s}(x_1)\} + \{f_N^{\bar{q}v}(x_2) + f_N^{\bar{q}s}(x_2)\}$$

$$\{f_M^{qv}(x_1) + f_M^{qs}(x_1) - f_{\overline{M}}^{qv}(x_1) - f_{\overline{M}}^{qs}(x_1)\}]$$

$$\begin{aligned}
& +C [g_N(x_2) \{f_M^{qv}(x_1) + f_M^{qs}(x_1) + f_M^{\bar{q}v}(x_1) + f_M^{\bar{q}s}(x_1) \\
& - f_M^{qv}(x_1) - f_M^{qs}(x_1) - f_M^{\bar{q}v}(x_1) - f_M^{\bar{q}s}(x)\} \\
& + \{g_M(x_1) - g_{\bar{M}}(x_1)\} \{f_N^{qv}(x_2) + f_N^{qs}(x_2) + f_N^{\bar{q}v}(x_2) \\
& + f_N^{\bar{q}s}(x_2)\}]] \quad (5.8a)
\end{aligned}$$

If we invoke equations (5.5) and (5.6), i.e.

$$\begin{aligned}
f_M^{qv}(x) &= f_M^{\bar{q}v}(x), \quad f_M^{\bar{q}v}(x) = f_M^{qv}(x), \quad f_M^{qs}(x) = f_M^{\bar{q}s}(x) = \\
f_M^{qs}(x) &= f_M^{\bar{q}s}(x)
\end{aligned}$$

$$f_N^{qs}(x) = f_N^{\bar{q}s}(x) ; \quad g_M(x) = g_{\bar{M}}(x), \quad f_N^{\bar{q}v}(x) = 0, \quad \text{we get}$$

$$\begin{aligned}
m^2 \frac{d^2 \sigma(MN)}{dm^2 dq_T^2} - m^2 \frac{d^2 \sigma(\bar{M}N)}{dm^2 dq_T^2} &= \int_0^1 dx_1 \int_0^1 dx_2 \theta [(\hat{s}-m^2)^2 - 4\hat{s}q_T^2] \\
\sum_{q=u,d,s} e_q^2 B \quad f_N^{qv}(x_2) [f_M^{\bar{q}v}(x_1) - f_M^{\bar{q}v}(x_1)] & \quad (5.8)
\end{aligned}$$

Similarly,

$$\begin{aligned}
m^2 \frac{d^2 \sigma(Mn)}{dm^2 dq_T^2} - m^2 \frac{d^2 \sigma(Mp)}{dm^2 dq_T^2} &= \int_0^1 dx_1 \int_0^1 dx_2 \theta \{(\hat{s}-m^2)^2 - 4\hat{s}q_T^2\} \\
\sum_{q=u,d,s} e_q^2 [B \{f_n^{qv}(x_2) + f_n^{qs}(x_2) - f_p^{qv}(x_2) - f_p^{qs}(x_2)\} \{f_M^{\bar{q}v}(x_1) \\
+ f_M^{\bar{q}s}(x_1)\} + \{f_n^{\bar{q}v}(x_2) + f_n^{\bar{q}s}(x_2) - f_p^{\bar{q}v}(x_2) - f_p^{\bar{q}s}(x_2)\} \\
\{f_M^{qv}(x_1) + f_M^{qs}(x_1)\}]] +
\end{aligned}$$

$$\begin{aligned}
& C [ \{ g_n(x_2) - g_p(x_2) \} \{ f_M^{qv}(x_1) + f_M^{qs}(x_1) + f_M^{\bar{q}v}(x_1) + f_M^{\bar{q}s}(x_1) \} \\
& + g_M(x_1) \{ f_n^{qv}(x_2) + f_n^{qs}(x_2) + f_n^{\bar{q}v}(x_2) + f_n^{\bar{q}s}(x_2) - f_p^{qv}(x_2) \\
& - f_p^{qs}(x_2) - f_p^{\bar{q}v}(x_2) - f_p^{\bar{q}s}(x_2) \} ] ] \quad (5.9a)
\end{aligned}$$

Using equations (5.5), (5.6) and (5.7), i.e.

$$f_n^{qs}(x) = f_p^{qs}(x), \quad f_n^{\bar{q}s}(x) = f_p^{\bar{q}s}(x), \quad g_p(x) = g_n(x), \quad \text{we have}$$

$$\begin{aligned}
m^2 \frac{d^2 \sigma(Mn)}{dm^2 dq_T^2} - m^2 \frac{d^2 \sigma(Mp)}{dm^2 dq_T^2} &= \int_0^1 dx_1 \int_0^1 dx_2 \theta [(\hat{s}-m^2)^2 - 4\hat{s}q_T^2] \\
&\sum_{q=u,d,s} e_q^2 [B \{ f_n^{qv}(x_2) - f_p^{qv}(x_2) \} \{ f_M^{\bar{q}v}(x_1) + f_M^{\bar{q}s}(x_1) \} \\
&+ C g_M(x_1) \{ f_n^{qv}(x_2) - f_p^{qv}(x_2) \} ] \quad (5.9)
\end{aligned}$$

With the help of equation (5.8) and (5.9) we get the following relations.

$$\begin{aligned}
& [m^2 \frac{d^2 \sigma(K^+p)}{dm^2 dq_T^2} - m^2 \frac{d^2 \sigma(K^-p)}{dm^2 dq_T^2}] / [m^2 \frac{d^2 \sigma(K^0n)}{dm^2 dq_T^2} - m^2 \frac{d^2 \sigma(\bar{K}^0n)}{dm^2 dq_T^2}] \\
&= [m^2 \frac{d^2 \sigma(K^+n)}{dm^2 dq_T^2} - m^2 \frac{d^2 \sigma(K^-n)}{dm^2 dq_T^2}] / [m^2 \frac{d^2 \sigma(K^0p)}{dm^2 dq_T^2} - m^2 \frac{d^2 \sigma(\bar{K}^0p)}{dm^2 dq_T^2}] = 4 \quad (5.10)
\end{aligned}$$

$$[m^2 \frac{d^2 \sigma(K^+p)}{dm^2 dq_T^2} - m^2 \frac{d^2 \sigma(K^+n)}{dm^2 dq_T^2}] / [m^2 \frac{d^2 \sigma(K^0p)}{dm^2 dq_T^2} - m^2 \frac{d^2 \sigma(K^0n)}{dm^2 dq_T^2}] = 1 \quad (5.11)$$

$$m^2 \frac{d^2 \sigma(\pi^+ p)}{dm^2 dq_T^2} - m^2 \frac{d^2 \sigma(\pi^- p)}{dm^2 dq_T^2} = \int_0^1 dx_1 \int_0^1 dx_2 \theta [(\hat{s}-m^2)^2 - 4\hat{s}q_T^2]$$

$$B \cdot \frac{1}{9} [d_p^v(x_2) - 4u_p^v(x_2)] \cdot u_\pi^v(x_1) \quad (5.12)$$

$$m^2 \frac{d^2 \sigma(K^+ p)}{dm^2 dq_T^2} - m^2 \frac{d^2 \sigma(K^- p)}{dm^2 dq_T^2} = \int_0^1 dx_1 \int_0^1 dx_2 \theta [(\hat{s}-m^2)^2 - 4\hat{s}q_T^2]$$

$$B[-\frac{4}{9} u_p^v(x_2) u_K^v(x_1)] \quad (5.13)$$

$$m^2 \frac{d^2 \sigma(\pi^+ n)}{dm^2 dq_T^2} - m^2 \frac{d^2 \sigma(\pi^- n)}{dm^2 dq_T^2} = \int_0^1 dx_1 \int_0^1 dx_2 \theta [(\hat{s}-m^2)^2 - 4\hat{s}q_T^2]$$

$$B \cdot \frac{1}{9} [u_p^v(x_2) - 4d_p^v(x_2)] \cdot u_\pi^v(x_1) \quad (5.14)$$

$$m^2 \frac{d^2 \sigma(K^+ n)}{dm^2 dq_T^2} - m^2 \frac{d^2 \sigma(K^- n)}{dm^2 dq_T^2} = \int_0^1 dx_1 \int_0^1 dx_2 \theta [(\hat{s}-m^2)^2 - 4\hat{s}q_T^2]$$

$$B[-\frac{4}{9} d_p^v(x_2) u_K^v(x_1)] \quad (5.15)$$

$$\frac{4}{5} [m^2 \frac{d^2 \sigma(\pi^+ p)}{dm^2 dq_T^2} - m^2 \frac{d^2 \sigma(\pi^+ n)}{dm^2 dq_T^2}] + \frac{1}{5} [m^2 \frac{d^2 \sigma(\pi^- p)}{dm^2 dq_T^2} - m^2 \frac{d^2 \sigma(\pi^- n)}{dm^2 dq_T^2}]$$

$$= \frac{1}{5} \int_0^1 dx_1 \int_0^1 dx_2 \theta [(\hat{s}-m^2)^2 - 4\hat{s}q_T^2] [u_p^v(x_2) - d_p^v(x_2)]$$

$$[C g_\pi(x_1) + B u_\pi^s(x_1)] \quad (5.16)$$

$$\frac{4}{5} [m^2 \frac{d^2 \sigma(\overline{K^0} p)}{dm^2 dq_T^2} - m^2 \frac{d^2 \sigma(\overline{K^0} n)}{dm^2 dq_T^2}] + \frac{1}{5} [m^2 \frac{d^2 \sigma(K^- p)}{dm^2 dq_T^2} - m^2 \frac{d^2 \sigma(K^- n)}{dm^2 dq_T^2}]$$

$$= \frac{1}{5} \int_0^1 dx_1 \int_0^1 dx_2 \theta [(\hat{s}-m^2)^2 - 4\hat{s}q_T^2] [u_p^v(x_2) - d_p^v(x_2)] [C g_K(x_1)$$

$$+ B u_K^s(x_1)] \quad (5.17)$$

### 5.III Discussion

These relations, especially (5.10) and (5.11), are not merely a consequence of isospin transformation. One needs both isospin transformation and the explicit QCD expression (5.1) for these relations to hold. An experimental check on such a relation thus is not a check on isospin transformation alone but also on the QCD expression.

The right hand side of the expressions (5.16) and (5.17) depend only on the sea and gluon distribution in meson and the valence quark distribution of the nucleon. The contribution due to the gluon is expected to be far more than the contribution due to the sea. Thus it could be a very reliable check on the various parametrisation of the gluon distribution in mesons. Similarly either of the equations (5.12) and (5.14) can be used as a test for the parametrisation of the valence distribution  $u_{\pi}^v(x)$ , and either of the equation (5.13) and (5.15) leads to the determination of the nonstrange valence quark distribution  $u_K^v(x)$  in kaons. This determination does not depend on the parametrization of the sea and gluon distributions in either of the incident particles. The above method will be superior to the present determination<sup>17</sup> using only the Drell-Yan expression and neglecting the sea.

An additional assumption about the sea and the gluon distribution that they are SU(3) singlets, i.e.  $g_{\pi}(x) = g_K(x)$ ,

$u_\pi^S(x) = u_K^S(x) = s_\pi^S(x) = s_K^S(x)$  and  $u_p^S(x) = d_p^S(x) = s_p^S(x)$  gives the following relations:

$$2 \frac{d^2 \sigma(\pi^- p)}{dm^2 dq_T^2} - m^2 \frac{d^2 \sigma(K^- p)}{dm^2 dq_T^2} = \frac{1}{9} \int_0^1 dx_1 \int_0^1 dx_2 \theta [(\hat{s}-m^2)^2 - 4\hat{s}q_T^2] \cdot$$

$$[B \{ [u_\pi^V(x_1) - u_K^V(x_1)] [4u_p^V(x_2) + 5u_p^S(x_2)] + [u_K^V(x_1) - s_K^V(x_1)]$$

$$u_p^S(x_2) \} + C g_p(x_2) \{ 5[u_\pi^V(x_1) - u_K^V(x_1)] + [u_K^V(x_1) - s_K^V(x_1)] \}]$$

$$(5.18)$$

$$2 \frac{d^2 \sigma(\pi^- n)}{dm^2 dq_T^2} - m^2 \frac{d^2 \sigma(K^- n)}{dm^2 dq_T^2} = \frac{1}{9} \int_0^1 dx_1 \int_0^1 dx_2 \theta [(\hat{s}-m^2)^2 - 4\hat{s}q_T^2]$$

$$[B \{ [u_\pi^V(x_1) - u_K^V(x_1)] \cdot [4d_p^V(x_2) + 5u_p^S(x_2)] + [u_K^V(x_1) - s_K^V(x_1)]$$

$$u_p^S(x_2) \} + C g_p(x_2) \{ 5[u_\pi^V(x_1) - u_K^V(x_1)] + [u_K^V(x_1) - s_K^V(x_1)] \}]$$

$$(5.19)$$

$$2 \frac{d^2 \sigma(\overline{K}^0 p)}{dm^2 dq_T^2} - m^2 \frac{d^2 \sigma(\overline{K}^0 n)}{dm^2 dq_T^2} = m^2 \frac{d^2 \sigma(\pi^+ p)}{dm^2 dq_T^2} - m^2 \frac{d^2 \sigma(\pi^+ n)}{dm^2 dq_T^2}$$

$$+ \frac{1}{9} \int_0^1 dx_1 \int_0^1 dx_2 \theta [(\hat{s}-m^2)^2 - 4\hat{s}q_T^2] B[u_\pi^V(x_1) - u_K^V(x_1)]$$

$$\cdot [u_p^V(x_2) - d_p^V(x_2)]$$

$$(5.20)$$

one further assumes  $SU(3)$  then  $u_\pi^V(x) = u_K^V(x) = s_K^V(x)$  and one gets the following relations from equations (5.18), (5.19), (5.20) and (5.12), (5.13), (5.14) and (5.15):

$$m^2 \frac{d^2\sigma(K^-p)}{dm^2 dq_T^2} = m^2 \frac{d^2\sigma(\pi^-p)}{dm^2 dq_T^2} \quad (5.21)$$

$$m^2 \frac{d^2\sigma(K^-n)}{dm^2 dq_T^2} = m^2 \frac{d^2\sigma(\pi^-n)}{dm^2 dq_T^2} \quad (5.22)$$

$$m^2 \frac{d^2\sigma(\bar{K}^0 p)}{dm^2 dq_T^2} - m^2 \frac{d^2\sigma(\bar{K}^0 n)}{dm^2 dq_T^2} = m^2 \frac{d^2\sigma(\pi^+ p)}{dm^2 dq_T^2} - m^2 \frac{d^2\sigma(\pi^+ n)}{dm^2 dq_T^2} \quad (5.23)$$

$$m^2 \frac{d^2\sigma(K^+ p)}{dm^2 dq_T^2} = 16m^2 \frac{d^2\sigma(\pi^+ p)}{dm^2 dq_T^2} - 4m^2 \frac{d^2\sigma(\pi^- n)}{dm^2 dq_T^2} + 4m^2 \frac{d^2\sigma(\pi^+ n)}{dm^2 dq_T^2} - m^2 \frac{d^2\sigma(\pi^- p)}{dm^2 dq_T^2} \quad (5.24)$$

$$m^2 \frac{d^2\sigma(K^+ n)}{dm^2 dq_T^2} = 16m^2 \frac{d^2\sigma(\pi^+ n)}{dm^2 dq_T^2} - 4m^2 \frac{d^2\sigma(\pi^- p)}{dm^2 dq_T^2} + 4m^2 \frac{d^2\sigma(\pi^+ p)}{dm^2 dq_T^2} - m^2 \frac{d^2\sigma(\pi^- n)}{dm^2 dq_T^2} \quad (5.25)$$

we also define the following parameters

$$L = [m^2 \frac{d^2\sigma(\pi^+ p)}{dm^2 dq_T^2} - m^2 \frac{d^2\sigma(\pi^- p)}{dm^2 dq_T^2}] / [m^2 \frac{d^2\sigma(\pi^+ n)}{dm^2 dq_T^2} - m^2 \frac{d^2\sigma(\pi^- n)}{dm^2 dq_T^2}] \quad (5.26)$$

$$\begin{aligned} L &= [m^2 \frac{d^2\sigma(K^+ p)}{dm^2 dq_T^2} - m^2 \frac{d^2\sigma(K^- p)}{dm^2 dq_T^2}] / [m^2 \frac{d^2\sigma(K^+ n)}{dm^2 dq_T^2} - m^2 \frac{d^2\sigma(K^- n)}{dm^2 dq_T^2}] \\ &= [m^2 \frac{d^2\sigma(\bar{K}^0 n)}{dm^2 dq_T^2} - m^2 \frac{d^2\sigma(\bar{K}^0 p)}{dm^2 dq_T^2}] / [m^2 \frac{d^2\sigma(K^0 p)}{dm^2 dq_T^2} - m^2 \frac{d^2\sigma(\bar{K}^0 p)}{dm^2 dq_T^2}] \end{aligned} \quad (5.27)$$



For large  $r_T = \frac{q_T}{\sqrt{s}}$ , the integrands in (5.12), (5.13), (5.14) and (5.15) contribute mainly near  $x_1, x_2 \approx 1$ . Then in this limit one gets,

$$R_1 \approx \frac{1 - 4 u_p(x)/d_p(x)}{u_p(x)/d_p(x) - 4}$$

$$R_2 \approx u_p(x)/d_p(x)$$

For SU(6) nucleon wave function  $R_2 = \frac{u_p}{d_p} = 2$  and  $R_1 = 3.5$  for

large  $r_T$ ; whereas for nucleon quark distribution as given by

Trueman, Peierls and Wang,<sup>23</sup>  $R_2 = \lim_{x \rightarrow 1} u_p(x)/d_p(x) = \infty$ ,  $R_1 = -4$ .

Hence  $R_1$  and  $R_2$  serve as good indicators for the tail distributions of  $u_p(x)$  and  $d_p(x)$ .

This work has been submitted to Phys. Rev. D for publication.

## Chapter 6

### CONCLUSION

The Drell-Yan<sup>12</sup> mechanism, involving on-shell quark-antiquark annihilation into a massive virtual photon, for lepton pair production in hadronic collisions does not explain all the details of the dilepton data.<sup>14</sup> One needs, in addition to the Drell-Yan mechanism, QCD effects such as  $q\bar{q} \rightarrow g\gamma^* \rightarrow \mu^+\mu^-$ ,  $gq \rightarrow q\gamma^* \rightarrow \mu^+\mu^-$  to explain the dimuon data particularly the transverse momentum and the absolute normalization of the dimuon cross-section. The contribution due to the first order QCD effects<sup>13</sup> is found to be of the order of Drell-Yan<sup>12</sup> contribution.

We have studied the angular distribution of the dimuon in their rest frame using first order QCD effects given by diagrams 2.3(a)&(b). The angular distribution is of the form  $1 + A \cos^2 \theta + B \sin 2\theta \cos \phi + C \sin^2 \theta \cos 2\phi$ . A, B and C are functions of  $m^2$ , s and  $q_T$  the transverse momentum of the dimuon. We restricted ourselves to large  $q_T$  in order to avoid mass singularity and infrared divergence and to justify neglecting primordial transverse momentum of the partons. We have computed A and B ( $C = \frac{1}{4}(1-A)$ ) in the

Gottfried-Jackson frame, i.e. in the dilepton restframe, angles are measured taking the beam as the z axis and the x axis being in the plane of the two hadron momenta for pp,  $p\bar{p}$ ,  $\pi^+p$ ,  $\pi^-p$  collisions at  $\sqrt{s} = 27.4$  Gev. For low value of  $r_T = q_T/\sqrt{s} < 0.05$ , the angular distribution is of the form  $1 + \cos^2\theta$ , identical to the Drell-Yan prediction, but for higher values of  $r_T > 0.05$ , there is a strong dependence on both  $\theta$  and  $\phi$ , which shows a striking departure from the Drell-Yan prediction. Hence we suggest the study of the dimuon angular distribution at large transverse momentum in order to investigate the role of QCD in the dimuon production.

Further we have studied the asymmetry associated with dilepton production in longitudinally polarized proton-proton and proton-antiproton collisions, using four different models of spin dependent quark and gluon distribution functions. For  $p-\bar{p}$  collision the asymmetry is quite large (greater than 15%) and shows striking variation with  $r_T = q_T/\sqrt{s}$  and is strongly dependent on the model of spin-dependent structure functions. For p-p collisions the asymmetry is not large ( $\sim 5\%$  to  $7\%$ ) and is also not strongly model dependent because in all the models, we use, the sea and the gluon are not strongly polarized. However, if one takes the model of Bajpai and Ramachandran,<sup>34</sup> which we have not considered in this thesis, where the gluon and the sea are polarized strongly but in opposite directions, the asymmetry is quite

large<sup>35</sup> ( $\sim 20\%$ ) for pp collisions also and changes sign if the number of flavours considered is taken to be greater than four. And thus the study of the asymmetry parameter  $A_L$  defined in equation (4.1) as a function of  $r_T$  will serve two purposes: (i) it distinguishes the first order QCD subprocesses giving rise to dilepton pair where  $A_L$  will be nonzero from the quark-meson scattering processes giving rise to dimuon for which  $A_L$  will be zero and (ii) and it serves as a good test for the spin dependent quark and gluon distributions in polarized nucleons.

Finally we have derived relations between dilepton differential cross-sections in meson-nucleon collisions:  $\pi^+N$ ,  $K^+N$ ,  $K^0N$ ,  $\bar{K}^0N$  ( $N = n, p$ ) collisions, assuming the sea and the gluon distribution to be SU(2) singlet. These relations lead to tests of the parametrizations of (i) non-strange valence quark distribution in mesons and (ii) gluon distribution in  $\pi$  and K mesons. The knowledge of the sea quarks either in mesons or nucleons and gluon distribution in nucleons is not required.

The effect of neutral vector boson  $Z^0$  has been neglected<sup>36</sup> because the maximum value of dimuon mass  $m$  considered is approximately 16 Gev (for  $\sqrt{s} = 27.4$  Gev and  $\tau = 0.4$ ).

# REFERENCES

1. H. D. Politzer, Physics Reports 14C, 129 (1974).  
W. Marciano and H. Pagels, Physics Reports 35C, 137 (1978).  
G. Rajasekaran, Recent developments in gauge theory,  
Lectures given at the Winter School on Theoretical High  
Energy Physics, Panchgani, India (1977).
2. D. Gross and F. Wilczek, Phys. Rev. D8, 3633 (1973);  
Phys. Rev. D9, 980 (1974).
3. B. Humpert, CERN preprint TH 2639-CERN (1979).
4. H. D. Politzer, Phys. Lett. 70B, 430 (1977).  
R. K. Ellis, H. Georgi, M. Machacek, H. D. Politzer  
and C. G. Ross, Phys. Lett. 78B, 281 (1979); Nucl. Phys.  
B152, 285 (1979); Caltech preprint CALT 68-684 and the  
references cited therein.  
B. Humpert and W. L. van Neerven, CERN preprint  
TH 2738-CERN.  
J. Kubar-Andre' and F. E. Paige, Phys. Rev. D19, 221 (1978).
5. J. D. Bjorken, Phys. Rev. 179, 1547 (1969).  
J. D. Bjorken and E. A. Paschos, Phys. Rev. 185, 1975 (1969);  
Phys. Rev. D1, 3151 (1970).  
R. P. Feynman, Photon-hadron Interactions, Benjamin,  
Reading, Mass., 1972.
6. G. Altarelli and G. Parisi, Nucl. Phys. B126, 298 (1977).  
G. C. Fox, Nucl. Phys. B131, 107 (1977).  
L. Baulieu and C. Kounnas, Nucl. Phys. B155, 429 (1979).
7. R. C. Ball et al. Phys. Rev. Lett. 42, 866 (1979) and  
the references therein.
8. T. Appelquist and H. Georgi, Phys. Rev. D8, 4000 (1973).  
A. Zee, Phys. Rev. D8, 4038 (1973).  
M. Dine and J. Sapiirstein, Phys. Rev. Lett. 43, 668 (1970).  
K. G. Chetyrkin, A. L. Kataev and F. V. Tkachov, Phys. Lett.  
85B, 277 (1979).  
William Celmaster and Richard J. Gonslaves, Phys. Rev.  
Lett. 44, 560 (1980).

9. R. D. Field, Applications of Quantum-Chromodynamics, Caltech preprint CALT-68-696 (1978).  
John Ellis, Quantum Chromodynamics and its Applications, Cern preprint TH-2782-CERN (1979).  
Yu. L. Dokshitser, D. I. D'yakonov, S. I. Troyan, Inelastic processes in Quantum Chromodynamics, SLAC. TRANS-183.
10. J. F. Owens, E. Reya and M. Gluck, Phys. Rev. D18, 1501 (1978).
11. D. P. Barber et al. Phys. Rev. Lett. 43, 830 (1970).
12. S. D. Drell and T. M. Yan, Phys. Rev. Lett. 25, 316 (1970); Ann. Phys. (N.Y.) 66, 578 (1971).
13. H. D. Politzer, Phys. Lett. 70B, 430 (1977).  
H. Fritzsch and P. Minkowski, Phys. Lett. 73B, 80 (1978).  
G. Altarelli, G. Parisi and R. Petronzio, Phys. Lett. 76B, 351 (1978); Phys. Lett. 76B, 356 (1978).  
R. Petronzio, CERN preprint TH-2495 (1978).
14. J. G. Branson et al., Phys. Rev. Lett. 38, 1334 (1977).  
D. Antreasyan et al., Phys. Rev. Lett. 39, 906 (1977); CERN preprint CERN-EP/79-116.  
D. M. Kaplan et al., Phys. Rev. Lett. 40, 435 (1978).  
J. K. Yoh et al., Phys. Rev. Lett., 41, 684 (1978).  
K. J. Anderson et al., Phys. Rev. Lett. 43, 944 (1979); Phys. Rev. Lett. 43, 948 (1979); Phys. Rev. Lett. 43, 1219 (1979).  
R. Barate et al., Phys. Rev. Lett., 43, 1541 (1979).  
J. Badier et al., CERN preprint CERN/EP 79-68; Phys. Lett. 89B, 145 (1979).
15. J. C. Collins and D. E. Soper, Phys. Rev. D16, 2219 (1977).
16. Edmond L. Berger, Slac preprint, SLAC-PUB-2314 (1979).
17. K. J. Anderson et al., Phys. Rev. Lett. 42, 944 (1979).  
G. E. Hogan et al., Phys. Rev. Lett. 42, 948 (1979).  
C. B. Newman et al., Phys. Rev. Lett. 42, 951 (1979).
18. Howard Georgi, Phys. Rev. D17, 3010 (1978).
19. R. D. Field, Applications of Quantum Chromodynamics, Caltech preprint CALT-68-696 (1978).  
Edmond L. Berger, Massive lepton pair production in hadronic collisions, Argonne National Lab. preprint, ANL-HEP-PR-78-12; Hadro production of massive lepton pairs in QCD, SLAC-PUB-2314 (1979).

- R. Stroynowski, Massive lepton pair production, SLAC-PUB-2402 (1979).
20. H. D. Politzer, Nucl. Phys. B129 301 (1977).  
K. Kajantie and R. Raitio, Univ. of Helsinki preprint HU-TFT-77-21 (1977).
  21. K. Kajantie, J. Lindfors and R. Raitio, Phys. Lett. 74B, 384 (1978); Nucl. Phys. B144, 422 (1978).
  22. M. Noman and Saurabh D. Rindani, Phys. Rev. D19, 207 (1979).
  23. R. F. Peierls, T. L. Trueman and L. L. Wang, Phys. Rev. D16, 1397 (1977).
  24. J. Kripfganz and A. P. Contogouris, McGill University preprint (1979).
  25. G. R. Farrar, Nucl. Phys. B77, 429 (1974).  
S. J. Brodsky and G. R. Farrar, Phys. Rev. Lett. 31, 1153 (1973).
  26. Keisho Hidaka, West Field College, University of London preprint (1979).
  27. L. M. Sehgal, Phys. Rev. D10, 1663 (1974).
  28. R. Carlitz and J. Kaur, Phys. Rev. Lett. 38, 673 and 1102 (1977); J. Kaur, Nucl. Phys. B128, 219 (1977).
  29. F. Close, Phys. Lett. 43B, 422 (1977).
  30. John Babcock, Evelyn Monsay and Dennis Sivers, Argonne National Lab. preprint ANL-HEP-PR-78-39 (1978).
  31. F. Close and D. Sivers, Phys. Rev. Lett. 39, 1116 (1977).  
K. Hidaka, E. Monsay and D. Sivers, Phys. Rev. D19, 1503 (1979).
  32. M. Noman and H. S. Mani, IV High Energy Symposium, Jaipur, India.
  33. M. Gluck and E. Reya, Nucl. Phys. B130, 76 (1977).
  34. R.P. Bajpai and R. Ramachandran, IIT Kanpur (India) preprint (1980).
  35. R.P. Bajpai, M. Noman and R. Ramachandran, IIT Kanpur (India) preprint (1980). *R.P.; S.*
  36. H. S. Mani, J. C. Rajpoot and A. Salam, Phys. Lett. 72B, 75 (1977). *~*  
H. S. Mani and S. D. Rindani, Phys. Lett. 84B, 104 (1979).